Molecular Signaling Pathways of Recombinant Human Cripto-1

Thesis submitted by

ASIM BIKAS DAS

For the award of the degree

of

Doctor of Philosophy

DEPARTMENT OF BIOTECHNOLOGY

INDIAN INSTITUTE OF TECHNOLOGY GUWAHATI

GUWAHATI - 781039, ASSAM, INDIA

MARCH 2012

Dedicated to my parents for their love, encouragement and support.

Department of Biotechnology

Indian Institute of Technology Guwahati

STATEMENT

I do hereby declare that the matter embodied in this thesis is the result of investigation carried out by me in the Department of Biotechnology, Indian Institute of Technology Guwahati, Guwahati, India, under the guidance of Dr. Biplab Bose.

In keeping with the general practice of reporting scientific observations, due acknowledgements have been made wherever the work described is based on the findings of other investigators.

March, 2012

Asim Bikas Das
(Roll No. 07610610)

Department of Biotechnology

Indian Institute of Technology Guwahati

Date: 5.03.2012

CERTIFICATE

This is to certify that the thesis entitled "**Molecular Signaling Pathways of Recombinant Human Cripto-1**", is being submitted by **Mr. Asim Bikas Das (Roll No. 07610610)** for the award of degree of Doctor of Philosophy is an authentic record of the results obtained from the research work carried out under my supervision in the Department of Biotechnology, Indian Institute of Technology Guwahati, India.

The results embodied in this thesis have not been submitted to any other University or Institute for the award of any degree.

March, 2012

Dr. Biplab Bose
(Research Supervisor)

Acknowledgements

I wish to express my deep sense of gratitude to my supervisor Dr. Biplab Bose for his ongoing support, encouragement and advice and for giving me the opportunity to work in such an inspiring environment. His dedication and commitment to research and teaching is truly inspiring and remarkable. I am very much thankful to Dr. S. S. Ghosh, Dr. A. Ramesh and Dr. L. Sahoo for their priceless suggestions, interesting discussions and for providing a great atmosphere and "state-of-art" facility at the Centre for Excellence (DBT Programme Support Laboratory), Department of Biotechnology, IIT Guwahati.

I am extremely grateful to Dr. S. S. Ghosh, whose valuable suggestions often gave new perspectives to our work. I would also like to thank his present and past lab members at the Department of Biotechnology as well as at the Centre for Nanotechnology for providing me the access to valuable instruments without which this study would have not been feasible. I sincerely thank Dr. A. M. Limaye, whose intellectual input gave us a new way to think and to carry forward our work. I must not forget to thank the present and past HODs of the Department of Biotechnology, Prof. A. Goyal and Prof. P. Goswami for creating excellent facilities and a great atmosphere at the department. I feel privileged to have been able to work with intelligent, interesting and most of all very co-operative present and past members of the Department of Biotechnology.

I'm heavily indebted to my lab members, Pojul and Ashok, who have provided me with ongoing support, inspiration and enjoyable working environment. I'm especially grateful to Urmila and my friends Vinod, Sukhvindar, Shadab, Kaushik da, Vijay, Subhamoy for their unassessable fondness which made my stay at IITG a gratifying and memorable one. I also extend my thanks to Chokalingam, Kohila, Manab, , Sudeep, Sandipan, Ritika, Kasturi, Rachna, Nidhi, Gouri, Sahil, Mitun, Ankana, Reddy, Souvika, Sagarika, Ganesh, Naresh, Abhay, Rishi, Manjit, Himangshu, Seraj, Vishwa, Amresh, Shilpa, Suprio, Bedabrata and former Ph.D. students Gopinath, Kiran, Atul, Abhishek, who have been of exceptional support during my PhD. Most especially, the sharing of news and views with my friends (Urmila, Vinod, Pojul, Ashok, Vishwa) during mid-morning and evening tea at institute coffee shop or KV gate tea stall used to give me utmost relaxation from my tedious work. I have thoroughly enjoyed my years in IIT Guwahati campus. The departmental picnics and my trips to different parts of Assam with friends were the most enjoyable and memorable days of

my PhD life. My sincere thanks to our departmental staff (Mr. Nurul, Mrs. Anita, Mr. Niranjan, Mrs. Prarthana , and Mr. Sharan).

Last but not the least, I express my deepest gratitude to my parents, Mr. Bimal Kumar Das and Mrs. Chhaya Rani Das, who taught me the values of honesty and hard work. Their love, support, and encouragement throughout my life heightened my strength to fulfill my goal. I am indebted to my brother Amit and other family members who always feel proud about me and have been giving constant encouragement that always give me energy to do more hard work. Finally, I want to remember some of my teachers who taught me to think, to do work in more wider and broader way, my father, my school teacher Kripanidhi Roy, Aswini Kumar Sen, Sanath Kumar Jana, Dilip Kumar Pal, Late Birendranath Bhowmik, my professor at BITS-Pilani, Prof Asish Kumar Das and Dr. B. N. Paul (Scientist, IITR). Many thanks to all of them.

March, 2012 ***Asim Bikas Das***

Contents

Abbreviations i
Abstract iii

Chapter 1: Introduction 1-3

Chapter 2: Review of Literature 4-17
Domain Architecture of Human Cripto-1 4
Expression of Human Cripto-1 6
Function of Human Cripto-1 7
Molecular Signaling of Human Cripto-1 9
Human CR-1 as a Therapeutic Target 14
Complexity in signaling networks of growth factors 14

Chapter 3: Materials & Methods 18-34
Bacterial cell culture 18
Maintenance of mammalian cell lines 18
Protein estimation 18
Quantification of DNA and RNA 19
Agarose gel electrophoresis 19
Elution of DNA from agarose gel 20
Plasmid DNA Isolation 20
Polymerase Chain Reaction 21
Preparation of Competent Cells 21
Transformation in bacterial cells 22
Colony PCR to Screen the recombinant clones 22
Restriction digestion 22
Ligation reaction 22
Cloning of PCR amplified DNA fragments in T/A vector 23
Sequencing of DNA fragments cloned in pGEMT - Easy 23
Cloning of CR-1 into bacterial expression Vector 24
Expression of GST tag CR-1 in E.coli BL21 24

Expression of GST tag CR-1 in E.coli Rosetta-gami-2(DE3) 25
Purification of GST tag CR-1 25
SDS-PAGE 25
Western blot 26
Transfection and Generation of Stably Transfected Cell 26
Protein Extraction from mammalian cells 27
Isolation of RNA from mammalian cells 27
Removal of Genomic DNA contamination from RNA 28
Reverse transcription for cDNA synthesis 28
Real-time PCR 29
MTT Assay 30
Trypan blue dye exclusion method 30
BrdU Cell proliferation ELISA 30
CFSE dyes dilution method 31
Cell cycle analysis 33
Detection of apoptosis 33
Lactate dehydrogenase assay 34
Data Analysis 34

Chapter 4: Results & Discussion 35-88
Expression of Recombinant Human Cripto-1 36
Selection of suitable cellular system 38
Effect of Cripto-1 on proliferation of different cell lines 47
Effect of recombinant CR1 on mitogenic pathways 54
Mechanism of the Anti-proliferation effect of CR-1 61
Effect of CR1-GST on transcription profile of cell cycle regulatory molecules 70
CR1-GST mediated anti-proliferative pathways 74

Chapter 5: Conclusions & Scope for future work 89

Bibliography 92
Appendix 103
Publications 115

Abbreviations

ANOVA	Analysis of variance
bp	Base pair
BrdU	5-bromo-2'-deoxyuridine
CHX	Cycloheximide
CR-1	Cripto-1
DMEM	Dulbecco's Modified Eagle Medium
DMSO	Dimethyl sulfoxide
DNA	Deoxyribonucleic acid
dNTP	Deoxyribonucleotide triphosphate
EGF	Epidermal growth factor
EGFR	Epidermal growth factor receptor
ERK	Extracellular signal-regulated kinase
FBS	Fetal bovine serum
GAPDH	Glyceraldehyde 3-phosphate dehydrogenase
GSH	Glutathione
GST	Glutathione S-transferase
hr	Hour
HRP	Horseradish peroxidase
JNK	c-Jun N-terminal kinase
kDa	Kilodalton
Kip1	Kinase-inhibitory protein1
MAPK	Mitogen-activated protein kinases
mg	Milligram
min	Minutes
ml	Milliliter
mM	Millimolar
MTT	3-(4,5-Dimethylthiazol-2-yl)-2,5-diphenyltetrazolium bromide
ng	Nanogram
nm	Nanometer

nM	Nanomolar
PBS	Phosphate buffered saline
PCR	Polymerase chain reaction
PI3K	Phosphatidylinositol 3-kinase
PIP2	Phosphatidylinositol-(4,5)-bisphosphate
PIP3	phosphatidylinositol-(3,4,5)-triphosphate
PMSF	Phenylmethanesulfonylfluoride
PPIA	Peptidylprolyl isomerase A
PTEN	Phosphatase and tensin homolog
PVDF	Polyvinylidene fluoride
RIPA	Radioimmunoprecipitation assay
RNA	Ribonucleic acid
rpm	Revolutions per minute
TDGF	Teratocarcinoma derived growth factor
TGF-β	Transforming growth factor beta
µg	Microgram
µl	Microliter
µM	Micromolar

Abstract

Human oncofetal protein Cripto-1 (CR-1) is considered as a potential biomarker and target for cancer therapy. CR-1 is overexpressed in various types of cancers, including colorectal, breast, nasopharyngeal and gastric cancer. It has been shown that Cripto-1 activates several processes linked with neoplasia, including cell proliferation. The mitogenic effect of CR-1 has been observed in various experimental systems. However, the finer molecular details of CR-1 mediated mitogenic signaling and the controls of those signaling pathways require further investigations. It is now well established that many growth factors can have contextual dichotomous effects. Epidermal growth factor (EGF), a well known mitogen, inhibits cellular proliferation and induces apoptosis, depending upon cell type, expression level of receptors and dosage. Similarly, members of TGF-β superfamily, including TGF-β itself, function in a context dependent fashion. CR-1 is a modulator of signaling by TGF-β ligands and has a modified EGF-like domain. Therefore, one can expect that CR-1 may also have such dichotomous effects. Here, in this thesis, we investigate differential effects of recombinant human CR-1 on cell proliferation in different cellular systems and identify a previously uncharacterized anti-proliferative pathway induced by CR-1.

We have expressed human CR-1 in both mammalian as well as in bacterial expression systems and have used recombinant CR-1 for our investigations. CR-1 interacts with cell surface Glypican-1 to induce the pro-proliferative pathways. We have used two different cell lines, human cervical adenocarcinoma cell line HeLa and human glioblastoma cell line U-87 MG, for most of our investigations. The expression of Glypican-1 is very low in Hela cells in comparison to U-87 MG. As expected, recombinant CR-1 activates pro-proliferative pathways and induces proliferation of U-87 MG cells. However, we have observed that treatment with recombinant CR-1 leads to decrease in proliferation of HeLa cells in a dose dependent fashion. This anti-proliferative effect is measured using different biochemical assays and is confirmed in two other cell lines. Using a series of experiments, we have proved that recombinant CR-1 reduces cell proliferation of HeLa cells by increasing the doubling time, without arresting cell cycle or inducing cell death.

We have further investigated into different signaling pathways involved in this phenomenon. Due to lower expression of Glypican-1, treatment with recombinant CR-1 failed to induce the pro-proliferative ERK1/2 MAPK and Akt pathways in HeLa cells. Interestingly, we have observed that such treatment increases PTEN in HeLa cells leading to downregulation of PI3K/Akt pathway. This leads further to increase in Cdk inhibitor $p27^{Kip1}$ which is known to stop or slow down the cell cycle. We have also observed a synchronized increase in activation of JNK in these cells. In contrast, no such anti-proliferative pathways are activated in U-87 MG as it is a PTEN null cell line.

This thesis leads us to two newer aspects of CR-1 signaling. Our observations indicate that treatment with CR-1 can trigger both pro- and anti-proliferative pathways and the fate of the cell is determined by the relative strength of these two pathways in a particular cell type. Further, treatment with recombinant CR-1 activates the PI3K/Akt pathway as well as increases PTEN that downreugulates for the same pathway. Therefore, CR-1 signaling may have an integral self-limiting control which can be contextually modulated to decide the fate of a cell.

1 Introduction

Polypeptide growth factors play cardinal role in controlling cellular homeostasis in multicellular organisms. They are involved in control of growth, differentiation and death of cells during embryonic development as well as in adult tissues. In addition, dysfunction of growth factors is associated with a variety of diseases. Growth regulatory mechanisms usually involve binding of a growth factor to specific receptor on the cell surface that leads to activation of a series of cytoplasmic proteins creating a cascade of events. This cascade eventually leads to activation or suppression of processes, including expression of molecules that control growth and differentiation. Although signaling pathways involving cascade of events seem simple, the complexity in cellular homeostasis originates from simultaneous involvement of multiple growth factors interacting with their cognate and some time promiscuous receptors. Additional layers of complexities arise as ligand-receptor interaction can activate multiple pathways, as there exists extensive cross-talks between several pathways and rather than being linear, most of the signaling pathways are non-linear with feedback and feed-forward loops. It is now evident that such complexity is crucial for fine-tuned and coordinated response to external stimuli. As cells work in noisy environment, such complex networks involving multiple pathways help to adapt and sustain cellular processes. However, this multiplicity also leads to contextual effects of external stimuli, both cell-specific and temporal.

Human Cripto-1 (CR-1) is an oncofetal protein of EGF-CFC family. It is expressed in embryonic cells and is absent or expressed in low quantity in normal adult tissues. During embryonic development, Cripto-1 controls formation of germ layers, correct orientation of the anterior–posterior axis, and migration of cells through primitive streak. Cripto-1 is also involved in cardiomyogenesis and in mammary gland development. CR-1 is known to function through multiple signal transduction pathways, including Glypican-1/c-Src/MAPK/Akt and Nodal/ALK4/ALK7/Smad-2 signaling pathways. In addition, it modulates the TGF-β, EGF and FGF signaling pathways. The pathway involving Nodal is crucial in cellular differentiation, whereas

Glypican-1 mediated pathway is involved in CR-1 induced cell proliferation and migration. Like other oncofetal proteins, CR-1 is overexpressed in cancer cells. Such overexpression leads to aberrant activations of signaling pathways of CR-1 triggering enhanced cell proliferation, migration, epithelial to mesenchymal transition, and angiogenesis. Therefore, CR-1 mediated oncogenic signaling is a typical example of abnormality in growth factor signaling leading to a disease.

Current understanding of CR-1 signaling shows that it works through multiple pathways. However, information about integration of these pathways is very little. Moreover, cross talks with other signaling pathways are also unknown to us. Being a crucial molecule for embryonic development, it is expected that CR-1 signaling would have multiple layers of connectivity with other pathways and must have very stringent controls. However, very little attention has been paid to such connectivities and controls. It is well known that signal transduction pathways involved in embryogenesis usually involve multiple non-linear loops, like feed-forward and feedback. These network motifs are crucial for auto-regulation, appropriate signal attenuation, cellular diversification and for robustness in signal transduction. However, such issues have not been investigated for CR-1 signaling.

The current work attempts to re-look into the well known signaling pathways of CR-1 to understand the control elements in those pathways. As mitogenic signaling of CR-1 is crucial in development of cancer, we have focused on those pathways. The mitogenic effect of CR-1 has been extensively investigated using different cellular systems and is well documented in existing literature. However, the primary impetus of our work originates from a rare observation that CR-1 can have growth inhibitory effect in a particular cell type, particularly at a high dose or in absence of certain critical growth factors. Although not extensively investigated, such observations indicate to hidden layers of complexities in seemingly simple mitogenic pathways of CR-1.

To investigate the mitogenic pathways of CR-1, we have used two different cellular systems: one with high expression of Glypican-1, the receptor through which CR-1 triggers mitogenic pathways, and the other with lower expression of Glypican-1. These cells were treated with recombinant CR-1 and a comparative study was performed to look into the differential effect of CR-1 on proliferation of these cells. Use of purified

recombinant CR-1 allowed us to perform quantitative dose-dependent studies which are crucial in such comparative investigations. Additionally, non-linear pathways are very sensitive to dose of stimulus. Growth factors are often overexpressed in cells in order to investigate their mitogenic pathways. However, such uncontrolled expression often overburdens the system with stimulus thereby disturbing the real dynamics of the signaling pathway. Such problem does not arise in our case, as we have used purified recombinant protein and in specific doses. Our investigations showed that treatment with CR-1 can trigger both pro- and anti-proliferative pathways and the fate of the cell is determined by the relative strength of these two pathways in a particular cell type. We have shown that the anti-proliferative effect originates from a hitherto unknown pathway of CR-1 involving PTEN and JNK. Treatment with CR-1 increases PTEN, a negative regulator of PI3K/Akt pathway, eventually down-regulating mitogenic pathways and activating inhibitors of cell cycle progression. Our observations lead us to a newer level of complexity in CR-1 signaling. It is well known that CR-1 activates PI3K/Akt pathway; whereas we have shown here that treatment with exogenous CR-1 can upregulate PTEN, a key inhibitory molecule of the same PI3K/Akt pathway. Therefore, our work has shown that CR-1 signaling has an integral self-limiting control which can be contextually modulated. There can be many such controls in CR-1 signaling pathways. Further investigation into the contextual effects of CR-1 would hopefully delineate those control modules.

The present thesis is organized into separate sections. After this introductory chapter, existing literature on Cripto-1 has been extensively reviewed in Chapter 2, Review of literature. Though, all the aspects of CR-1 biology have been discussed in this section, special emphasis is given on the mitogenic effect of CR-1. Chapter 3 describes materials and methods used in the present work. The methodologies for various experiments have been given in details. Additional information on common reagents, kits, cells used in different experiments is given in the appendix. The results of our experiments and a thorough discussion on those have been provided in Chapter 4, Results & Discussion. The conclusions drawn from our present work, along with their implications in cancer cell biology are discussed in Chapter 5.

2 Review of Literature

Human Cripto-1 (CR-1) is an oncofetal protein, which functions as a modulator during embryogenesis and oncogenesis. It is a member of the EGF-CFC family (Cripto-FRL-1-Criptic family), that includes human CR-1, Cryptic in mice [1], FRL-1 in *xenopus* [2], and one-eyed pinhead (*oep*) in zebrafish [3]. Human CR-1 is also known as Teratocarcinoma-Derived Growth Factor-1 (TDGF-1). Sequence conservation among different EGF-CFC family members is relatively very low. Overall sequence identity among human CR-1 and human Cryptic, another EGF-CFC family member, is ~25% [4]. Like other members of EGF-CFC, CR-1 is also primarily expressed during embryonic development and rarely in adults. However, CR-1 is over expressed in a number of human breast, colon, gastric and pancreatic cancer cells, suggesting that CR-1 may function as growth factor in these tumor cells [5-8].

Domain Architecture of Human Cripto-1:

CR-1 is a 188 amino acid long protein and its molecular weight varies from 24 – 36 kDa, depending upon the extent of glycosylation [9]. Like other members of EGF-CFC family of proteins, CR-1 has an N-terminal signal peptide domain, an epidermal growth factor (EGF)-like motif, a conserved cysteine rich domain (CFC region), and a short hydrophobic C-terminus that is essential for membrane anchorage by a glycosylphosphatydilinositol (GPI) moiety (Figure 2.1). However, The EGF domain present in CR-1 is a variant of EGF-like motif of other members in EGF super-family. It is approximately 40 amino acids long, containing six cysteine residues that can form three intramolecular disulfide bonds. While in the canonical EGF motif, three loops (A, B and C) can be recognized, the variant of EGF-like motif in the EGF-CFC proteins lacks the A loop, possesses a truncated B loop and has a complete C loop [10]. Due to modified EGF like domain, CR-1 can not bind to epidermal growth factor receptor (EGFR) [11].

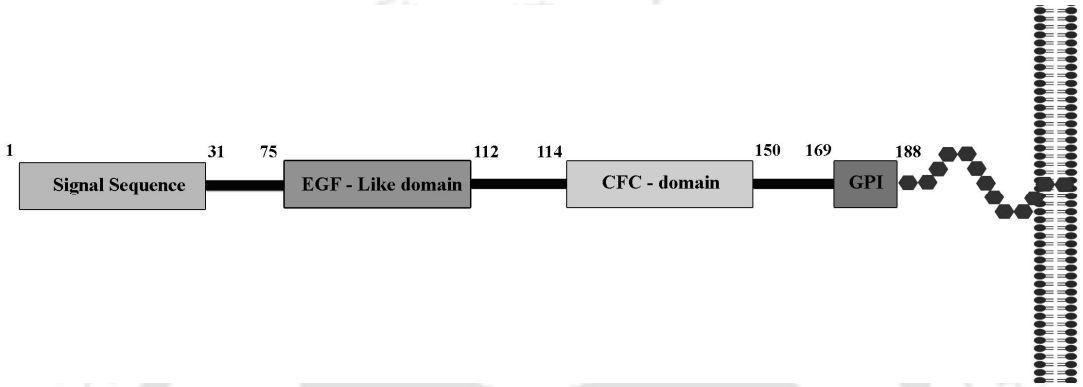

Figure 2.1 Domain architecture Human Cripto-1. Cripto-1 (1-188 amino acid) has a signal sequence, epidermal growth factor -like motif (EGF- like domain), a conserved cysteine rich domain (CFC-domain), and a short hydrophobic C-terminus that is essential for membrane anchorage by a glycosylphosphatydilinositol (GPI) moiety.

Full-length CR-1 is a fucosylated protein with C-terminal GPI-anchor region. However, it has been shown that fucosylation and C-terminal anchor region are not essential for CR-1 signaling [12, 13]. Seno *et al.* [14] have shown that treatment with recombinant CR-1 expressed in *E. coli* induces mitogenic signaling and facilitates branching morphogenesis in mouse mammary epithelial cells. Several reports have demonstrated that removal of the C-terminal GPI-anchor domain of CR-1 does not alter the CR-1 functionality [15-19]. This indicates that CR-1 can act both as a membrane bound molecule and as a soluble ligand. Soluble and functional form of CR-1 has been identified in human milk [20] and in serum of breast and colon cancer patients [21]. EGF-like domain of Cripto, fused either to human Fc or to GST, also induces mitogenic signaling [17, 22]. Furthermore, even refolded peptides corresponding to the EGF-like domain of CR-1 stimulate growth of several types of cell lines when added to culture medium [9, 23].

Expression of Human Cripto-1:

A 2.2 kb long CR-1 transcript was initially identified in a cDNA library derived from undifferentiated human NTERA2 teratocarcinoma cells [24]. This was further mapped to human chromosomal location 3p21.3. Subsequently, five other human CR-1–related pseudogenes have been identified. These are CR-2, CR-3, CR-4, CR-5 and CR-6 (also known as TDGF-2, TDGF-3, TDGF-4, TDGF-5 and TDGF-6 respectively) [25].

It is known that the members of EGF-CFC family are involved in early vertebrate development. During embryonic development, mouse Cripto-1(Cr-1) is expressed in a spatially restricted fashion [26]. Initially, Cr-1 is expressed in the mouse blastocyst, primitive streak, and later, is restricted to the developing heart. Cr-1 is also expressed in the developing mouse mammary gland [27, 28]. Expression pattern of human CR-1 during embryonic development has not been elucidated yet. However, expression of CR-1 has been detected in Human embryonic stem (huES) cells [29].

Human CR-1 is generally absent or present at very low level in some normal adult tissues [30]. Expression of CR-1 in normal adult tissue is limited to mammary cells. Expression of biologically active CR-1 has been detected in human milk [20]. Mouse Cr-1 expression is upregulated in mammary epithelial cells during pregnancy and lactation [31]. However, CR-1 is overexpressed in a majority of human colorectal carcinomas [5], breast carcinomas [8], testicular germ cell tumors [22], lung cancer

[32], ovarian carcinomas [33], and pancreatic cancer [7]. Expression pattern of CR-1 indicates that it has a crucial role during embryogenesis, oncogenesis and mammary gland development.

Function of Human Cripto-1:

CR-1 is involved in embryonic development, mammary gland development and oncogenesis. Functions of CR-1 in these processes are discussed below.

Role of CR-1 in embryonic development:

The precise function of human CR-1 in embryonic development is not clearly elucidated. In general, several EGF-CFC family members are involved in early vertebrate development. During embryonic development, mouse Cr-1 is expressed in a spatially restricted fashion [26]. Initially, Cr-1 is expressed in the mouse blastocyst, and in primitive streak. Subsequently it is expressed only in developing heart. Ding *et. al.* [34] have shown that Cr-1 is required for correct orientation of the anterior–posterior axis in the mouse embryo. Disruption of Cr-1 alleles, by homologous recombination, leads to embryonic lethality due to impaired gastrulation and anterior-posterior axis perturbation. *oep*, the CR-1 homologue in zebra fish, is essential for cellular movement during embryonic development [35]. In human, loss-of-function mutations, in human Criptic protein (CFC1), is associated with left-right lateral defects [36].

Role of CR-1 in mammary gland development:

CR-1 can modulate mammary epithelial cell migration, branching morphogenesis and milk protein expression *in vitro*. Mouse Cr-1 is expressed in the stromal cells, luminal epithelial cells, and myoepithelial cells of the branching ducts of mouse mammary glands [28]. It is expressed at low level during mammary gland development and its expression increases during pregnancy and lactation [27, 37]. Human CR-1 has also been detected in human milk [20], indicating that this may have the same function as its homologue in mouse. CR-1 stimulates the growth of HC-11 mouse mammary epithelial cells. In these cells, prior treatment with exogenous CR-1 promotes a competency response to the lactogenic hormones inducing expression of milk protein β-casein. However, simultaneous treatment with CR-1 in the presence of lactogenic

hormones inhibits beta-casein expression through a Ras dependent, PI3K-dependent pathway [23].

Role of CR-1 during oncogenesis:

CR-1 is involved in several cellular responses linked with neoplasia, such as stimulation of cell proliferation, migration, branching morphogenesis and transformation [38]. Overexpression of CR-1 in breast cancer cell line, MCF-7, enhances resistance to anoikis and increases the invasiveness of these cells [39]. *In vivo* overexpression of human CR-1 in mammary glands of transgenic mouse causes development of hyperplasia and papillary adenocarcinoma [40]. Antisense therapy against CR-1 mRNA can inhibit growth of cancer cells both *in vivo* and *in vitro* [41]. CR-1 is also involved in tumor angiogenesis. Its overexpression stimulates various endothelial cell responses that are associated with microvessel formation *in vivo* [12]. Treatment with monoclonal antibody against CR-1 can inhibit such CR-1-induced neovessel formation [12]. Overexpression of CR-1 in MCF-7 human breast cancer cells enhances tumor neovascularization in a xenograft model [42]. In addition, overexpression of CR-1 supports colony formation and anchorage-independent growth in NOG-8 mammary epithelial cells [43]. Transfection of human CR-1 into NIH3T3 cells induces morphological changes and colony formation [24]. Similarly, overexpression of CR-1 in normal rat fibroblasts was shown to induce growth of these cells in soft agar [9].

CR-1 also plays a role in inducing epithelial to mesenchymal transition (EMT) of mammary epithelial cells [42]. EMT marker expression study has shown that E-cadherin, which is responsible for intactness of junction complex in epithelial cells, was significantly downregulated in mammary gland hyperplasias, tumors of CR-1 transgenic mice and CR-1 transfected HC-11 cells [44]. Furthermore, zinc-finger repressor transcription factor Snail was detected in elevated levels in mammary tumor lesions of CR- 1 transgenic mice [44]. Snail is known to downregulate or interfere with the normal expression of E-cadherin [45]. Another EMT marker, vimentin, which is the major cytoskeletal component of mesenchymal cells [46, 47], was upregulated in human cervical carcinoma cells following overexpression of CR-1. These cells also exhibited increased migration and invasion [48].

Molecular Signaling of Human Cripto-1:

CR-1 is involved in the activation of several different signaling pathways during embryonic development and cellular transformation [49]. CR-1 mediated signaling pathways and there functions are discussed here.

Glypican-1/c-Src/MAPK/Akt signaling pathway:

MAPK and AKT pathways are important mitogenic pathways which are activated by various external stimuli. Activation of canonical MAPKs pathway begins with stimulation of tyrosine kinase receptors (RTKs) present on cell surface. Activation of RTKs activates a cascade of protein kinases, defined sequentially as MAPKKK (represented by c-Raf-1), and MAPKK such as MEK1 and MEK2. MEKs ultimately phosphorylate p44 MAPK and p42 MAPK, also known as ERK1 and ERK2. The activated ERKs then translocate to the nucleus where they transactivate transcription factors altering gene expression to promote growth, differentiation or mitosis [50].

In Akt (also known as protein kinase B or PKB) signaling pathway, the Akt cascade is activated by receptor tyrosine kinases (RTKs) that induce the production of phosphatidylinositol 3,4,5 triphosphates (PIP3) by phosphoinositide 3-kinase (PI3K). These lipids serve as plasma membrane docking sites for proteins that harbor pleckstrin-homology (PH) domains, including Akt and its upstream activator phosphoinositol-dependent kinase PDK1. The binding of Akt to inositol lipids alters its conformation so that the protein can be phosphorylated and activated by PDK1. The activated Akt gets dissociated from plasma membrane and participates in a series of events like phosphorylation of BAD, inhibition of cell cycle inhibitory proteins p21 and p27, and thereby promotion of cell survival.

CR-1 can activate both MAPK as well as PI3K/Akt pathways. These two pathways are activated when CR-1 binds to the heparan sulfate proteoglycan Glypican-1, which in turn activates the tyrosine kinase c-Src, leading to activation of downstream MAPK and Akt [18, 51, 52]. Full-length CR-1 expressed in mammalian system has been shown to activate MAPK pathway in several *in vitro* experiments leading to enhanced phosphorylation of ERK1/2. Similar phenomenon has also been observed with a refolded 47-mer peptide representing EGF domain of CR-1 [12, 53]. In Akt signaling pathway, CR-1 enhances the tyrosine phosphorylation of the p85 regulatory subunit of

PI3K and induces the phosphorylation of Akt and GSK-3β [42, 54]. CR-1 mediated cell proliferation and survival is regulated by MAPK and Akt signaling pathways. Deregulated activation of these two pathways by CR-1 leads to enhanced cell proliferation. Exogeneous CR-1 activates MAPK and Akt pathways and induces proliferation, migration, invasion and angiogenesis in HUVECs cells [12]. CR-1 functions as a survival factor in human cervical cancer cell line SiHa and Caski where CR-1 inhibits apoptosis through enhancement of phosphorylation of Akt and GSK-3β [54]. In addition, increase in active c-Src and Akt was observed in mammary tumors from the CR-1 transgenic mice and in HC-11 cell over expressing Cr-1 [44]. Activation of Akt is associated with the EMT and increased migration of these cells. Glypican-1/c-Src/MAPK/Akt signaling pathways of CR-1 are briefly described in Figure 2.2.

Involvement of CR-1 in EGF and FGF signaling pathways:

The epidermal growth factor (EGF) signaling pathway is one of the most important pathways that regulate growth, survival, proliferation, and differentiation in mammalian cells. Binding of EGF to the epidermal growth factor receptor (EGFR) activates the Ras/MAPK pathway, resulting in transcriptional activation of many genes which induce cellular transformation [55]. CR-1 can also indirectly activate EGF signaling. Though a member of EGF super-family, CR-1 does not bind to EGFR [53]. However, it does cross-talk with one of the EGFR, ErbB4 indirectly, triggering tyrosine phosphorylation of this receptor and activating downstream signaling through ERK1/2 [11].

Fibroblast growth factors (FGFs) and their receptors (FGFR) also control a wide range of biological functions regulating cellular proliferation, survival, migration and differentiation. The predominant signaling pathways activated downstream of FGFRs are MAPK signaling pathways [56]. In *Xenopus* oocytes, a *Xenopus* Cripto-1 protein homolog, FRL1, can increase the phosphorylation of *Xenopus* FGFR-1 without directly binding to it [2].

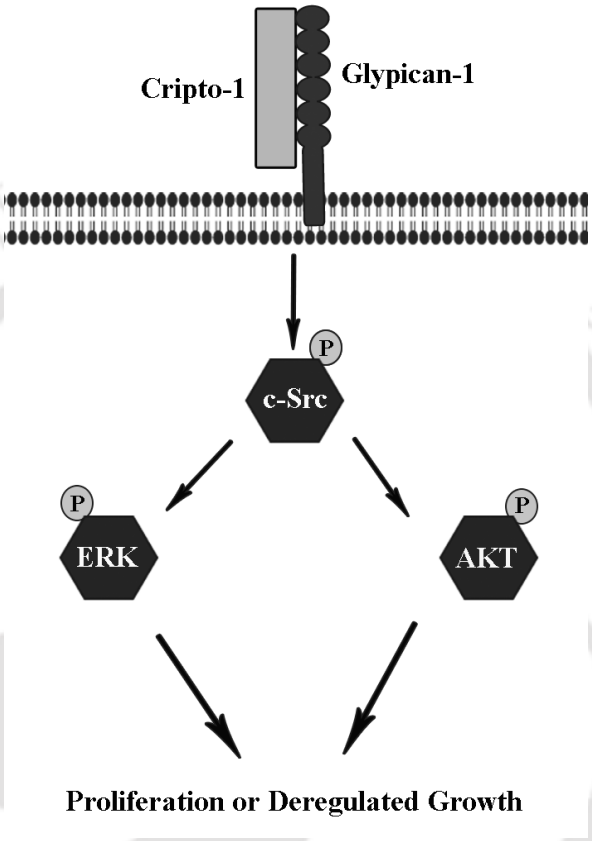

Figure 2.2. Cripto-1 activates MAPK and AKT signaling pathway. Cripto-1 binds with glypican-1, and activates c-Src which subsequently activates Erk1/2 and Akt. Activation of these two pathways eventually leads to cell proliferation through modulation of molecules involved in cell cycle progression.

CR-1 in TGF-β signaling pathway:

TGF-β signaling controls a plethora of cellular responses. TGF-β binds to two different serine/threonine kinase receptors, i.e. type I and type II receptors. Upon ligand binding, type I receptors specifically activate intracellular Smad proteins, which in turn regulate the expression of target gene and control the cell growth [57]. CR-1 inhibits the function of TGF-β. CR-1 binds TGF-β, thereby blocks its association with its type I receptor, TβRI. *In vitro* experiments have shown that CR-1 mediated inhibition of TGF-β leads to reduced phosphorylation of downstream signaling molecule Smad2 and induced growth of TGF-β dependent cells [58]. Recently, Shani *et. al* have shown that glucose regulated protein 78 (GRP78) associates with CR-1 to block TGF-β signaling [59].

Nodal/ALK4/ALK7/Smad-2 signaling pathway:

CR-1 mediated Nodal/ALK4/Smad-2 signaling pathway is mainly involved in embryonic development. CR-1 is known to be a co-receptor for Nodal, a ligand of the transforming growth factor beta (TGF-β) family. Similar to other ligands of the TGF-β family, including activin and bone morphogenetic proteins (BMPs), Nodal signals through transmembrane serine/threonine kinase receptor [60]. Nodal signaling utilizes the type I activin receptor ActRIB (ALK4) and the type II receptors, ActRIIA and ActRIIB, leading to phosphorylation and nuclear accumulation of the cytoplasmic signal transducers Smad2 and/or Smad3 together with Smad4 [61]. The activated Smad complex interacts with nuclear transcription factors, like transcription factors of the FAST subfamily, to induce gene expression [19]. Mutational studies have shown that CR-1 binds to Nodal through its EGF domain and the CFC domain of CR-1 is responsible for binding to ALK4 (ActRIB) [13, 62]. Membrane bound CR-1 recruits Nodal to an Activin receptor complex composed of ActRIB (ALK4) and ActRIIB [51, 63]. CR-1 can also directly interact with another serine/threonine kinase orphan receptor ALK7 enhancing the ability of ALK7 to respond to Nodal [64]. The Nodal/ALK4/ALK7/Smad-2 pathway of CR-1 is briefly described in Figure 2.3.Several findings suggest that in addition to activation of Nodal/ALK4/ALK7/Smad-2 and Glypican-1/c-Src/MAPK/Akt pathways, CR-1 signaling can also cross talk with wnt/β-catenin/Lef-1 signaling pathway. In fact, CR-1 has been identified as a primary target gene in the wnt/β-catenin signaling pathway during embryonic development [42, 65].

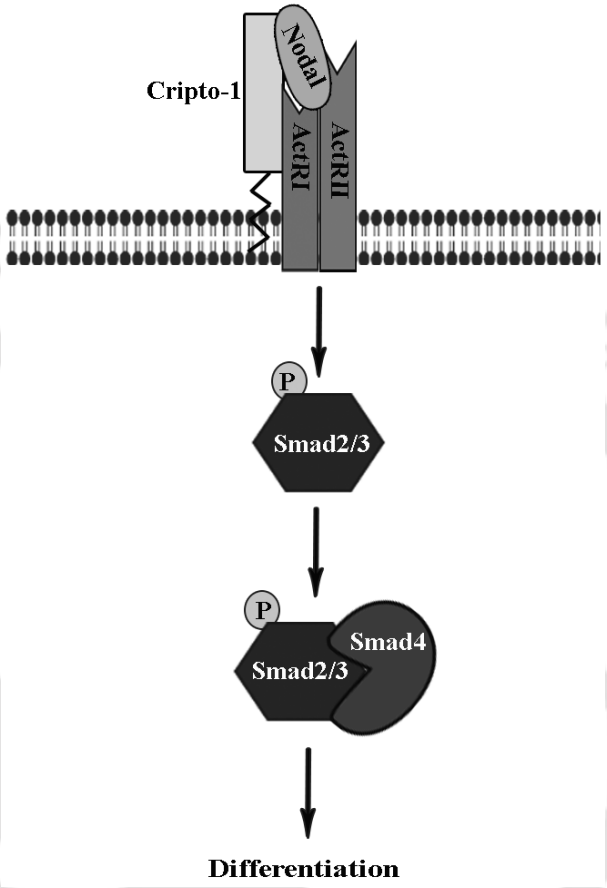

Figure 2.3 Cripto-1 activates Smad-2/3 signaling pathway. Cripto-1 acts as co-receptor in this signaling pathway. Cripto-1 binds to Nodal through its EGF domain and recruits Nodal to type I activin receptor ActRIB (ALK4). Binding of Nodal to the receptor activates Smad2/3 pathway.

Human CR-1 as a Therapeutic Target:

As it has been shown that CR-1 has a potential role in oncogenesis, it is considered as a suitable target for cancer therapeutics. Adkins *et.* al [66] developed a mouse monoclonal antibody (IgG) against the CFC domain of CR-1. This monoclonal inhibits Cripto-Nodal signaling and Cripto-Activin interaction, thereby arresting the growth of tumor cells in mouse xenograft models *in vivo*. Xing *et. al* [67] developed a rat antibody (IgM) which binds to the EGF-like domain of human CR-1. This monoclonal antibody inhibits growth of cancer cells *in vitro* and with greater effect in combination with cytotoxic drugs like 5-fluorouracil, epirubicin and cisplatin. In addition, this antibody prevents tumor development *in vivo*, inhibits growth of established tumors in mice with colon xenografts and induces apoptosis.

Complexity in signaling networks of growth factors:

Normal growth and development require a proper balance between cell proliferation and cell death. Perturbation of this balance, such as increased cellular proliferation, can lead to the development of pathological conditions such as hyperplasia and eventually cancer. Conversely, reduced proliferation or elevated cell death can result in loss of specific cell populations leading to development of degenerative diseases [68]. Control of the cellular balance is achieved by extraordinary complex signaling networks involving extracellular signaling molecules like growth factors.

Growth factors serve diverse functions in a cell. They promote proliferation, differentiation and survival of cells [69]. Each of these processes is tightly controlled and functions even in a noisy cellular environment. Processes like cell proliferation are usually controlled by more than one signaling molecule. Each of these molecules interacts with their cognate receptors thereby triggering a cascade of molecular reactions and processes within the cell that eventually leads to a particular cellular function. Such cascade of events constitutes signal transduction pathways, working as channels of cellular information transfer. However, growth factor driven cellular signaling pathways are not isolated from each other but are interconnected to form complex signaling networks. Cells receive information through multiple signal transduction pathways. They must then integrate this information to achieve a cellular function [70-72]. Therefore, the primary complexity in signaling networks originates

from involvement and integration of multiple pathways. Such complexity is critical for control and robustness of cellular response and also responsible for contextual response. A signaling network with linear cascade of events without any interactions with other pathways will work like an all or null system: the external signal will trigger a cellular process when all the components of the pathway are present and would fail in absence of even one component. However, interaction of multiple pathways allows transfer of information even when one or more component is absent [73]. As the expression of various signaling molecules varies contextually, a growth factor can also have contextual effect. Integration of multiple extracellular signals also gives rise to contextuality.

A typical example of contextual effect of a growth factor is TGF-β signaling. It activates MAPK pathway that induces cell proliferations [74]. On the other hand, it can activate Smad signaling which induces transcription of the cell cycle inhibitory molecules like p21 resulting in the suppression of cell growth [75, 76]. Therefore the relative strength of these two pathways in a particular cell would decide the effect of TGF-β, either enhanced cell proliferation or retardation of proliferation. Such contextual effect of TGF-β is well documented [77]. The signaling pathways of TGF-β have extensive cross-talks with pathways of other signaling molecules. Such cross-talk often leads to contextual effect of TGF-β. For instance, TGF-β is known to synergize with platelet-derived growth factor to stimulate colony formation of 3T3 fibroblast cells, but inhibits the colony formation induced by epidermal growth factor [78].

Another well known example of such contextual behavior is Epidermal growth factor (EGF). EGF stimulates growth of a wide variety of normal and malignant cells [79] and in many cases EGF prevents cell death [80, 81]. In contrast, EGF is also known to induce apoptosis in several cell lines overexpressing the EGF receptor (EGFR) [79, 82-85], suggesting a relationship between EGF receptor expression and EGF-induced cell fate. A low level of EGFR expression is associated with growth stimulation by EGF, whereas a high level of receptor expression correlates with growth inhibition and cell death [86].

Association of growth factor with two different types of receptors often results in two opposite types of cellular responses. For example, Nerve Growth Factor (NGF) binds to two classes of receptors: the p75 LNGFR (“low-affinity nerve growth factor

receptor") and TrkA (high-affinity tyrosine kinase receptor), a transmembrane tyrosine kinase [87]. NGF induces apoptosis in cells which express the low-affinity receptor (p75LNGFR) [88-90]. On the other hand, binding of NGF to high-affinity (trk) receptors promotes cell survival, induces cell proliferation and differentiation [91, 92]. Binding to two different types of receptors generates opposing signaling cascades whose relative strength ultimately decides the fate of the cell [92].

Cripto-1 signals through multiple signaling pathways, namely Smad, MAPK, PI3K/Akt pathways, leading to cell survival, proliferation and differentiation. Signaling through several extracellular cues converges on Smad, MAPK and PI3k/akt pathways. Therefore, existence of cross-talks between CR-1 and other growth factors is obvious. CR-1 works as a modulator of signaling by TGF-β ligands and has a modified EGF-like domain. As discussed earlier, TGF-β and EGF show contextual effects. Therefore one can expect that CR-1 may also have contextual effect. Still, the existing literature does not emphasize on the contextual effect of CR-1. The pro-proliferative signaling of CR-1 is extensively investigated and is well documented. However, there are only two reports that indicate that CR-1 can have contextual effect. De Santis *et al.* [23] have shown that at lower concentration CR-1 induces proliferation in mouse mammary epithelial cell HC-11 but at higher dose it marginally reduces proliferation giving rise to a biphasic dose-dependent effect. However, the origin and consequence of such biphasic effect have not been investigated. Similar dose-dependent biphasic effect on cell proliferation has been observed with TGF-β as well as with EGF [93, 94]. Presence of low and high-affinity receptor-ligand interactions activating different signaling pathways can lead to such biphasic effect [94]. In another work, De Santis *et al.* have shown that treatment with CR-1 induces apoptosis in HC-11 cells in low serum condition in absence of EGF and insulin [95]. EGF and insulin are survival factors for HC-11 cells and absence of these two makes this cell sensitive to apoptosis [96]. Such contextual effect may have implications in normal physiological role of CR-1. The dose-dependent biphasic effect may be a mechanism to control CR-1 signaling through self-attenuation. On the other hand, induction of apoptosis in absence of EGF and Insulin indicates that signaling of CR-1 has cross-talks with other growth factors. Such cross-talks and dependence, can give rise to cell-specific/temporal variation in effect of CR-1.

The biphasic effect of CR-1, as observed by De Santis *et al.* [23], also raises questions about the control mechanism of CR-1 signaling. Being a modulator of differentiation and proliferation, the signaling network CR-1 should have inbuilt mechanisms to tightly control the dynamics of signaling. Dynamics of signaling networks can determine the fate of a cell. It is often observed that transient activation of a mitogenic pathway triggers cell proliferation, while sustained activation leads to cellular differentiation [97]. The architecture of a signaling network determines its dynamics. The complexity in dynamics originates from non-linear network motifs like feed-forward and feedback motifs. While feed-forward network motifs are crucial for signal amplification, feedback loops act as pulse generators, signal attenuators and help to make the system robust [98-100]. Mitogenic pathways like Erk1/2 MAPK and PI3K/Akt pathways are tightly controlled by several feedback loops [101-103]. Though CR-1 acts through these two pathways, effect of such feedback mechanisms on CR-1 signaling has not been investigated. As the cardinal paths of CR-1 signaling are already identified, it is high time for us to look into the issues of network architecture, cross-talks and dynamics of CR-1 signaling. That would eventually help us to understand the role of this molecule in growth and development as well as in diseases, with finer details.

3 Materials & Methods

Details of the common reagents used in this work along with their source are given in appendix.

Bacterial cell culture:

E. coli strains and clones were stored at -70 °C as glycerol stocks (20% glycerol) and were cultured in LB medium or 2xTY medium containing suitable antibiotics. *E. coli* strains used in this work and the composition of culture media are given in Table A2 and A3 respectively in the appendix.

Maintenance of mammalian cell lines:

Human cervical adenocarcinoma cell line HeLa, human glioblastoma cell line U87-MG, human breast cancer cell line MCF-7, human colon adenocarcinoma cell line HT29, and human embryonic kidney cell line HEK293, were procured from NCCS, Pune, India. They were maintained in DMEM (Gibco), with 10% Fetal bovine serum and 1X antibiotic–antimycotic (Gibco) at 37 °C with 5% CO_2, in a humidified incubator. Medium was replenished at intervals of 3 days. Cells were subcultered by trypsinization once they reached 80-90% confluence. After removal of medium, the monolayer of cells was washed with sterile PBS and 0.5 ml to 1 ml of Trypsin (0.25%) /EDTA (0.02%) was added to the flask and kept at 37 ^{0}C. After few minutes, trypsin was aspirated out of the flask and cells were flushed with the medium to make a uniform cell suspension. Around 30% of the cell suspension was transferred to a new flask having fresh growth media and cells were kept at 37 °C with 5% CO_2. Medium and other reagents used in mammalian cell culture are given in Table A4 and A5 in appendix.

Protein estimation:

The total protein content in a sample was estimated by either Bradford assay [104] or by Lowry's method [105]. Protein content was estimated by following the 96 well

plate assay format. BSA was used as protein standard. BSA was dissolved in same buffer system which was used during sample preparation.

Protein estimation by Bradford assay:

The protein sample which was dissolved in PBS, was estimated by Bradford assay. Bradford reagent was purchased from Sigma. As per the manufacturer protocol, 200 µl of protein sample was mixed with 200 µl Bradford Reagent and kept at room temperature for 15 min. After incubation, 200 µl of the reaction mixture of each sample was transferred to the 96 well plate and the optical density was measured at 595 nm.

Protein estimation by Lowry's method:

The protein sample which was isolated by RIPA buffer, was estimated according to the Lowry's method. 100 µl of diluted crude protein sample was mixed with 500 µl of freshly prepared complex forming reagent (2% Na_2CO_3 in 0.1 N NaOH : 1.0% $CuSO_4.5H_2O$: 2% potassium sodium tartrate ≡ 100:1:1). The reaction mixture was vortexed and incubated at room temperature for 10 min and 50 µl of freshly prepared diluted Folin reagent with distilled water (1:1) was added to the reaction mixture and vortexed for 5 s. This reaction mixture was incubated in the dark at room temperature for 30 min. After 30 min of incubation, 200 µl the reaction mixture of each sample was transferred to 96 well plate and the optical density was measured at 660 nm.

Quantification of DNA and RNA:

Quantities of DNA and RNA in samples were measured by spectrophotometry. Samples were diluted in water and optical densities were measured at 260 nm and at 280 nm. 1 O.D at 260 nm was considered to represent 40 µg/ml of RNA and 50 µg/ml of double stranded DNA. Concentrations of DNA and RNA samples were calculated from the optical densities by using suitable dilution factors.

Agarose gel electrophoresis:

DNA samples were resolved by agarose gel electrophoresis using agarose gel (0.8-1.5%, containing 0.5 µg/ml of ethidium bromide) in 1X TAE at 80 V until the desired resolution was achieved. The DNA fragments were visualized on a UV-Trans-Illuminator and imaged using gel documentation system (Gel logic 1500, Kodak).

Elution of DNA sample from agarose gel:

PCR amplified products, digested plasmids and inserts were eluted out of agarose gel by using QIAquick Gel Extraction Kit, as per manufacturer's protocol. For gel elution of DNA, required fragments were excised from the gel and stored at –20 °C for further use. 3 volumes of Buffer QG was added to 1 volume of gel (i.e. 300 µl for 100 mg of gel slice) and heated at 50 °C to melt and dissolve the gel. 1 gel volume of isopropanol was added to the sample and mixed. A QIAquick spin column was placed in a 2 ml collection tube. 750 µl of sample was applied to the column to bind DNA, followed by centrifugation at maximum speed for 1 min. The flow through was discarded and 500 µl of QG buffer was added to the column. After centrifugation for 1 min, 0.75 µl of PE buffer was added to wash the column and centrifuged. Another hard spin was given for 1 min to remove residual traces of wash buffer. 50 µl of EB buffer (10 mM Tris-HCl, pH 8.5) or nuclease-free water was added to the column to elute out the DNA. After incubation for 3-4 min at room temperature, DNA was eluted out by centrifugation at maximum speed for 1 min. Eluted DNA was stored at -20 °C for further use.

Plasmid DNA Isolation (Mini-Prep Method):

Plasmid DNA was isolated from 3 ml of overnight cultures by alkaline lysis method [106]. Reagents used for plasmid isolation are given in Table A5 in appendix. A single *E.coli* colony carrying a recombinant plasmid was grown for 14-18 hr in LB medium containing specific antibiotic, at 37 °C with shaking at 180 rpm. The culture was harvested and the cells were resuspended in 100 µl of solution I. The cells were lysed with 200 µl of freshly prepared solution II. The contents were thoroughly but gently mixed by inversion of the tube. Bacterial genomic DNA and bacterial cell debris were differentially precipitated by adding 150 µl of ice cold solution III and incubating on ice for 5 min followed by centrifugation at 12000 g for 10 min at 4 °C. The supernatant was transferred to a fresh tube and equal volume of phenol/chloroform (1:1 v/v; here chloroform means chloroform/isoamylalcohol (24:1 v/v)) was added. The resulting mixture was mixed gently by inversion and the phases were separated by centrifugation at 12,000 g for 10 min at 4 °C. The aqueous phase was aspirated out in a fresh tube and 2 volumes of ethanol were added to precipitate the plasmid DNA. After incubation at room temperature for 10 min, plasmid DNA was precipitated by centrifugation at 12,000g for 10 min at 4 °C. The DNA pellet was washed with 70% ethanol, air-dried and resuspended in the required amount of nuclease-free water.

Polymerase Chain Reaction (PCR):

Taq DNA polymerase was used for all PCR reactions. 25-50 ng of DNA sample was used in 20 µl reaction mixture. The composition of reaction mix was as follows:

10x Assay buffer (10mM Tris-HCl (pH 9), 1.5mM MgCl2, 50mM KCl, 0.01% gelatin)	2.00 µl
dNTP (10mM each)	0.50 µl
Taq DNA polymerase (3U/µl)	0.33 µl
5'primer (20 pmole/µl)	1.00 µl
3'primer (20 pmole/µl)	1.00 µl
DNA	25.00 ng
Nuclease-free water to final volume	20.00 µl

PCR amplification was performed by thermal cycling. A typical thermal cycling involved initial denaturation for 5 min at 94°C, followed by 40 cycles as follows: 1min at 94°C, 1min at 60 °C, 1min at 72 °C and the final extension was performed for 10 min at 72 °C. Sequence of primers and reaction conditions used are given in appendix (Table A7).

Preparation of Competent Cells:

Competent *E. coli* cells were prepared by $CaCl_2$ method [1]. A single colony was inoculated in 5 ml LB media and incubated overnight at 37 °C under shaking condition. 500 µl of the primary culture was inoculated in 25 ml of LB media and grown till OD_{600} reached 0.4-0.5. The culture was kept on ice for 10 min and centrifuged at 3000 g for 10 min at 4 °C. The pellet was resuspended uniformly in 12.5 ml of ice-cold sterile 50 mM $CaCl_2$ and kept on ice for 45 min. The cells were harvested at 1000 g for 10 min at 4 °C and the pellet was resuspended in 2 ml chilled 50 mM $CaCl_2$. Sterile glycerol (20 % of final volume) was added to the cell suspension and aliquots of 200 µl each were made in sterile vials and stored at -70 °C for further use.

Transformation in bacterial cells:

Recombinant plasmids were transformed in chemically competent *E.coli* cells by heat shock method [106]. Plasmid/ligation mixtures (usually 10-20 µl) were mixed with 200 µl of competent cells and placed on ice for 45 min without any disturbances. The cells were subjected to heat shock at 42 °C in a water bath for 90 s and chilled on ice immediately afterwards. 800 µl of pre-warmed LB media was added and the cells were incubated for 1 hr at 37 °C with shaking. Cells were harvested by centrifugation at 3000 g for 10 min at 4 °C and resuspended in 100 µl of LB media. Resuspended cells were plated on TYA plates containing the appropriate antibiotic followed by incubation at 37 °C for 12-16 hr. Subsequently, the colonies were picked, grided on a TYA plate containing appropriate antibiotic and screened by colony PCR and restriction digestions.

Colony PCR to Screen the recombinant clones:

Clones obtained after transformation were screened for the insert by colony PCR analysis. Colony PCR was performed by inoculating a very small amount of bacterial colony in the sample mix for PCR. The PCR was performed just like other PCR reactions with an exception that the initial 5 min heating at 94 °C in hot start PCR was extended to 8 min to break bacterial cells. PCR products were resolved on agarose gel and analyzed. Recombinant clones were further analyzed by digestion with restriction endonucleases.

Digestion of DNA by Restriction Enzyme:

Plasmids or PCR amplified DNA fragments were subjected to digestion by restriction endonuclease. An aliquot of plasmid DNA (~2 µg) was digested overnight with the required amount of restriction endonuclease according to the conditions specified by the manufacturer. The reaction was terminated by heating at 68 °C for 10 min. An aliquot was loaded on an agarose gel for analysis and resolved by electrophoresis. Whenever needed, RNase (0.25µl/20µl reaction) was added to the reaction mix to remove RNA.

Ligation reaction.

The restriction enzyme digested vector and insert were resolved by agarose gel electrophoresis and the digested DNA fragments were eluted out of the agarose gel by

QIAquick Gel Extraction Kit. The gel-eluted products were ligated using T4 DNA ligase. For ligation reaction, linearized vector and insert fragment were mixed in 1:3 molar ratios respectively and incubated with 1X ligation buffer and 2 units of T4 DNA ligase enzyme. The ligation reaction was carried out at 4 °C for 12-16 hr and terminated by incubating at 65 °C for 10 min.

Cloning of PCR amplified DNA fragments in T/A vector system:

PCR amplified DNA fragments were cloned in T/A cloning vector, pGEMT-easy (Promega) for sequencing and downstream processing. In brief, PCR amplified products were resolved by agarose gel electrophoresis and the correct DNA fragment was eluted out of the gel using QIAquick Gel Extraction Kit. Eluted DNA was cloned into the pGEMT-easy vector as per manufacturer's protocol.

The ligation mix:

Insert DNA	25.0 ng
pGEMT-easy vector	50.0 ng
2x rapid ligation buffer	5.00 µl
T4 DNA ligase	1.00 µl
Nuclease-free water to final volume	10.0 µl

The reaction mix was incubated at 4 °C in ice-water bath overnight and the ligated mix was transformed in *E. coli* DH5α cells by standard chemical transformation method. Transformed cells were plated over TYA/Amp plate containing X-gal/IPTG. After overnight growth at 37 °C, white colonies were picked and checked by colony PCR. Plasmids were isolated from positive clones and digested with *EcoRI* and checked on agarose gel. Clones with proper insert were grown in LB media and stored at –70 °C with 20 % glycerol.

Sequencing of DNA fragments cloned in pGEMT - Easy:

PCR amplified products cloned in pGEMT – Easy were subjected for sequencing before further modification and cloning in expression vectors. Sequencing was done by dideoxy method using M13 universal primers. Sequencing was performed by Axygen.

Cloning of C-terminal truncated CR-1(CR-1-ΔC) into bacterial expression Vector:

C-terminal truncated CR-1 (corresponding to 1st - 169th amino acid) was amplified by PCR using human full-length CR-1 cDNA as a template. The cDNA was provided by Dr. D. S. Salomon, NIH, USA. The primer set which was used for amplification contain restriction enzyme sites for *BamHI* and *XhoI* at 5' and 3' end respectively (Appendix Table. A7). The PCR amplified CR-1-ΔC and bacterial expression vector pGEX-4T-2 (GE Healthcare) were double digested with *BamHI* and *XhoI* (NEB). Vector and insert were ligated in 3:1 molar ratio as described previously. An aliquot of this ligated product was subsequently used to transform in chemically competent *E. coli* DH5α using the heat shock method mentioned earlier. Transformed cells were plated on TYA/Amp/Glu plate. After 16 hr of incubation at 37 °C, bacterial colonies were picked and grided in another TYA/Amp/Glu plate and clones were checked by colony PCR. Clones containing the recombinant CR-1 were further confirmed by restriction digestion and stored as glycerol stocks at -70 °C. The recombinant pGEX-CR-1-ΔC construct or empty vector pGEX-4T-2, were further transformed to *E.coli* BL21 or *E. coli* Rosetta-gami-2(DE3) for protein expression.

Expression of GST tag CR-1 (CR1-GST) in *E.coli* BL21:

A single colony of *E. coli* BL21, carrying the recombinant pGEX-CR-1-ΔC construct or empty vector pGEX-4T-2, was inoculated in 5 ml 2xTY medium containing ampicillin (100 µg/ml) and 1% glucose. This was incubated with shaking at 30 °C for overnight. 500 µl of this overnight culture was subcultured into 50 ml 2xTY medium containing the same concentration of ampicillin and incubated with shaking (250 rpm) at 30 °C till OD_{600} reached ~ 0.5. Expression of the recombinant protein was induced by IPTG (0.5 mM) for 4 hr at 30 °C with shaking. Cells were harvested by centrifugation, and washed with 6 ml of STE buffer (Appendix Table A5). Cells were again resuspended in 3 ml of ice cold STE containing lysozyme (100 µg/ml) and incubated on ice for 15 min. DTT and sodium lauroyl sarcosine were added to final concentration of 5 mM and 1.5% to the mixture respectively. After vortexing for 5 s, cell lysate was sonicated for 6 cycles each of 10 s, at 25% amplitude. Homogenate formed after sonication was clarified by centrifugation for 10 min at 11,000 g, 4 °C. The supernatant was collected and mixed with Triton-X-100 to the final concentration of 2%. Then the supernatant was incubated for 30 min at 4 °C and stored at -20 °C.

Expression of GST tag CR-1 (CR1-GST) in *E.coli* Rosetta-gami-2(DE3):

Single colony of *E. coli* Rosetta-gami-2(DE3), carrying the recombinant pGEX-CR-1-ΔC construct or empty vector pGEX-4T-2, was inoculated in 5 ml 2xTY medium containing, tetracycline (12 µg /ml), chloramphenicol (25 µg/ml) ampicillin (50 µg/ml) and 1% glucose. This was incubated with shaking at 30 °C for overnight. 500 µl of this overnight culture was subcultured into 50 ml 2xTY medium containing same concentration of chloramphenicol, ampicillin and incubated with shaking (250 rpm) at 30 °C till OD_{600} reached ~ 0.5. Expression of the recombinant protein was induced by IPTG (0.5 mM) for 4 hr at 30 °C with shaking. Cells were harvested by centrifugation, washed and resuspended in ice cold PBS containing 1 mM EDTA, followed by lysing with mechanical cell disruptor (Constant Systems, UK) at 14×10^7 Pa. The cell homogenate formed after disruption was immediately mixed with PMSF (1 mM). To solubilize the insoluble protein Triton-X-100 (1%) was added to the cell homogenate and incubated on ice for 30 min. Cell lysate was clarified by centrifugation for 10 min at 11,000 g, 4 °C. The supernatant was collected and stored at -20 °C.

Purification of GST tag CR-1 (CR1-GST):

The supernatant which contained the recombinant fusion protein CR1-GST or GST, was purified using Glutathione–Agarose beads (Sigma) as per the manufacturer's protocol. In brief, clarified cell lysate was mixed with Glutathione–Agarose beads and shaken for 1 hr at room temperature, and then the column was washed with 5 volume of PBST and 2 volume of PBS. Bound protein was eluted using 20 mM GSH in 50 mM Tris–HCl, pH 8.0. Purified protein was dialyzed for 8 hr against PBS at 4 °C to remove residual GSH. Concentration of recombinant protein was estimated by Bradford assay.

Sodium dodecyl sulfate polyacrylamide gel electrophoresis (SDS-PAGE) of protein:

SDS-PAGE was performed to analyze the expression of recombinant proteins and western blot. Required amount of purified protein or cell lysates were mixed with 4x SDS-PAGE gel loading buffer with reducing agent (2-mercaptoethanol) and heated in boiling water bath for 3 min. The denatured protein samples along with standard SDS-PAGE protein markers were subjected to SDS-PAGE following the method of Laemmli [107]. The electrophoresis was carried out using 5 % stacking and 12 %

separating gels of thickness 0.75 mm at constant 20 mA and 30 mA current for stacking and separating gel, respectively, in a MiniVE vertical electrophoresis system (G.E Healthcare). After the completion of electrophoresis, the gels were stained with the coomassie brilliant blue or silver staining method (Appendix. Table A5).

Western blot:

Western blot was performed to analyze the recombinant protein expression in mammalian and in bacterial system as well as to study the expression level of cell signaling molecules. Concentrated cell extract was resolved on a 12 % SDS -PAGE and subsequently electro blotted on PVDF membrane for 4 hr using semi-dry Trans-Blot apparatus with the buffer system recommended by the manufacturer (G.E Healthcare). Transfer of proteins on membrane was confirmed by Ponceau S staining. Membranes were washed with TBST to remove Ponceau S stain and then blocked with 5 % milk TBST or 5 % BSA TBST for 2 hr at room temperature. Membranes were exposed to particular dilution of primary antibody in 5 % BSA in TBST for 2 hr at room temperature or for over night at 4 °C. This was followed by incubation with appropriate secondary antibodies coupled with horse radish peroxidase (HRP) for 1 hr at room temperature. After washing the membranes three times with TBST for 10 min, blot was developed using chemiluminescence (Super Signal West Dura, Thermo Scientific) and imaged using gel documentation system (Gel logic 1500, Kodak). Details of reagents used are given in Table A5 and A6 in appendix.

Transfection and Generation of Stably Transfected Cell line:

All transfections in this study were done by Electroporation using ElectroSquarePorator ECM 830 (BTX, Harvard Apparatus) electroporator. Mammalian cells were detached by trypsinization and washed with DMEM containing 10 % FBS. Cell were again washed with DMEM containing 2.5 % FBS (without antibiotic) and resuspended in a density of $1x10^7$ cells/ml. 400 µl of cell suspension and 20 µg of purified recombinant plasmid were mixed and kept at room temperature for 5 min. Electroporation was done at 140 volt for 70 ms. After electroporation cells were resuspended in culture media (DMEM /10 % FBS / antibiotic) and seeded in 6 well plates. Cells were kept in CO_2 chamber at 37 °C for another 48 hr. Transfected cells were selected for stable transfectomas using G418 as selection marker. After 48 hr of transfection, medium was aspirated off and cells were replenished with DMEM /

10 % FBS having G418 (final concentration 800 µg/ml). Medium was replenished at 72 hr intervals. About 9-12 days after transfection, majority of cells started dying and drug resistant clones formed distinct colonies. Drug resistant clones were picked up using sterile cotton swabs and inoculated in new 6 well plates and maintained with medium having G418. After 3 days, culture supernatant was collected from each well and screened for expressed recombinant protein. Stable transfected cells were maintained in DMEM / 10 % FBS with G418 (400 µg/ml).

Protein Extraction from mammalian cells:

Isolation of total protein from mammalian cell lines was done using RIPA (Radioimmunoprecipitation assay) buffer (Appendix Table. A5). Media was discarded from culture plate and cells were washed with ice cold PBS to remove the residual media. Keeping the culture plate on ice, required amount of RIPA buffer containing the protease inhibitor PMSF (1 mM), phosphatase inhibitor sodium fluoride (50 mM) and sodium orthovanadate (1 mM) was added to the cells. After 5 min of incubation on ice, cells were scrapped and sonicated for 10s. Cell lysate was clarified by centrifugation for 10 min at 10,000 rpm, 4 °C. The supernatant was collected and mixed with required amount of SDS-PAGE sample loading buffer, boiled for 3 min at 100 °C and stored at -80 °C. Concentrations of proteins were estimated by Lowry's method.

Isolation of RNA from mammalian cell lines:

Total RNA was isolated from mammalian cell line for preparation of cDNA. RNase free materials were used for isolation of RNA and for all downstream processing. All plasticwares including micropipette tips and centrifuge tubes were treated by 0.1 % DEPC for 2 hr at 37 °C, followed by removal of DEPC by autoclaving. Total RNA was extracted by TRI reagent (Sigma). 1 ml of TRI reagent was used to isolate RNA from 5-7 x 10^6 cells in 25 cm^2 culture flasks. RNA was isolated according to the manufacturer's protocol. After addition of the reagent on monolayer of cell, the cell lysate was passed several times through a syringe to form a homogenous lysate. To ensure complete dissociation of nucleoprotein complexes, samples were allowed to stand for 5 min at room temperature. Then 0.2 ml of chloroform per ml of TRI Reagent was added. After 30-60 s of vigorous shaking samples were allowed to stand for 10 min at room temperature. Resulting mixture was centrifuged at 12,000 *g* for 15

min at 4 °C. The aqueous phase having RNA was transferred to a fresh tube and 0.5 ml of isopropanol per ml of TRI Reagent was added to precipitate the RNA. After incubation at room temperature for 10 min with occasional mixing by inversion, the sample was centrifuged at 12,000g for 10 min at 4 °C. The supernatant was removed and the RNA pellet was washed with 1ml of 75 % chilled ethanol and re-centrifuged at 12,000 g for 10 min at 4 °C. The RNA pellet in ethanol was either stored at –70 °C for long-term storage or the RNA pellet was air-dried and was dissolved in suitable amount of sterile water and stored at –20 °C for immediate use.

Removal of Genomic DNA contamination from RNA:

To remove the genomic DNA contamination, each RNA sample was treated with RNase-free DNase (Promega) according to the manufacturer's protocol with some modification. The composition of reaction mix was as follows:

RNA	5.00 µg
RNase-Free DNase 10X Reaction Buffer	5.00 µl
RNase-Free DNase (1,000 U/ml)	5.00 µl
Nuclease-free water to final volume	50.0 µl

The reaction mixture was incubated at 37 °C for 45 min. Subsequently, RNA was re-extracted from the mixture by TRI reagent following the same protocol described in previous section. DNA free RNA samples were dissolved in nuclease-free water and estimated by spectrophotometer for cDNA synthesis.

Reverse transcription for cDNA synthesis:

Around 1µg of total RNA was used for reverse transcription using H Minus reverse transcriptase (RT) (Fermentas) and random hexamer. For a 20 µl of reaction mix, following protocol was followed:

A sample mix was prepared:

RNA	1.00 µg
Random Hexamer (100 pmol/ µl)	1.00 µl
Nuclease-free water to final volume	10.00 µl

The sample mix was incubated at 65 °C for 5 min to break RNA secondary structures and immediately chilled on ice. 8 µl of reaction mix was added to the heat-treated sample mix. A reaction mix was prepared as:

5X Reaction Buffer RT	4.00 µl
dNTP mix (10mM each) (1mM final concentration)	2.00 µl
H Minus reverse transcriptase (200units/µl)	1.00 µl
Nuclease-free water	3.00 µl

Reverse transcription was carried out at 37 °C for 60 min. The reaction was stopped by heating at 70 °C for 10 min followed by chilling on ice. 1 µl of RT products were used as template for downstream PCR amplification steps.

Real-time PCR:

Expression level of mRNA was quantified by real-time PCR. ~10 µg of RNA equivalent cDNA and optimized concentration of gene specific primer were used in each reaction (Appendix Table. A7). SYBR green was used as the reporter dye (Power SYBR Green PCR Master mix, Applied Biosystem). A 20 µl reaction mix was prepared as

2X SYBR Green PCR Master Mix	10.0 µl
5'primer	1.00 µl
3'primer	1.00 µl
cDNA (10ng/5µl)	5.00 µl
Nuclease-free water	3.00 µl

All real-time PCRs were performed on 7500 Real-Time PCR System (Applied Biosystem). Absence of non-specific amplification was confirmed by melting curve, using the Applied Biosystems real-time PCR system software (Melting curve profile of amplicons of all primer sets used in this study are shown in appendix Figure A1 and A2). GAPDH, β-actin and PPIA were used as endogenous controls. Efficiency of each

reaction was calculated using LinRegPCR [108] and fold change in expression of target genes in comparison to the geometric mean of the three endogenous control genes was calculated by ΔΔCt method as used in REST [109].

MTT Assay:

To measure viability of cells at different experimental conditions MTT assay was used. MTT is a colorimetric assay that is based on the cleavage of the tetrazolium salt 3-[4,5-dimethylthiazol-2-yl]-2,5- diphenyl tetrazolium bromide or MTT to formazan by mitochondrial dehydrogenase in viable cells [110]. Cells were seeded in a 96 well plate at a concentration of 1 x 10^4 cell/well. After 24 hr of seeding, cells were treated as per the requirement. At specific time point 10 µl of MTT (Himedia) solution (5 mg / ml in PBS) was added to each well and incubated for 4 hr at 37 °C in a 5% CO_2 humidified incubator. The reaction product was quantified by measuring the optical density of the soluble formazan in DMSO at 550 nm and the background subtraction was done at 650 nm.

Trypan blue dye exclusion method:

This method was used to determine the number of viable cells present in a sample. Live cells exclude trypan blue due to intact cell membrane where as dead cells do not [111]. Cells were detached from the culture plate after certain time period by trypsinization to make the cell suspension. One part of 0.4% trypan blue (Gibco) was mixed with one part of cell suspension and allowed to incubate at room temperature for 2-3 min. 10 µl of mixture was put on hemocytometer and the live cells were counted under light microscope.

BrdU Cell proliferation ELISA:

BrdU (5'-bromo-2'-deoxyuridine) incorporation assay was used to detect the proliferation of cell. The protocol of *Huong et al* [112] was followed with some modification. 3 hr before the end of the culture period, BrdU was added (10^{-5} M final oncentration) (BD bioscience) to each well. At the end of the culture period, the cells were washed twice with PBS (200 µl/ well). After each wash step, the supernatant was carefully removed, leaving about 25-50 µl in each well. After the last wash step, the plate was dried under a dryer (15-30 min), and cells were fixed with 200 µl /well of ethanol for 10 min at RT and air dried. To denature the DNA, plate containing the ethanol fixed cells were incubated for 30 min at RT with 2 N HCl. To stop the

denaturation process, 100 µl 0.1 M $Na_2B_4O_7$ was added and incubated for 10 min. The plate was washed once with PBS. Following the denaturation step, the plate was blocked by 1% BSA in PBS and incubated for 1 hr at RT and then washed three times with PBST. Monoclonal anti-BrdU antibody (BD bioscience), l/200 diluted in PBST, was added and incubated for 1 hr at RT. The incubation with PBST alone instead of anti-BrdU antibody in PBST was used as a negative control for the ELISA. After washing for another four times with PBST, HRP conjugated anti-mouse antibody (Sigma) 1/1000 diluted in PBST was added and further incubated for 45 min at RT. The plate was washed again with PBST for four times and OPD based substrate solution (Appendix Table. A5) (100 µl/ well) was added. The reaction was stopped by adding 4 M H_2SO_4 (50 µl/ well) after 15 min. Absorbance was measured at 492 nm using microplate reader (Tecan, Infinite 200).

Carboxyfluorescein succinimidyl ester (CFSE) dyes dilution method:

Carboxyfluorescein succinimidyl ester (CFSE) assay was used to calculate the doubling time of cells. Cells were detached, pelleted and resuspended at concentration of 1 x 10^6/ml in 1 ml of PBS containing 5% serum. Cells were labeled by incubating with 5 µM CFDA-SE (Sigma) with slow shaking for 6 min. After staining, cells were washed three times with 10 ml of PBS containg 5% serum to remove the excess amount of CFSE dye. Subsequently, labeled cells were seeded in 96 well plates (~10^4 cells/well) and after 24 hr of seeding, cells were treated as specified in the results section. This time point was considered as the zero hour in our analysis. Untreated cells without staining were used as a negative control. After a specified duration of treatment, cells were harvested, washed, and analyzed by flow cytometry. FACSCalibur flow cytometer (BD Biosciences) was used for all flow cytometric analysis. Data was acquired using CellQuest software (BD Biosciences) and analyzed using WinMDI. Measurements for CFSE were made in FL-1 channel in log mode and data for 20,000 cells were collected in each case. As our cell populations were homogenous with unimodal CFSE fluorescence intensity histograms, we used a simplified model to calculate the average doubling time of a cell population. Assuming that all cells are dividing and there is no cell death during the period of our study, the mean doubling time, $\langle T_d \rangle = T/\log_2(\langle F_0 \rangle/\langle F_T \rangle)$; here, $\langle F_0 \rangle$ = geometric mean fluorescence intensity at zero hour and $\langle F_T \rangle$= geometric mean fluorescence intensity at T hr.

The derivation of the formula as follows,

Let , T_d = Mean doubling time of cell and T = Time required for n number of cell divisions.

So, $n = T/T_d$

Now, if initial mean fluorescence intensity is $<F_0>$,

Then mean fluorescence intensity after 1st cell cycle is $F_1 = \frac{< F_0 >}{2}$

Mean fluorescence intensity after 2nd cell cycle is $F_2 = \frac{< F_0 >}{2^2}$

Therefore, after nth cell cycle if the mean fluoresces intensity would be,

$$< F_T >= \frac{< F_0 >}{2^{\frac{T}{T_d}}}$$

$$\Rightarrow 2^{\frac{T}{T_d}} = \frac{< F_0 >}{< F_T >}$$

Taking $\log_2$ on both sides,

$$\log_2(2^{\frac{T}{T_d}}) = \log_2(\frac{< F_0 >}{< F_T >})$$

$$\Rightarrow \frac{T}{T_d}.\log_2 2 = \log_2(\frac{< F_0 >}{< F_T >})$$

$$\Rightarrow \frac{T}{T_d} = \log_2(\frac{< F_0 >}{< F_T >})$$

$$\Rightarrow T_d = \frac{T}{\log_2(\frac{< F_0 >}{< F_T >})}$$

Cell cycle analysis:

Flow cytometric analysis of cells stained with propidium iodide (PI) was used for cell cycle analysis. Cells were seeded in 6 well plates (~10^5 cells/well) and after 24 hr of seeding, cells were treated as per the requirement. At specified time point, cells were detached from the culture plate by trypsinization, harvested, fixed and stained with PI as per the protocol of Riccardi and Nicoletti [113]. In brief, after trypisinization, cells were harvested by centrifugation. Harvested cells were resuspended at a concentration of ≈1 x 10^6/ml in DMEM and pelleted down by centrigugation. Cells were washed by resuspending in ice-cold PBS and centrifuged. Finally the cells were resuspended in 500 µl of ice cold PBS. For fixing the cells, 4.5 ml of prechilled 70% ethanol was added to the resuspended cells slowly with intermittent vortexing and keeping the cells on ice. Fixed cells were stored at 4 °C for 48h. Cells were then re-pelleted and resuspended in 0.5 ml of PBS, 0.5 ml of DNA extraction buffer was added and incubated at room temperature for 5 min. Supernatant was removed by centrifugation and cells were resuspended in 1 ml of DNA staining solution (Appendix Table. A5). Cells were incubated at 4 ºC in DNA staining solution in dark for at least 1 h. Cell cycle profile analysis was performed on 20,000 cells on a FACSCalibur flow cytometer using the Cellquest analysis program (Becton Dickinson). All the centrifugation steps for cell cycle analysis were carried out at 400 g for 5 min at 4 ºC. Untreated cells without staining were taken as negative control. Cell cycle analysis was performed using Modfit LT (Verity Software). Fluorescence intensities of PI stained cells were measured in FL2 channel in log mode and doublet discrimination was achieved using FL2 as DDM parameter.

Detection of apoptosis:

Extent of apoptosis was estimated by flow cytometry using Annexin V-FITC Apoptosis Detection Kit I (BD Biosciences) as per the manufacturer's protocol. Briefly, cells were seeded in 6 well plates (~10^5 cells/well) and after 24 hour of seeding, specific treatment was given. At specified time point cells were detached from the culture plates by trypsinization and harvested by centrifugation at 400 g for 5 min at 4 ºC. Cells were washed in PBS and re-suspended in 100 µl of 1X Binding Buffer (provided by manufacturer). Cells were then stained with 5 µl Annexin V-FITC and 5 µl propidium iodide (PI) in the dark for 15 min at room temperature. After adding the 400 µl of 1X binding buffer to each tube samples were analyzed by flow

cytometry with a FACSCalibur instrument (Becton-Dickinson). Compensation and quadrants were set up using unstained cells, cells stained with Annexin V- FITC (no PI) and cells stained with PI (no Annexin V- FITC) as control. Fluorescence intensity of FITC and PI stained cells was measured in FL1 and FL3 channel in log mode, respectively. Data of each experiment was extracted using FlowPy (http://flowpy.wikidot.com/), analyzed with WinMDI and plotted using SigmaPlot.

Lactate dehydrogenase assay:

Lactate dehydrogenase (LDH) assays were performed by assessing LDH released into the media as a marker of necrosis. The assay was performed using LDH assay kit from Randox Laboratories, as per the manufacturer's protocol. This assay is based on conversion of pyruvate to L-lactate by LDH in presence of NADH which gets oxidized to NAD^+ [8]. In brief, cells were seeded in 96 well plates (~10^4 cells/well) and after 24 hr of seeding, cells were treated as specified in the results section. At specified time point, culture media was collected and cellular debris were removed by centrifugation at 1000 rpm at 4 °C. 40 µl of culture supernatant was mixed with 1 ml freshly prepared pyruvate solution having NADH and the optical density was measured immediately for next 3 min at 340 nm (Carry 100 Bio, Varian). LDH activity in each sample was calculated from the slope of the absorbance over this time period (-ΔA/min). Total LDH activity was measured in fresh cell lysates prepared by sonication on ice and this was used to calculate the percentage of LDH released into the medium in the samples. Cells lysed with 0.1% tween 20 was used as a positive control.

Data Analysis:

Two-way ANOVA or one-way ANOVA followed by pairwise multiple comparisons, was used depending upon the type of experiment. For real time PCR experiments, data of fold change in expression was analyzed using non-parametric Kruskal Wallis One Way Analysis of Variance on Ranks, followed by Dunnett's test for pair-wise comparisons. SigmaPlot (Systat Software, Inc), was used for all statistical analysis and to generate graphs. Means of multiple data points were plotted. Error bars represent standard deviations if not otherwise mentioned.

4 Results & Discussion

Human Cripto-1 binds to cell surface receptor glypican-1, leading to activation of MAPK and Akt pathways [18, 51, 53]. Activation of MAPK and Akt pathways results in cell proliferation. It is now well established that CR-1 induces cell proliferation when expressed inside a cell as well as when used as an exogenous growth factor [9, 58]. However, it has been reported that treatment with high dose of CR-1 shows slight growth inhibitory effect in HC-11 mammary epithelial cells [23]. Treatment with CR-1 can even trigger apoptosis in these cells, when maintained in absence of EGF and Insulin which are critical for viability of HC-11 cells [95]. Although growth inhibitory effect of human CR-1 has not been thoroughly investigated, these observations indicate that CR-1 may activate both pro- and anti-proliferative pathways in different cellular systems. As CR-1 induces proliferation primarily through glypican-1, we decided to use two different cellular systems to investigate the effect of CR-1 on cell proliferation: one which expresses glypican-1 and the other with comparatively lower expression of glypican-1. We expressed recombinant human CR-1 and then used the recombinant protein to investigate the effect of exogenous CR-1 in these cell lines.

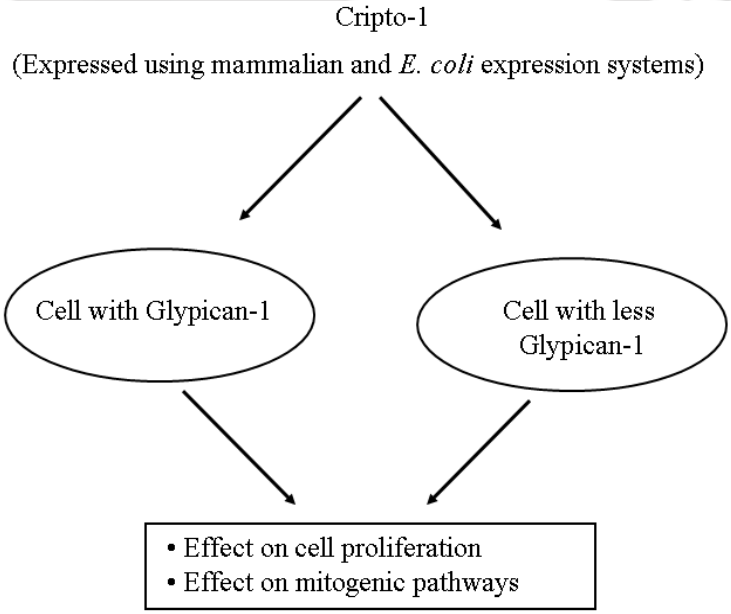

Expression of Recombinant Human Cripto-1:

Expression of Full-length CR-1 in mammalian system:

Full-length human CR-1 was overexpressed in MCF-7 cells. Human CR-1 cDNA cloned in pCI-neo vector and pCI-neo vector alone were electroporated into MCF-7 cells. The cDNA clone [54] was gifted by Dr. D. Salomon, NIH, USA. The design of the recombinant construct is shown in Figure 4.1a. Stably transfected clones were selected by G418 treatment. Subsequently, release of recombinant CR-1 into the culture media was detected by western blot (Figure 4.1b) using conditioned media (CM) of a selected clone. Five days old CM was used for all assays. Full-length CR-1 is 188 amino acids long protein and the theoretical molecular weight of this molecule is 21.1 kDa. However, CR-1 expressed in mammalian cells usually has higher molecular weight (ranging from 27 to 36 kDa) due to varying glycosylation [9]. As shown in Figure 4.1b, molecular weight of the CR-1 detected in the CM of the stably transfected clone is approximately 29 kDa. The CM of this clone was further used for functional assays.

Quantitative dose-dependent experiments can not be performed with crude conditioned media as other constituents are present in media. Moreover, purification of CR-1 from CM is difficult as quantity of CR-1 in CM is very less. Therefore we decided to produce purified CR-1 using E. *coli* expression system.

Expression of recombinant CR-1 in *E. coli*:

Hydrophobicity plot of human CR-1 shows that it has multiple hybrophobic regions (Figure 4.2a). The C-terminal end of CR-1 (170-188 amino acid residues) is essential for membrane anchorage by a glycosylphosphatydilinositol (GPI) and this part contains large number of hydrophobic amino acids. Expression of soluble human CR-1 in *E. coli* is challenging as presence of hydrophobic regions may reduce the solubility of the recombinant protein and may even cause misfolding in *E. coli*. Earlier, it has been shown that when expressed in *E. coli*, CR-1 accumulates in inclusion bodies and requires *in vitro* refolding [14]. To circumvent this problem, we have fused the protein to bulkier GST at the N-terminal and truncated the hydrophobic C-terminal GPI-anchor region. It is expected that folding of GST at N-terminal would help in folding of CR-1. It is known that C-terminal GPI-anchor region is not essential for CR-1 signaling [12, 114]. CR-1 expressed in human cells is a fucosylated protein. However,

it has been shown that fucosylation is not required for CR-1 signaling [13]. Additionally it has been shown that peptides corresponding to the EGF-CFC domain of CR-1 are functional [9, 12, 17, 18, 22, 23]. Therefore, it can be expected that GST-tagged C-terminal truncated CR-1 expressed in *E. coli* will be functional. Different forms of recombinant CR-1 those have been used by other research groups to investigate the mitogenic effect is shown in Table 4.1.

Our cloning strategy is shown in Figure 4.2b. DNA fragment corresponding to C-terminal truncated human CR-1 (1 – 169 amino acid residues) was amplified by PCR using pCI-neo-CR-1 construct as template (Figure 4.3a). This amplified fragment (CR-1-ΔC) was cloned in pGEX-4T-2 expression vector. The cloning was confirmed by colony PCR (Figure 4.3b) and restriction digestion (Figure 4.3c). Subsequently, the sequence of the insert in the selected clone was confirmed by DNA sequencing. It was confirmed that the sequence of the insert is in right frame with the GST sequence at N-terminal and is identical with the CR-1 sequence (from 385 to 891 base position of NCBI RefSeq: NM_003212.3) available in GenBank, NCBI. The annotated sequence is shown in Figure 4.4.

This recombinant construct was used for expression of the fusion protein in *E. coli* BL21 (DE3). When expressed in *E. coli* BL21, GST tagged CR-1 (CR1-GST) accumulated in inclusion bodies (Figure 4.5a and b). To resolve this problem, total cell extract was prepared by solubilizing the bacterial pellet in detergent (1.5% sodium lauroyl sarcosine and 2% Triton-X-100). This method improved the amount of CR1-GST in soluble fraction (Figure 4.5c). Subsequently, CR1-GST was purified by affinity chromatography using glutathione-agarose. But large amount of detergent present in cell extract led to low yield of purified CR1-GST after affinity purification (Figure 4.5d). On an average, the yield of purified CR1-GST was ~50 µg/L of culture.

Therefore, we changed our host strain to *E. coli* Rosetta-gami-2(DE3). This strain of *E. coli* allows disulfide bond formation in cytoplasm and is suitable for soluble expression of eukaryotic proteins which contain number of cysteine residues and generally go to the insoluble fraction when expressed in bacteria [115]. Using *E. coli* Rosetta-gami-2(DE3) we have successfully expressed CR1-GST in soluble form without using any detergent (Figure 4.6a) and this was purified from the cell lysate in

a single step using affinity chromatography (Figure 4.6b). The calculated molecular weight of this protein is ~44 kDa. The recombinant protein was characterized by SDS-PAGE (Figure 4.6b). The yield of purified recombinant CR1-GST was more when expressed in *E. coli* Rosetta-gami-2 and varied from 300 to 450 µg/L of culture. The recombinant CR1-GST was further characterized by Western Blot with anti-GST antibody (Figure 4.6c) and anti-CR-1 antibody (Figure 4.6d). Results of these Western blot experiments confirmed that the expressed CR-1 is fused with GST in correct reading frame. This recombinant CR1-GST expressed in *E. coli* Rosetta-gami-2 was further used for most of the functional studies.

Selection of suitable cellular system:

Glypican-1 is a cell surface receptor for CR-1. Binding of CR-1 to glypican-1 induces MAPK and AKT pathways that leads to the proliferation and metastasis [18, 42]. Therefore, presence of different amount of glypican-1 on cell surface is expected to affect the cellular response upon treatment with CR-1. RT-PCR was used to check the status of glypican-1 mRNA in four different cell lines (Figure 4.7a and b). Difference in mRNA expression level was further quantitatively estimated by real time PCR (Figure 4.7c and d). We observed that expression of glypican-1 is almost 10 times lower in HeLa cells in comparison to U-87 MG (Figure 4.7c). Subsequently, these two cells lines were used for comparative studies.

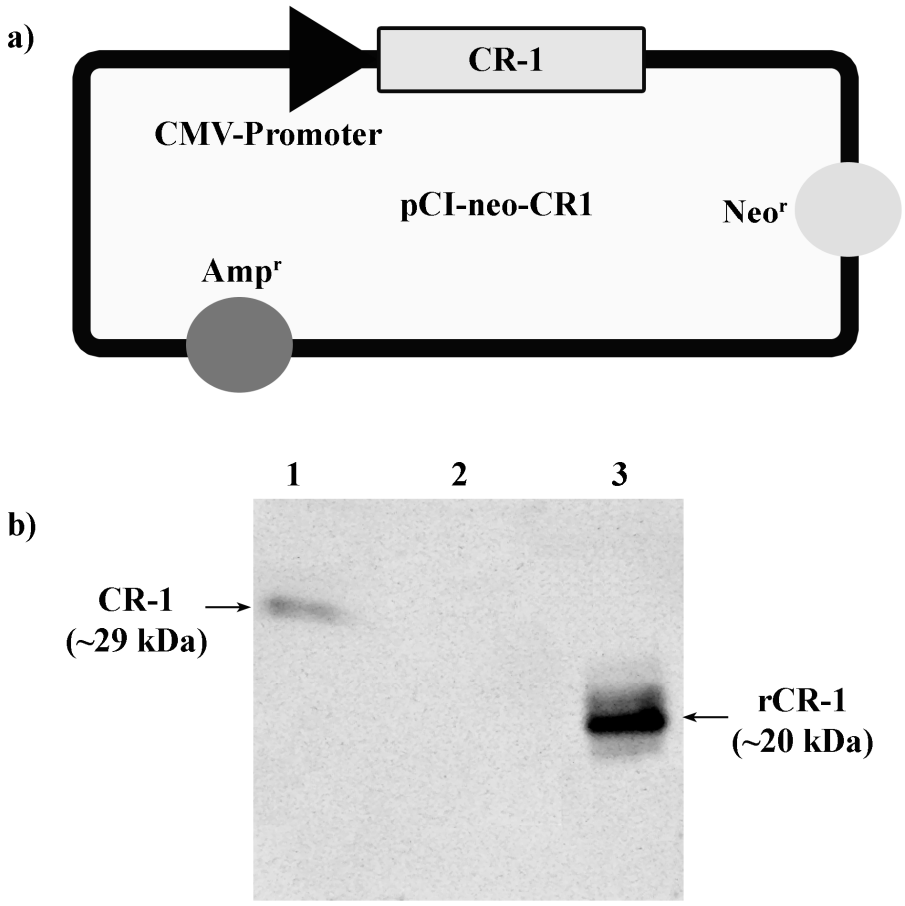

Figure 4.1 Expression of human CR-1 in MCF-7 cells. a) Vector construct of pCI-neo-CR1 transfected to MCF-7 cells. Full-length CR-1 was cloned at *EcoRI* site of pCI-neo Vector. Neo^r and Amp^r represent neomycin and ampicillin resistance gene b) Western blot to detect CR-1 in condition media (CM) of stably transfected MCF-7 cells, lane 1: CM of MCF-7 cells transfected with pCI-neo-CR-1, lane 2: CM of MCF-7 cells transfected with pCI-neo vector, lane 3: Purified C-terminal truncated CR-1 (rCR-1) expressed in insect cell line (R & D system). rCR-1 was used as a positive control in this experiment. In lane 1 and 2, 40 µl of CM and in lane 3, ~150 ng rCR-1 were loaded. Proteins were detected using anti-human CR-1 antibody.

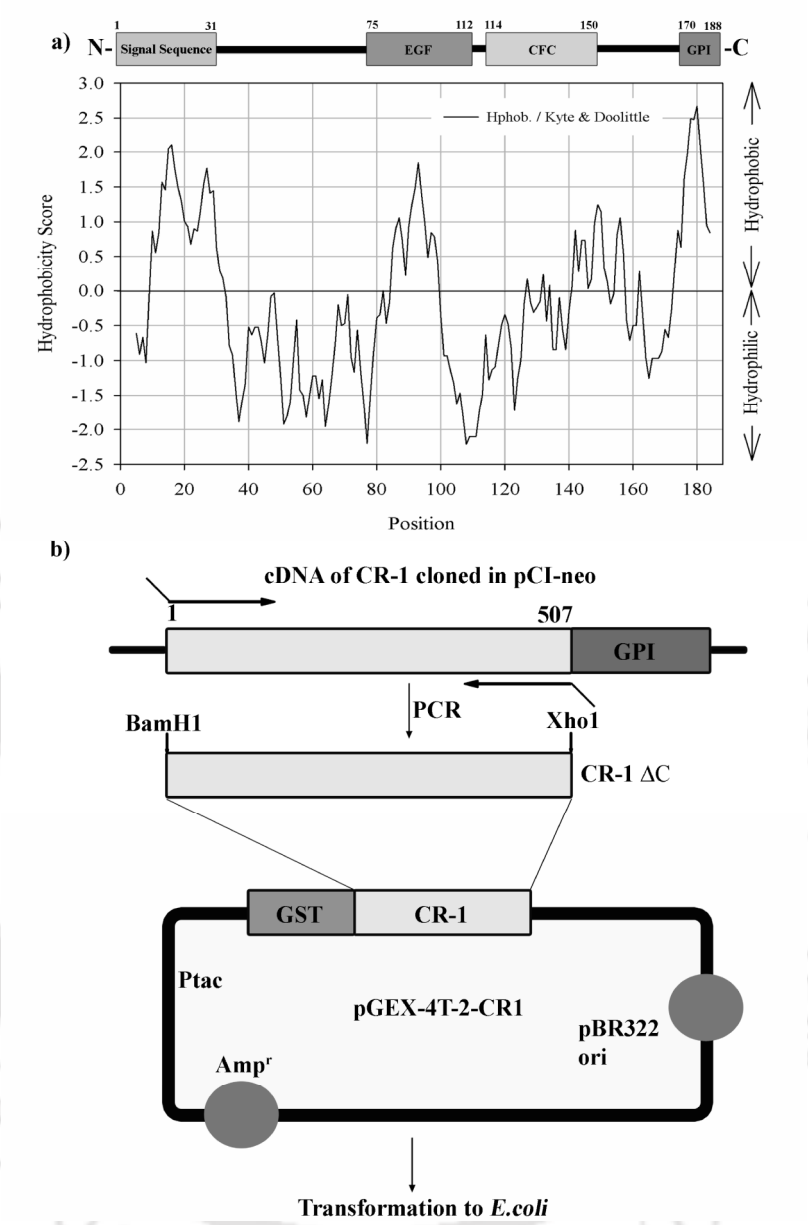

Figure 4.2 Strategy for cloning and expression of human CR-1 in *E.coli*. a) Hydropathy plot of amino acids sequence of CR-1 by using Kyte & Doolittle method. Region having score more than zero is hydrophobic. The C-terminal GPI anchor region has 8 hydrophobic amino acid residues. b) Plan for cloning of human CR-1 in pGEX-4T-2 bacterial expression vector. C-terminal truncated (corresponding to 1-169th amino acid) CR-1 was amplified by PCR using the primer set having *BamHI* and *XhoI* overhangs. Amplified product was cloned into pGEX-4T-2 expression vector at C-terminal end of GST. Amp^{r}: ampicillin resistance gene.

Table 4.1 Different forms of recombinant cripto-1 those can induce mitogenic pathways.

Form of CR-1	Expression system	Domains	Reference
Full length Glycosylated	Mammalian		[54]
Full length Non glycosylated	Mammalian		[13]
Full-length	Bacterial		[14]
GST-tagged EGF domain	Mammalian		[22]
Fc-tagged EGF domain	Mammalian		[17]
Refolded peptide	Synthetic		[23]

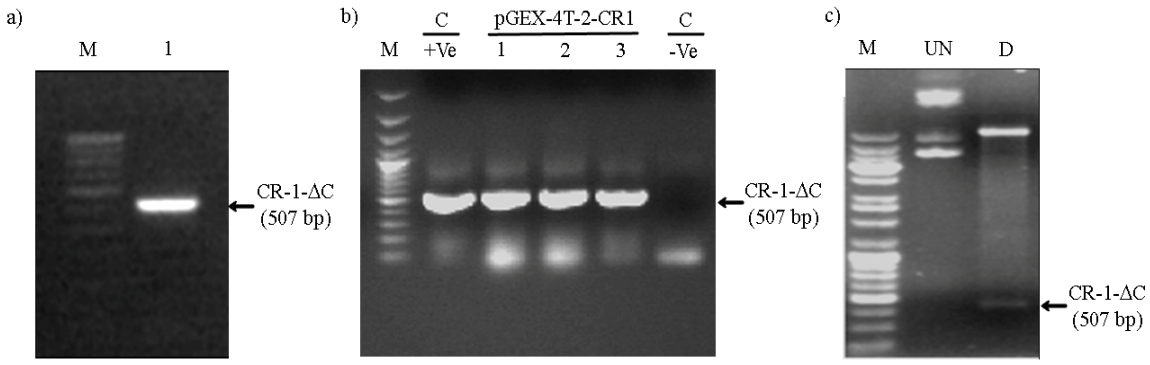

Figure 4.3 Cloning of C-terminal truncated CR-1 into pGEX-4T-2 vector. a) CR-1-ΔC was amplified by PCR using pCI-neo-CR1 as template. The amplified product was resolved in agarose gel. Amplified CR-1-ΔC is shown in lane 1. This amplified product was eluted out and cloned in pGEX-4T-2. b) Colony PCR was performed to screen clones. PCR was done by using CR-1 specific cloning primers. pCI-neo-CR1 clone was used as positive control. Lane 1, 2, and 3 are clones of pGEX-4T-2-CR1. C: control. c) Restriction digestion of one positive clone with *BamH1* and *XhoI*. Digested products were resolved in agarose gel. UN and D indicate undigested and digested plasmid respectively. Lane M: DNA molecular weight marker.

a)
ATGTCCCCTATACTAGGTTATTGGAAAATTAAGGGCCTTGTGCAACCCACTCGACTTCTTTTGGAATATCTT
GAAGAAAAATATGAAGAGCATTTGTATGAGCGCGATGAAGGTGATAAATGGCGAAACAAAAAGTTTGAAT
TGGGTTTGGAGTTTCCCAATCTTCCTTATTATATTGATGGTGATGTTAAATTAACACAGTCTATGGCCATCAT
ACGTTATATAGCTGACAAGCACAACATGTTGGGTGGTTGTCCAAAAGAGCGTGCAGAGATTTCAATGCTTG
AAGGAGCGGTTTTGGATATTAGATACGGTGTTTCGAGAATTGCATATAGTAAAGACTTTGAAACTCTCAAA
GTTGATTTTCTTAGCAAGCTACCTGAAATGCTGAAAATGTTCGAAGATCGTTTATGTCATAAAACATATTTA
AATGGTGATCATGTAACCCATCCTGACTTCATGTTGTATGACGCTCTTGATGTTGTTTTATACATGGACCCA
ATGTGCCTGGATGCGTTCCCAAAATTAGTTTGTTTTAAAAAACGTATTGAAGCTATCCCACAAATTGATAAG
TACTTGAAATCCAGCAAGTATATAGCATGGCCTTTGCAGGGCTGGCAAGCCACGTTTGGTGGTGGCGACC
ATCCTCCAAAATCGGATCTGGTTCCGCGTGGATCCATGGACTGCAGGAAGATGGCCCGCTTCTCTTACAGT
GTGATTTGGATCATGGCCATTTCTAAAGTCTTTGAACTGGGATTAGTTGCCGGGCTGGGCCATCAGGAATT
TGCTCGTCCATCTCGGGGATACCTGGCCTTCAGAGATGACAGCATTTGGCCCCAGGAGGAGCCTGCAATT
CGGCCTCGGTCTTCCCAGCGTGTGCCGCCCATGGGGATACAGCACAGTAAGGAGCTAAACAGAACCTGCT
GCCTGAATGGGGGAACCTGCATGCTGGGGTCCTTTTGTGCCTGCCCTCCCTCCTTCTACGGACGGAACTGT
GAGCACGATGTGCGCAAAGAGAACTGTGGGTCTGTGCCCCATGACACCTGGCTGCCCAAGAAGTGTTCCC
TGTGTAAATGCTGGCACGGTCAGCTCCGCTGCTTTCCTCAGGCATTTCTACCCGGCTGTGATGGCCTTGTG
ATGGATGAGCACCTCGTGGCTTCCAGGACTCCAGAACTACCACCGTCTGCTCGAGCGGCCGCATCGTGA

b)
MSPILGYWKIKGLVQPTRLLLEYLEEKYEEHLYERDEGDKWRNKKFELGLEFPNLPYYIDGDVKLTQSMAIIRYIA
DKHNMLGGCPKERAEISMLEGAVLDIRYGVSRIAYSKDFETLKVDFLSKLPEMLKMFEDRLCHKTYLNGDHVTH
PDFMLYDALDVVLYMDPMCLDAFPKLVCFKKRIEAIPQIDKYLKSSKYIAWPLQGWQATFGGGDHPPKSDLVPR
GSMDCRKMARFSYSVIWIMAISKVFELGLVAGLGHQEFARPSRGYLAFRDDSIWPQEEPAIRPRSSQRVPPMGI
QHSKELNRTCCLNGGTCMLGSFCACPPSFYGRNCEHDVRKENCGSVPHDTWLPKKCSLCKCWHGQLRCFPQ
AFLPGCDGLVMDEHLVASRTPELPPSARAAAS

Figure 4.4: Annotation of the sequence of CR1-GST. a) The DNA sequence. The blue region is the cloned C-terminal truncated CR-1 fragment. Underlined regions are *BamHI* and *XhoI* sites used for cloning. The green region represents GST sequence present in the vector itself. The pink region codes for the thrombin cleavage site present in the vector. The red colored codon is a stop codon. b) The amino acid sequence. Same color coding is used. The blue colored underlined region represents the EGF-CFC domain. The GST tagged CR-1 as shown here has 401 amino acids.

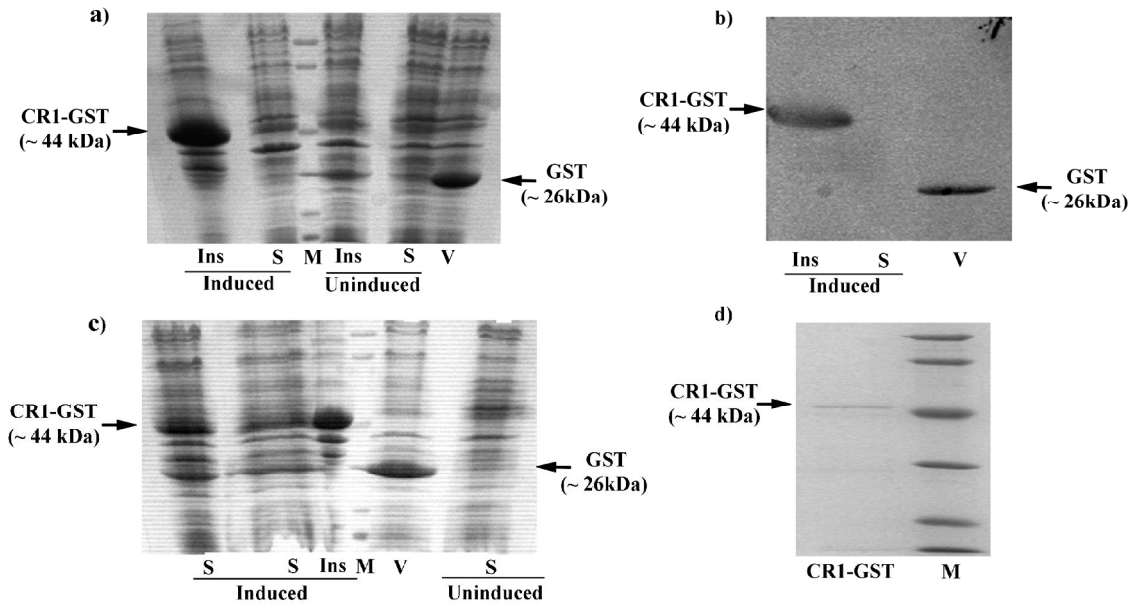

Figure 4.5 Expression of GST tagged CR-1 in E.coli BL21. a) SDS-PAGE to detect expression of CR1-GST. The clone having pGEX-4T-2-CR1 was induced at 30 ºC with 0.5 mM IPTG for 4 hr. Cells were lysed and centrifuged to remove insoluble cellular debris as a pellet. Proteins in clarified lysate (soluble fraction) and in pellet (insoluble fraction) were resolved by SDS-PAGE. CR1-GST accumulated in the insoluble fraction. (b) Western blot to detect CR1-GST in different fractions. The protein was detected by mouse anti-GST antibody, followed by anti-mouse HRP antibody. c) SDS-PAGE to detect CR1-GST after solubilization using detergents. Solubilization improved the amount of CR1-GST in soluble fraction. Soluble fractions of two different experiments are shown in the figure. d) SDS-PAGE to detect purified CR1-GST. 12% Polyacrylamide gels were used and gels were stained by coomassie brilliant blue. Ins: Insoluble fraction, S: Soluble fraction, V: Induced soluble fraction of a clone with pGEX-4T-2 vector only, M: Protein Molecular weight marker.

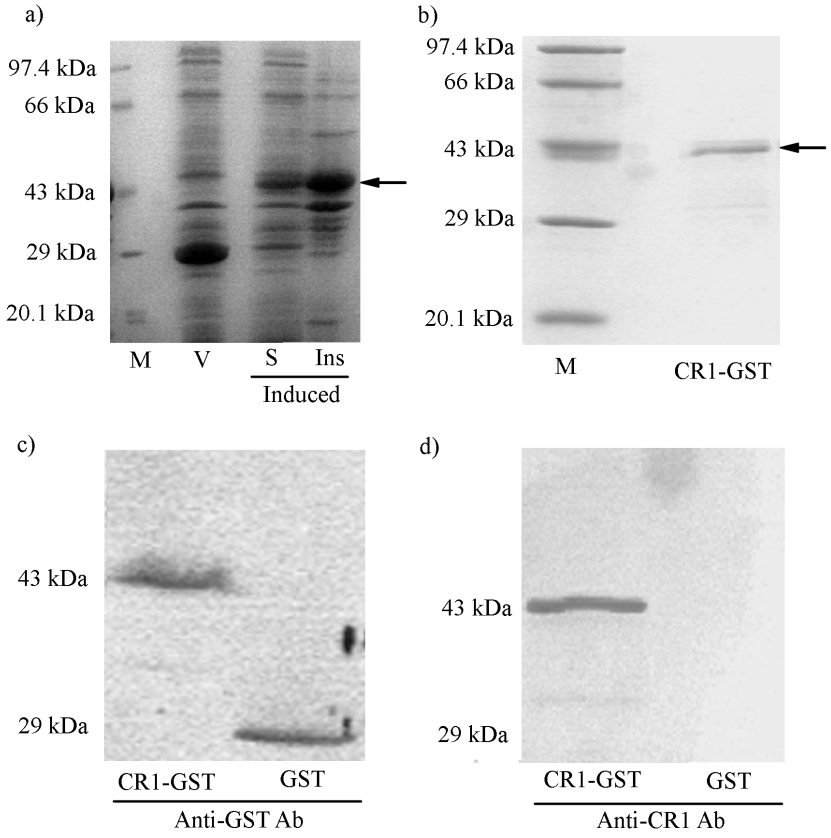

Figure 4.6 Purification and characterization of recombinant CR1-GST expressed in E. coli Resetta Gami-2(DE3): a) SDS-PAGE to detect expression of CR1-GST. When expressed in E. coli Rosetta-gami-2, CR1-GST was detected in soluble fraction. Ins: Insoluble fraction, S: Soluble fraction, V: Induced soluble fraction of a clone with pGEX-4T-2 vector only and M: Protein Molecular weight marker. The recombinant protein was purified by affinity chromatography using glutathione–agarose. The purified protein was characterized by SDS-PAGE (b) and Western Blots (c & d). In Western Blots, proteins were detected either by mouse anti-GST antibody (c) or mouse anti-CR-1 antibody (d), followed by anti-mouse HRP. Recombinant GST (26 kDa) expressed in E. coli Resetta-gami-2 using pGEX-4T-2 vector was used as a control. 12% Polyacrylamide gels were used and gels were stained by coomassie brilliant blue.

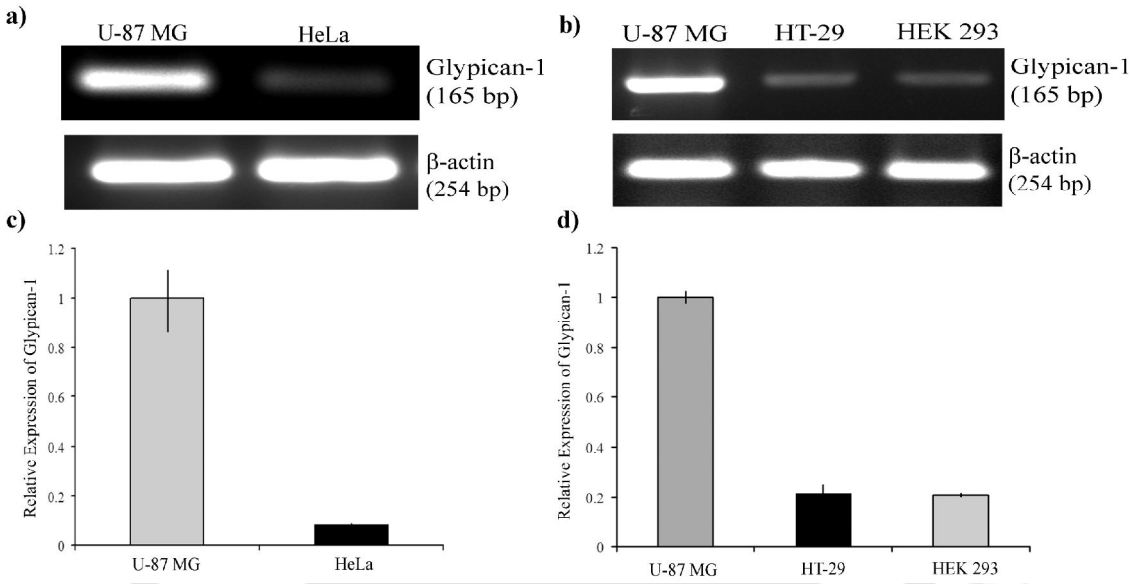

Figure 4.7 Expression of Glypican-1 in different human cell lines. a) and b) RT-PCR to detect expression of Glypican-1 in four different cell lines. β-actin was used as endogeneous control. c) and d) Real-time PCR was used to calculate relative expression of glypican-1 in these cell lines. GAPDH, β-actin and PPIA were used as endogenous controls for data normalization. Each bar represent mean of three data points. Error bars represent maximum and minimum values. Relative expression of Glypican-1 was significantly lower in HeLa, HT-29 and HEK 293 cells with respect to U-87 MG cells (Mann-Whitney Rank Sum Test, $p<0.05$).

Effect of CR-1 on proliferation of different cell lines:

Effect of conditioned media having CR-1:

To elucidate the effect of CR-1 on cell proliferation, U-87 MG and HeLa cells were treated with different dilutions of conditioned media (CM) of the clone expressing Full-length human CR-1. The treatment was done for 48 hr in serum free condition and subsequently MTT assay was used to measure the cell viability. Treatment with CM containing CR-1 induced proliferation of U-87 MG (Figure 4.8a). This confirmed that the CR-1 overexpressed in MCF-7 is mitogenic. However, higher amount of CM showed some inhibitory effect. Such biphasic effect of CR-1, with slight inhibitory effect only at higher concentration, has been earlier reported by De Santis *et al* [23]. In contrast to U-87 MG cells, treatment with the CM reduced viability of HeLa cells in a consistent dose-dependent fashion (Figure 4.8b). This study demonstrated that treatment with CR-1 has cell specific effect on cell proliferation. To further investigate this differential effect in a quantitative fashion, we have used purified recombinant CR-1 (CR1-GST) expressed in *E. coli* Rosetta-gami-2 in subsequent experiments.

Effect of recombinant CR1-GST expressed in *E. coli*:

To study the effect of CR-1 on different cell lines, purified, dialyzed and filter sterile CR1-GST was used. U-87 MG cells were treated with different dosage of CR1-GST. As shown in Figure 4.9, this recombinant protein increases viability of U-87 MG cells in a dose-dependent fashion with a biphasic effect, just like CR-1 overexpressed in MCF-7 cells. To understand the effect of CR1-GST on HeLa cells, HeLa cells were treated for 48 hr with different doses of CR1-GST in absence of serum and cell viability was measured using MTT assay. We observed that in contrast to U-87 MG cells, CR1-GST reduced the viability of HeLa cells in a dose-dependent fashion, without any biphasic effect (Figure 4.10a). Such monotonic decrease in cell viability was also observed when HeLa cells were treated in presence of serum (Figure 4.10b). Therefore, the results obtained with recombinant CR1-GST are consistant with those obtained with conditioned media having full-length CR-1.

The MTT assay depends upon the metabolic activity of a cell. So the observation of MTT based cell viability assay in HeLa cells was further confirmed by counting viable cells by trypan blue dye exclusion assay. HeLa cells were treated with 200 ng/ml CR1-GST for 72 hr and viable cells were counted under light microscope. As shown in

Figure 4.10c, it was observed that treatment with CR1-GST reduced viability of HeLa cells. The anti-proliferative effect of recombinant CR-1 on HeLa cells was further confirmed by BrdU incorporation assay. In this assay, cells are pulsed with BrdU. BrdU gets incorporated in newly synthesized DNA in replicating cells. Incorporated BrdU is measured by ELISA to estimate the extent of cell proliferation. As shown in Figure 4.11, treatment with CR1-GST (200ng/ml) reduces proliferation of HeLa cells in a time-dependent fashion.

We have observed the anti-proliferative effect of CR-1 in HeLa cells, both in absence and in presence of serum. Such monotonic anti-proliferative effect of CR1 has never been reported. To re-confirm this anti-proliferative effect, we treated HeLa cells with recombinant CR-1 (rCR-1) procured from R&D Systems. This rCR-1 is expressed in an insect cell line and contains 23-172 residues of human CR-1. As shown in Figure 4.12, rCR-1 also reduced the viability of HeLa cells in a dose-dependent fashion. The consistent anti-proliferative effect observed using three different recombinant proteins confirmed that the anti-proliferative effect of CR-1 is not an artifact arising due to expression of the protein in a particular form using a particular expression system. Rather, these observations confirmed that CR-1 can reduce cell proliferation in a context dependent fashion and HeLa cells treated with CR1-GST can be used to investigate the anti-proliferative pathway.

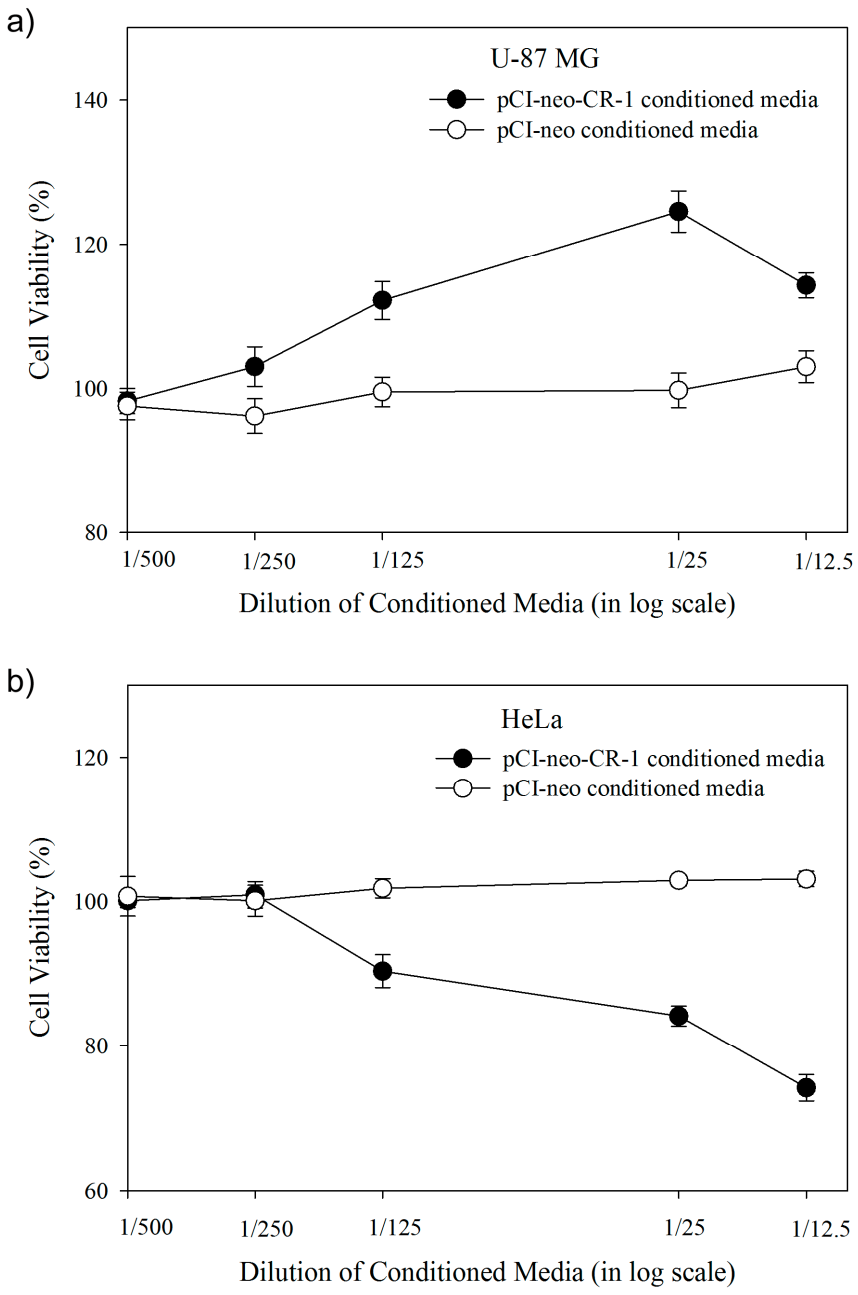

Figure 4.8 Differential effect of CR-1 on viability of a) U87 MG cells and b) HeLa cells. Viability of cells was measured by MTT assays after 48 hr treatment in absence of serum with different dilutions of CM of MCF cells transfected with pCI-neo-CR-1 and pCI-neo vector. Percentage cell viability was estimated by dividing the measurement for treated cells by that of untreated cells. In both the plots, each data point represents mean of four different wells. Two-way ANOVA with pairwise multiple comparison indicates that CR1 containing CM effects cell viability in a dose-dependent fashion ($p < 0.001$) and CM of pCI-neo vector only does not have any significant effect ($p > 0.05$).

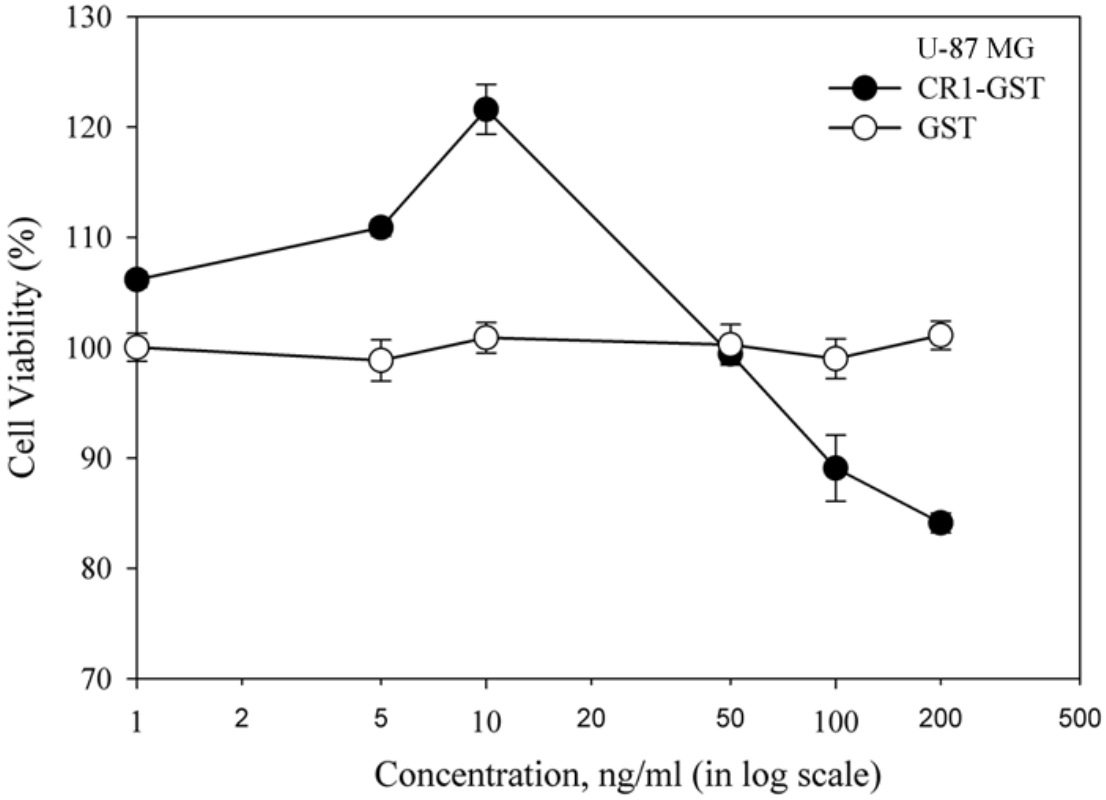

Figure 4.9 Effect of Recombinant CR1-GST on viability of U-87 MG cells. Cell viability was measured by MTT assay after 48 hr treatment in absence of serum with different doses of CR1-GST or GST. Percentage cell viability was estimated by dividing the measurement for treated cells by that of untreated cells. The experiment was repeated and a representative experiment is shown here. Each data point represents mean of four different wells. Two-way ANOVA with pairwise multiple comparison indicates that CR1-GST effects cell viability in a dose-dependent fashion ($p < 0.001$) and GST does not have any significant effect ($p > 0.05$).

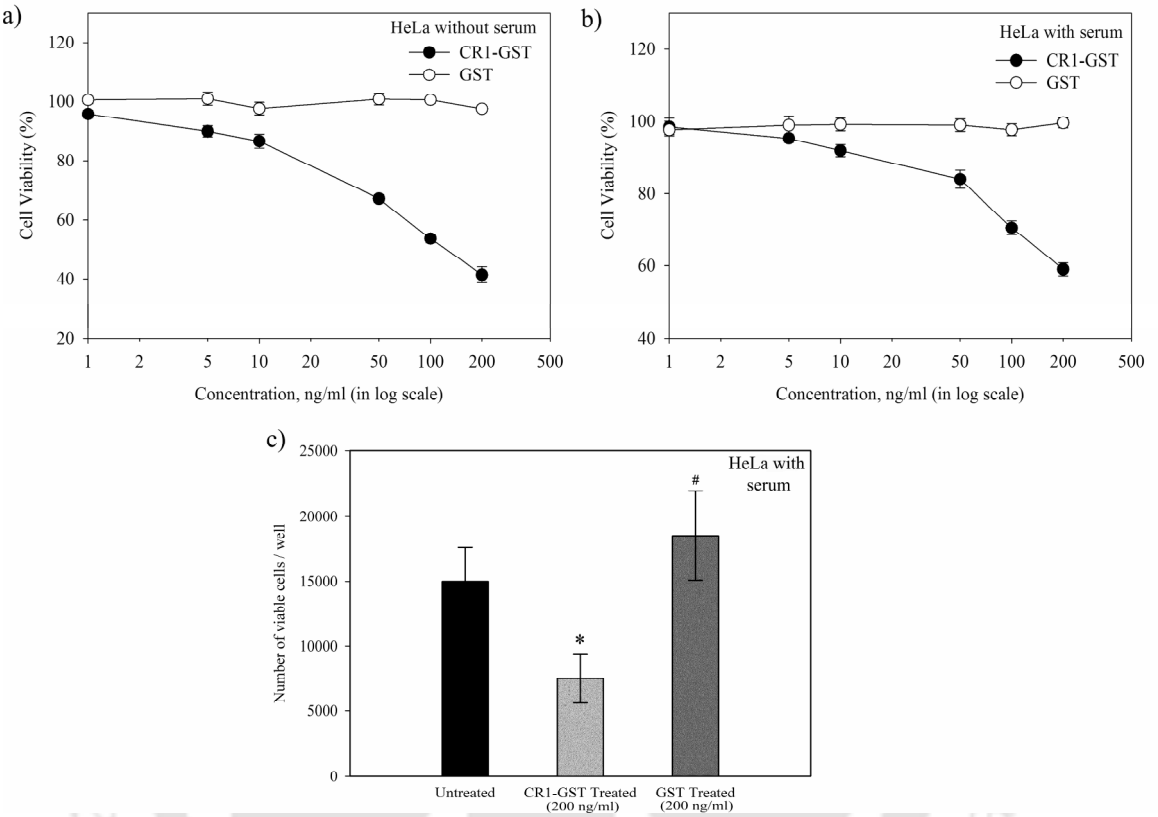

Figure 4.10 Recombinant CR1-GST reduces viability of HeLa cells. Viability of HeLa cells were measured by MTT assays after 48 hr treatment with different doses of CR1-GST or GST in absence (a) and in presence (b) of serum. Experiments were repeated and two representative experiments are shown here. Each data point represents mean of four different wells. Two-way ANOVA with pairwise multiple comparison indicates that in both the experiments CR1-GST effects cell viability in a dose-dependent fashion ($p < 0.001$). (c) Number of live cells was counted using trypan blue dye exclusion method, after 72 hr treatment with either CR1-GST or GST (200 ng/ml) in presence of serum. Approximately 10^3 cells were seeded in each well prior to treatments. Each bar represents mean of four independent wells. One way ANOVA with pairwise multiple comparison: *, significantly different from other treatment groups, $p < 0.005$ and #, not significantly different from untreated, $p > 0.05$.

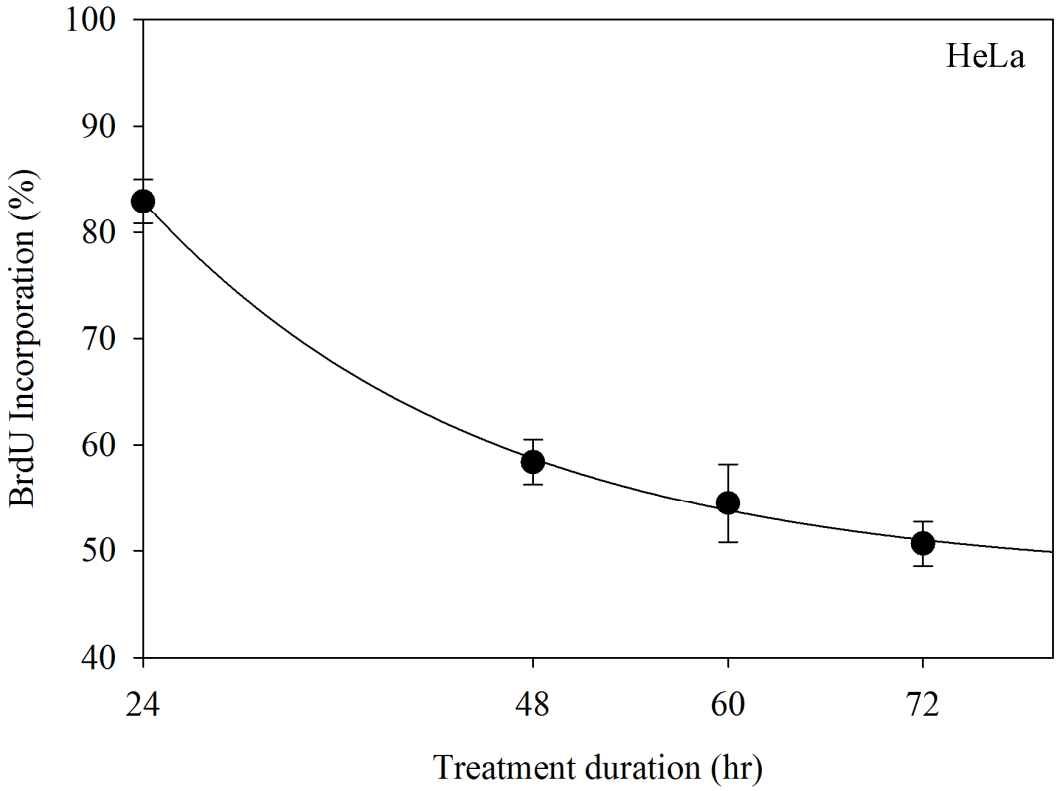

Figure 4.11 Recombinant CR1 reduces proliferation of HeLa cells. Proliferation of HeLa cells were measured by BrdU incorporation assay. HeLa cells were treated with CR1-GST (200 ng/ml) for different durations in presence of serum. Cells were pulsed with BrdU for 3 hr just before the end of specific treatment duration. BrdU Incorporation (%) was estimated by dividing the measurement for treated cells by that of untreated cells. Experiments were repeated and one representative experiment is shown here. Each data points represent mean of four different wells. One way ANOVA indicates that the effect of CR1-GST on proliferation of HeLa cells depends upon treatment duration ($p < 0.001$).

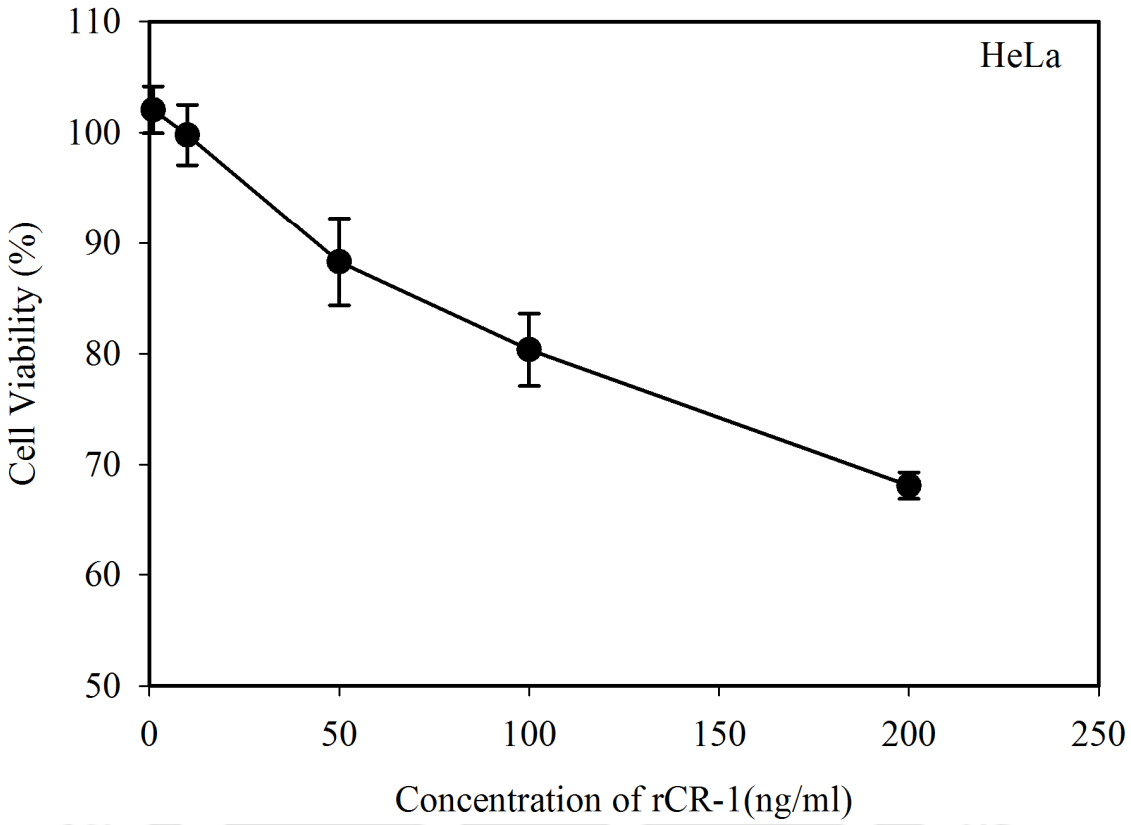

Figure 4.12 Recombinant CR-1(rCR-1) expressed in insect cells (R&D system) reduces viability of HeLa cells. Viability of HeLa cells were measured by MTT assays after 72 hr treatment with different doses of CR1 in presence of serum. Cell viability was estimated by dividing the measurement for treated cells by that of untreated cells. Each data point represents mean of four different wells. One way ANOVA indicates that rCR-1 (R&D) effects viability of HeLa cell in a dose-dependent fashion ($p < 0.001$).

Effect of recombinant CR1 on mitogenic pathways:

CR-1 binds to Glypican-1 and activates ERK1/2 MAPK and PI3K/Akt pathways to induce cell proliferation [18, 42, 51, 54]. Treatment with CR-1 induces phosphorylation of ERK1/2 and Akt in many cell lines [12]. After 24 hr of serum starvation, U87 MG and HeLa cells were treated with CR1-GST. Subsequently, phosphorylation status of ERK1/2 and Akt was determined by Western Blot. We observed that CR1-GST induced approximately two fold increase in phosphorylation of p44/42 and three fold increase in phosphorylation of Akt in U-87 MG cells, after 15 min and 5 min of treatment respectively (Figure 4.13). Such observation is expected as Glypican-1 is expressed in U-87 MG cells and we have shown that recombinant CR-1 can induce proliferation of this cell. However, Glypican-1 is expressed in comparatively very low amount in HeLa cells. We observed that treatment with CR1-GST did not induce phosphorylation of p44/42 and Akt in HeLa cells, even when treated for long period of time (Figure 4.14). This clearly explains the inability of CR-1 to induce proliferation of HeLa cells.

The proposition that CR-1 fails to activate its pro-proliferative pathways due to the lower expression of glypican-1, was further substantiated by our observations in two other cell lines HT-29 and HEK 293. Like HeLa cells, expression of glypican-1 is also low in these two cell lines (Figure 4.7b, & d). As expected, CR1-GST failed to induce proliferation of these cells. Rather, treatment with CR1-GST reduced the cell viability in a dose-dependent fashion (Figure 4.15).

To investigate the role of MAPK and AKT pathway in CR-1 mediated modulation of cell proliferation in U-87 MG and HeLa cells, viability assays were performed in presence of two inhibitors, U0126 and LY294002. U0126 inhibits MEK1/2 of MAPK pathways and LY294002 inhibits PI3 kinase of PI3K/Akt pathway (Figure 4.16a). Complete blockage of these two pathways may hinder the normal physiology of cells. Therefore we used these two inhibitors at suboptimal concentration (6 µM each). At this concentration, these two inhibitors reduced the cell viability of HeLa and U87 MG cells to ~ 85 and 73 % respectively (Figure 4.16b). Further, we treated both the cells with different concentration of CR1-GST in presence of these inhibitors (6 µM each). As shown in Figure 4.17a, in presence of these inhibitors, CR1-GST failed to induce proliferation of U-87 MG cells. But the anti-proliferative effect on HeLa cells was

potentiated (Figure 4.17b). Treatment with 100 ng/ml of CR-1 reduced viability of HeLa cells to ~ 75 %. When treated in presence of inhibitors, viability of these cells reduced to ~ 45 %.

Taken together, these observations indicate that treatment with CR-1 can activate the well characterized pro-proliferating ERK1/2 MAPK and Akt pathway as well as a hitherto uncharacterized anti-proliferative pathway. The fate of the cell depends upon the relative strengths of these two pathways. When the CR-1 fails to trigger effective induction of pro-proliferative pathways, as observed in HeLa cells, the antiproliferative effect becomes predominant.

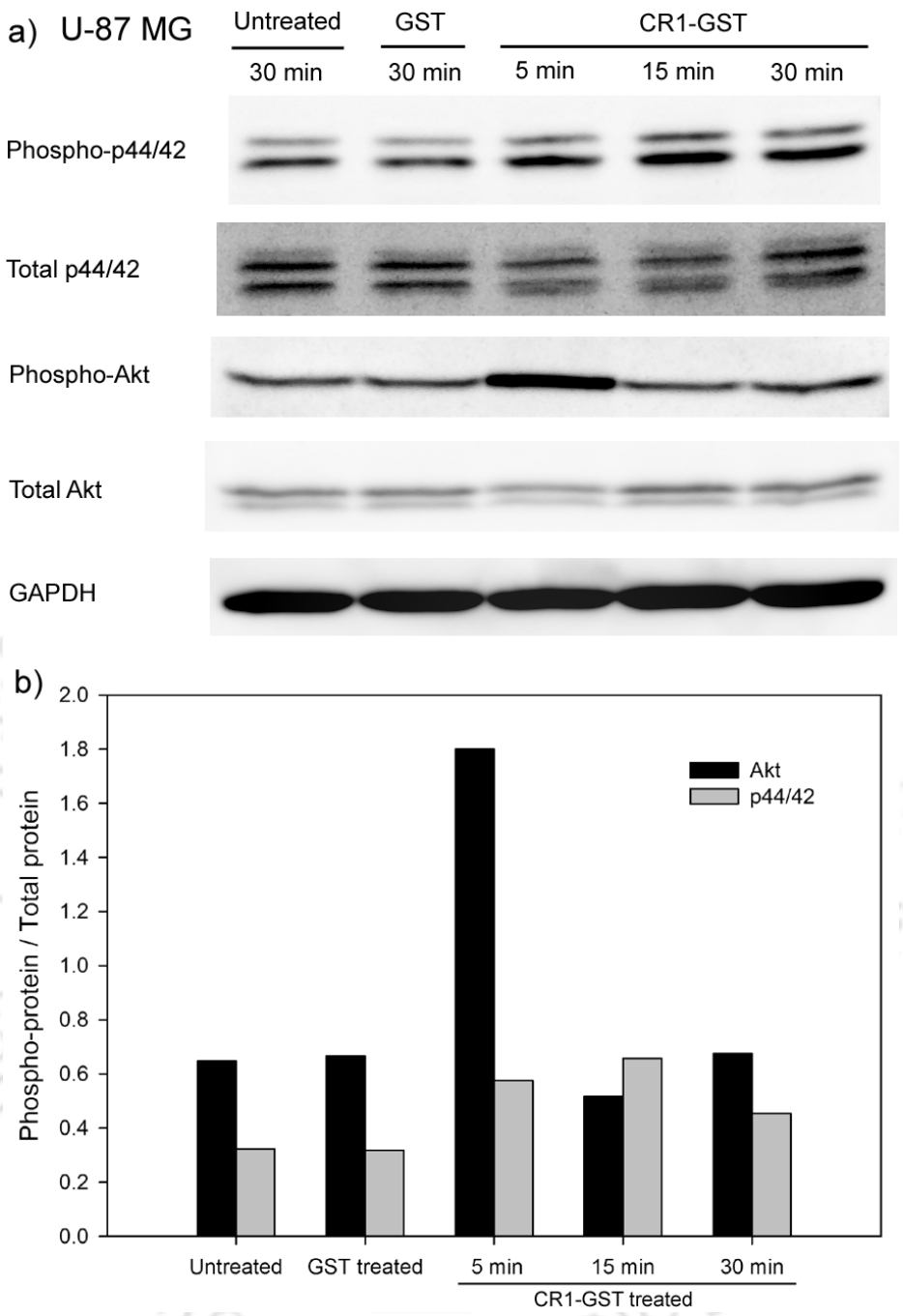

Figure 4.13 Recombinant CR1-GST activates mitogenic pathways in U-87 MG cells. a) Western blots to detect phosphorylation status of p44/42 and Akt in U-87 MG cells treated with 200 ng/ml of CR1-GST or GST in absence of serum for 5 to 15 minutes. GAPDH was used as loading control. Primary antibodies (dilution: 1/1000) used to probe the blots were: rabbit anti-phospho-p44/42 MAPK (Thr202/Tyr204), rabbit anti-p44/42 MAPK, rabbit anti-phospho-Akt (Ser473), rabbit anti-Akt (pan) and rabbit anti-GAPDH. Goat anti-rabbit HRP-conjugate (dilution: 1/6000) was used as secondary antibody. Blots were developed using chemiluminescence. b) Densitometric analysis of Western blots to quantify the ratio of phosphorylated to total protein for p44/42 and Akt in different treatment groups.

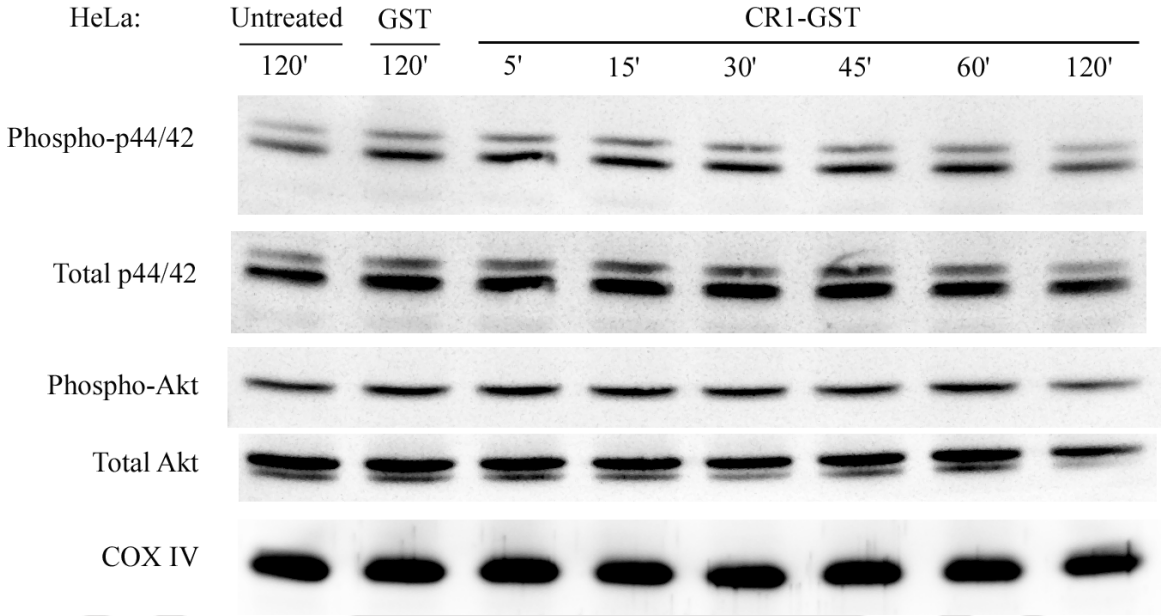

Figure 4.14 Recombinant CR1-GST does not activate mitogenic pathways in HeLa cells. Western blots to detect phosphorylation status of p44/42 and Akt in HeLa cells treated with 200 ng/ml of CR1-GST or GST in absence of serum for 5 to 120 min. Cox IV was used as loading control. Primary antibodies (dilution: 1/1000) used to probe the blots were: rabbit anti-phospho-p44/42 MAPK (Thr202/Tyr204), rabbit anti-p44/42 MAPK, rabbit anti-phospho-Akt (Ser473), rabbit anti-Akt (pan) and rabbit anti-COX IV. Goat anti-rabbit HRP-conjugate (dilution: 1/6000) was used as secondary antibody. Blots were developed using chemiluminescence.

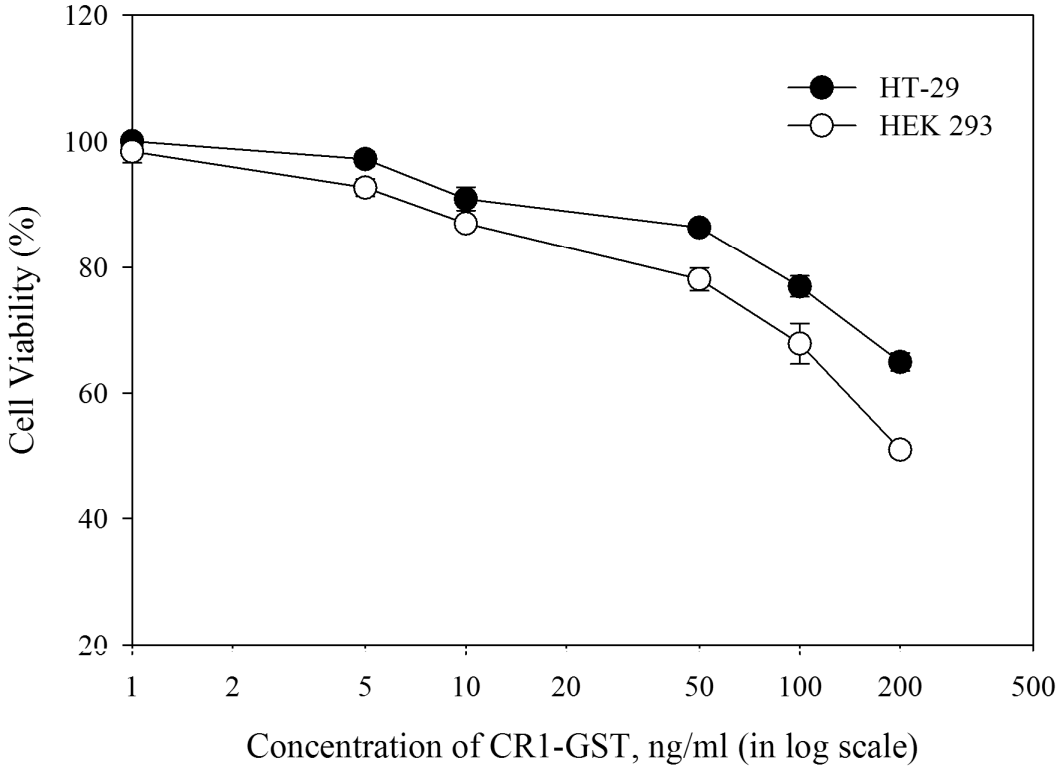

Figure 4.15 Recombinant CR1-GST reduces viability of HT-29 and HEK 293 cells. Viability was measured by MTT assays after 48 hr treatment with different doses of CR1-GST or GST in presence of serum. Percentage cell viability was estimated by dividing the measurement for treated cells by that of untreated cells. Treatment with recombinant CR1-GST reduces viability of HT-29 and HEK 293 cells in a dose-dependent fashion (One-way ANOVA, $p < 0.001$, for both the cell lines).

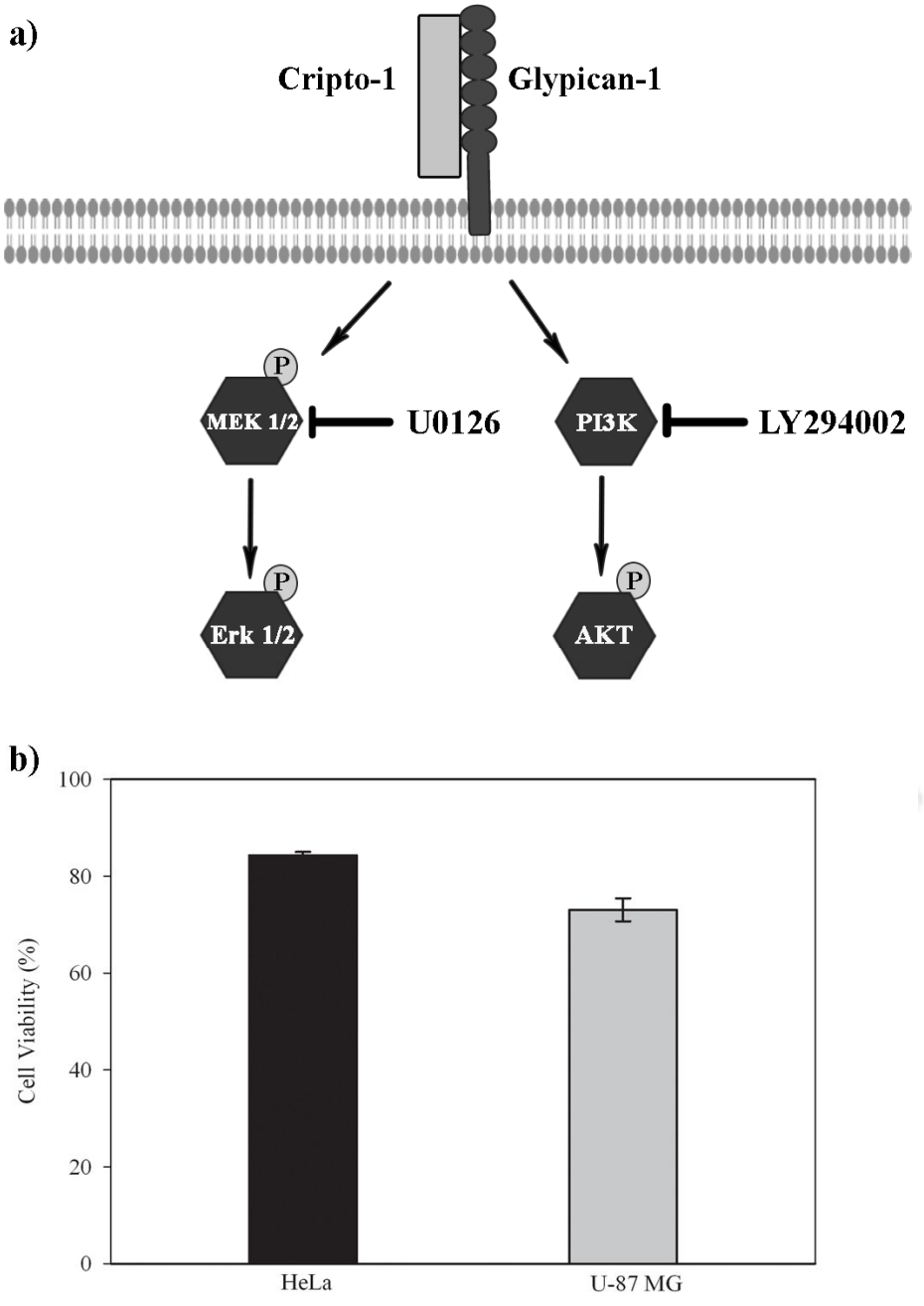

Figure 4.16 Strategy to inhibit pro-proliferative pathways of CR-1. (a) Schematic diagram showing some key molecules of Erk1/2 MAPK and Akt pathway. U0126 inhibits MEK1/2 of MAPK pathway reducing the Erk1/2 phosphorylation and LY294002 inhibits PI3 kinase of PI3K/Akt pathway reducing AKT phosphorylation (b) Cell viability of HeLa and U-87 MG cells treated with both the inhibitors, U0126 (6 µM) and LY294002 (6 µM). Cells were treated for 48 hr in absence of serum and cell viability was measured by MTT assays.

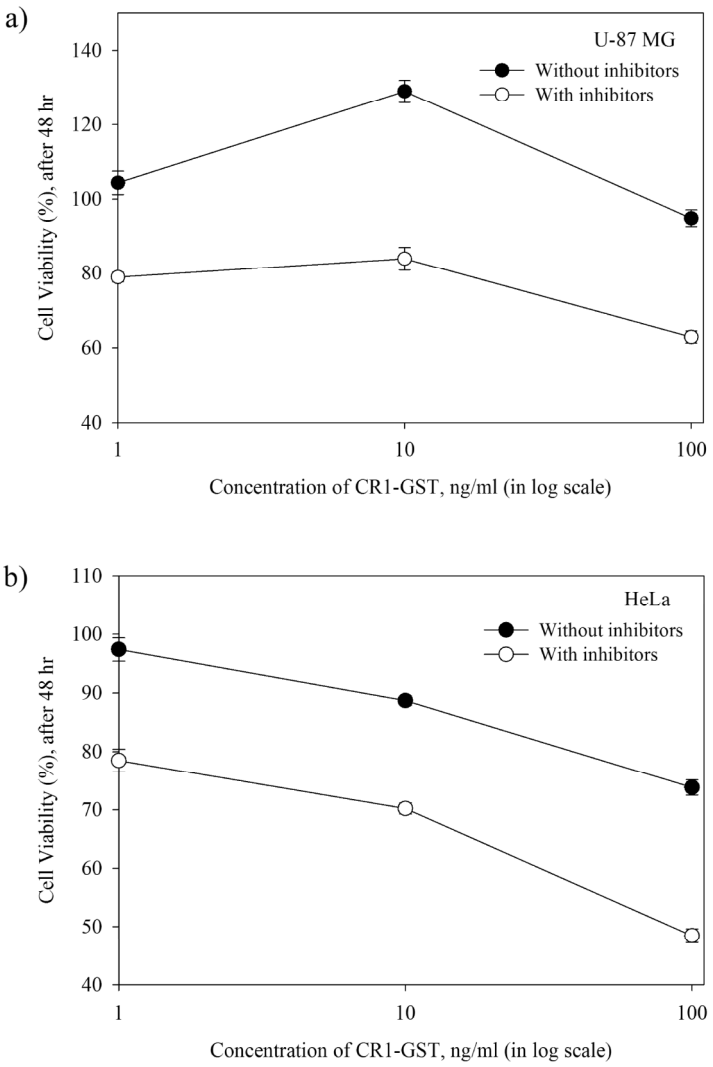

Figure 4.17 Effect of CR-1 on cell proliferation, in presence of inhibitors of mitogenic pathways. U-87 MG cells (a) and HeLa cells (b) were treated with different concentration of CR1-GST (1 to 100 ng/ml) in presence/absence of LY294002 and U0126 (6 µM each) for 48 hr. Subsequently, cell viability was measured by MTT assay. Percentage cell viability was estimated by dividing the measurement for CR1-GST treated cells by that of untreated cells. The experiment was repeated and a representative experiment is shown here. Each data point represents mean of four different wells.

Mechanism of the anti-proliferative effect of CR-1:

The differential expression of Glypican-1 can explain why recombinant CR-1 failed to induce proliferation of HeLa, HT-29 and HEK-293 cells. However, the existing models for mitogenic signaling of CR-1 can not explain the dose and time-dependent reduction in cell proliferation that was observed when these cells were treated with recombinant CR-1. We took an organized approach to investigate the possible mechanisms involved in such reduction in cell proliferation. We did all these investigations using HeLa cells treated with recombinant CR1-GST.

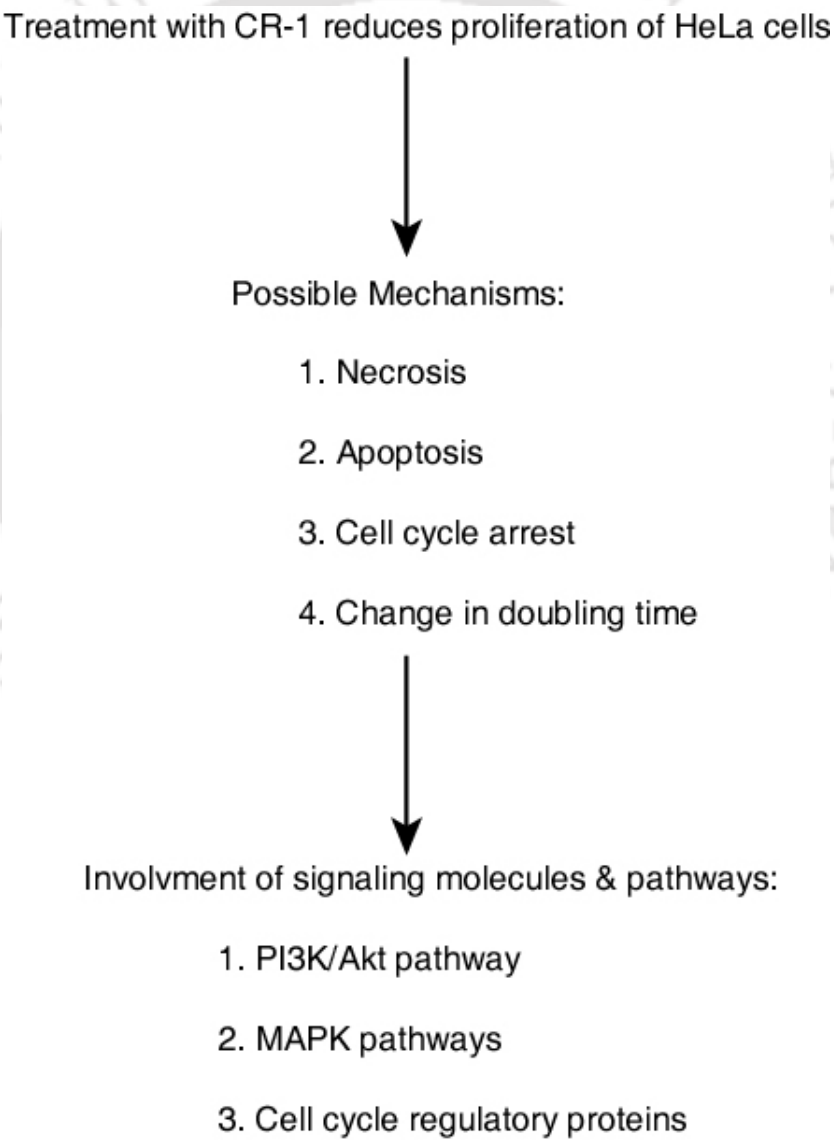

CR1-GST does not induce necrosis in HeLa cells:

Induction of necrosis can reduce the number of viable cells in an experiment. Necrosis is a process of cell death which is accompanied by mitochondrial swelling and increased plasma membrane permeability. Eventually, the cell membrane ruptures, resulting in the release of the cell's components into the surrounding media [116]. Lactate dehydrogenase (LDH) is a soluble cytosolic enzyme that is released into the culture medium following loss of membrane integrity resulting from necrosis [117]

We measured the amount of LDH into the culture supernatant, released due to disruption of cell membrane, to determine the degree of necrosis. HeLa cells were treated with 200 ng/ml of CR1-GST for 24 hr, 48 hr and 72 hr. At the end of each time point, culture supernatant was collected to determine the amount of released LDH. Level of LDH in CR1-GST treated cells was found to be similar to untreated cells, even after treatment for 72 hr (Figure 4.18). This experiment confirmed that reduction in cell viability upon treatment with recombinant CR-1 was not due to enhanced cell death by necrosis.

Recombinant CR-1 does not induce apoptosis in HeLa cells:

Induction of apoptosis can also reduce the number of viable cells in an experiment. Apoptosis is a programmed, physiological mode of cell death. The apoptotic program is characterized by certain morphological features, including loss of plasma membrane integrity, condensation of the cytoplasm and nucleus, and internucleosomal cleavage of DNA [116].

Loss of plasma membrane integrity is one of the earliest features of apoptosis. In apoptotic cells phosphatidylserine (PS) gets translocated from the inner to the outer leaflet of the plasma membrane, thereby exposing PS to the outer part of the cell membrane. Annexin V is a phospholipid-binding protein that has high affinity for PS, and binds to cells with exposed PS. Since externalization of PS occurs in the earlier stages of apoptosis, FITC Annexin V staining can identify apoptosis at an earlier stage. Extensive disruption of cell membrane happens at the late phase of apoptosis. Cells with compromised cell membrane, like in late phase of apoptosis or in necrosis, can be stained with propidium iodide (PI). Viable cells with intact membranes exclude PI. To differentiate the apoptotic and necrotic death, staining with FITC Annexin V is

used in conjunction with PI to identify early apoptotic cells (PI negative, FITC Annexin V positive) and late apoptotic cells (PI positive, FITC Annexin V positive).

We treated HeLa cells with CR1-GST or GST (200 ng/ml) for 72 hrs. Subsequently, we stained those cells with Annexin V-FITC and PI, and analyzed by flow cytometry. Result of one such flow cytometry experiment after double staining with Annexin V-FITC and PI is shown in Figure 4.19a. Cells present in the upper-right and the lower-right quadrant of the Annexin-V-FITC/PI dot plot belong to cells undergoing apoptosis. Percentage of Apoptotic cells in different treatment groups, measured in three independent experiments, is shown in Figure 4.19b. It is evident from the plot that treatment with 200 ng/ml of CR1-GST for 72 hr, did not induce apoptosis in HeLa cells. Cisplatin, which is known to induce apoptosis in HeLa cells, was used as a positive control in this experiment.

Necrotic and apoptotic cells can also be recognized by their morphologies. Therefore, we observed CR1-GST treated HeLa cells under light microscope to check any possible morphological changes and presence of necrotic/apoptotic cells. The images are shown in Figure 4.20. However, no such morphological changes were observed in cells treated with CR1-GST in comparison to untreated or GST treated cells (Figure 4.20).

Treatment with CR-1 does not induce cell cycle arrest in HeLa cells:

We looked into the possibility of cell cycle arrest as the reason for reduced viability of CR-1 treated HeLa cells. Distribution of cells in different phases of cell cycle was measured by flow cytometry after staining with PI. PI is a fluorogenic compound that binds to DNA by intercalating between the bases. PI binds stoichiometrically to nucleic acids so that fluorescence emission is proportional to the DNA content of a cell. HeLa cells were treated with 200 ng/ml of CR1-GST for 72 hr. After staining with PI, cell cycle analysis was done by flow cytometry. Result of a particular experiment is shown in Figure 4.21a. It is evident from the histograms that treatment with CR1 did not arrest these cells in any particular phase of cell cycle. The experiment was repeated and percentage of cells in different phases of cell cycle in different treatment groups is shown in Figure 4.21b. A marginal but statistically significant increase in percentage of cells in S phase was observed for CR1-GST treated cells with slight decrease in G1 phase (Figure 4.21b). However, one can not

consider such little change in distribution as a signature of cell cycle arrest. Such slight difference in distribution of cells may arise as CR1-GST treated cells were growing slowly and were out of phase with untreated cells.

The data obtained in cell cycle assays, also provides information about percentage of apoptotic cells in these treatment groups. During apoptosis, chromosomal DNA gets fragmented. This leads to loss of chromosomal DNA from apoptotic cells, during processing for PI staining. Therefore, cells undergoing apoptosis are under-stained and contribute to sub-G1 population in the histogram for PI-stained cells. We observed that sub-G1 population in our experiments were low and similar in all treatment groups (3.48 ± 0.59% in CR1-GST treated, 3.64 ± 0.91% in GST treated and 3.86 ± 0.48% in untreated cells). This reconfirmed that treatment with CR1-GST did not induce apoptosis.

Effect of CR1-GST on doubling time of HeLa cells:

Increase in the doubling time due to the treatment with CR1-GST, can lead to our observations in cell viability and proliferation assays. To determine the rate of cell divisions we have used CFSE dye dilution assay. Carboxyfluorescein diacetate succinimidyl ester (CFDA-SE) is a cell membrane permeable non-fluorescent molecule. When it enters the cytoplasm of a cell, intracellular esterases remove acetate groups and convert this molecule to a fluorescent one, Carboxyfluorescein succinimidyl ester (CFSE). The cell membrane is impermeable to CFSE and therefore, it is retained within a cell for a long time. During the cell division, CFSE gets distributed almost equally between daughter cells, allowing discrimination of successive rounds of cell division by flow cytometry [118].

To identify overall delay in cell division, we pulse-labeled HeLa cells with CFDA-SE followed by treatment with CR1-GST for specified period of time. As expected, division of cells led to decrease in the fluorescence intensity of labeled cells due to dye dilution (Figure 4.22a). However, the shift in peak for cells treated with CR1-GST was lesser than untreated/GST treated cells. This indicates that CR1-GST treated cells had lesser number of cell divisions in 72 hr than the untreated cells. Assuming that all cells in a treatment group were dividing at the same rate, average doubling time was calculated using the geometric mean fluorescence values as described in the methods section. We observed that treatment with CR1-GST, increased the doubling time of HeLa cells to 37.28 ± 2.75 hr from 27.29 ± 1.14 hr (Figure 4.22b).

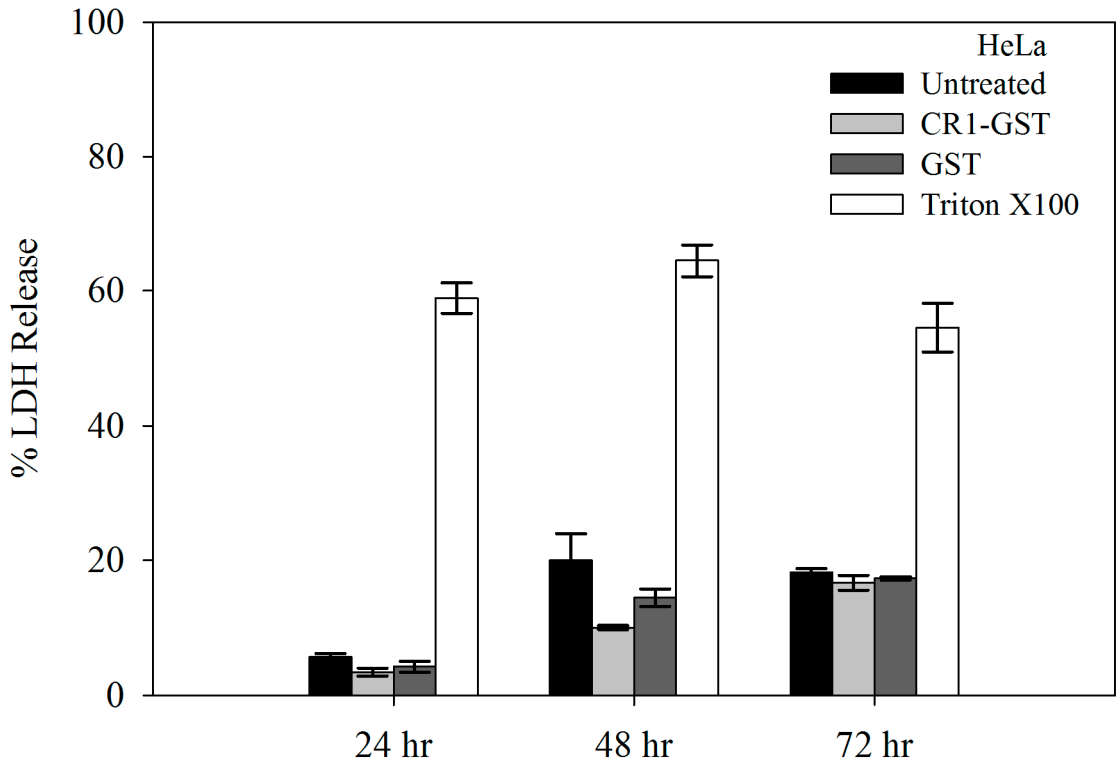

Figure 4.18 Recombinant CR1-GST does not induce necrosis in HeLa cells. LDH released from cells in culture media was used as a measure of necrotic cell lysis. Cells were treated with either CR1-GST or GST (200 ng/ml) or left untreated for three different durations in presence of serum and LDH activity in culture medium was measured. Total LDH activity was measured in fresh cell lysates prepared by sonication on ice and used to calculate the percentage of LDH released into the medium. Cells treated with Triton X-100 (0.1%) were used as a positive control for cell lysis in this experiment. Each bar represents mean of three data points.

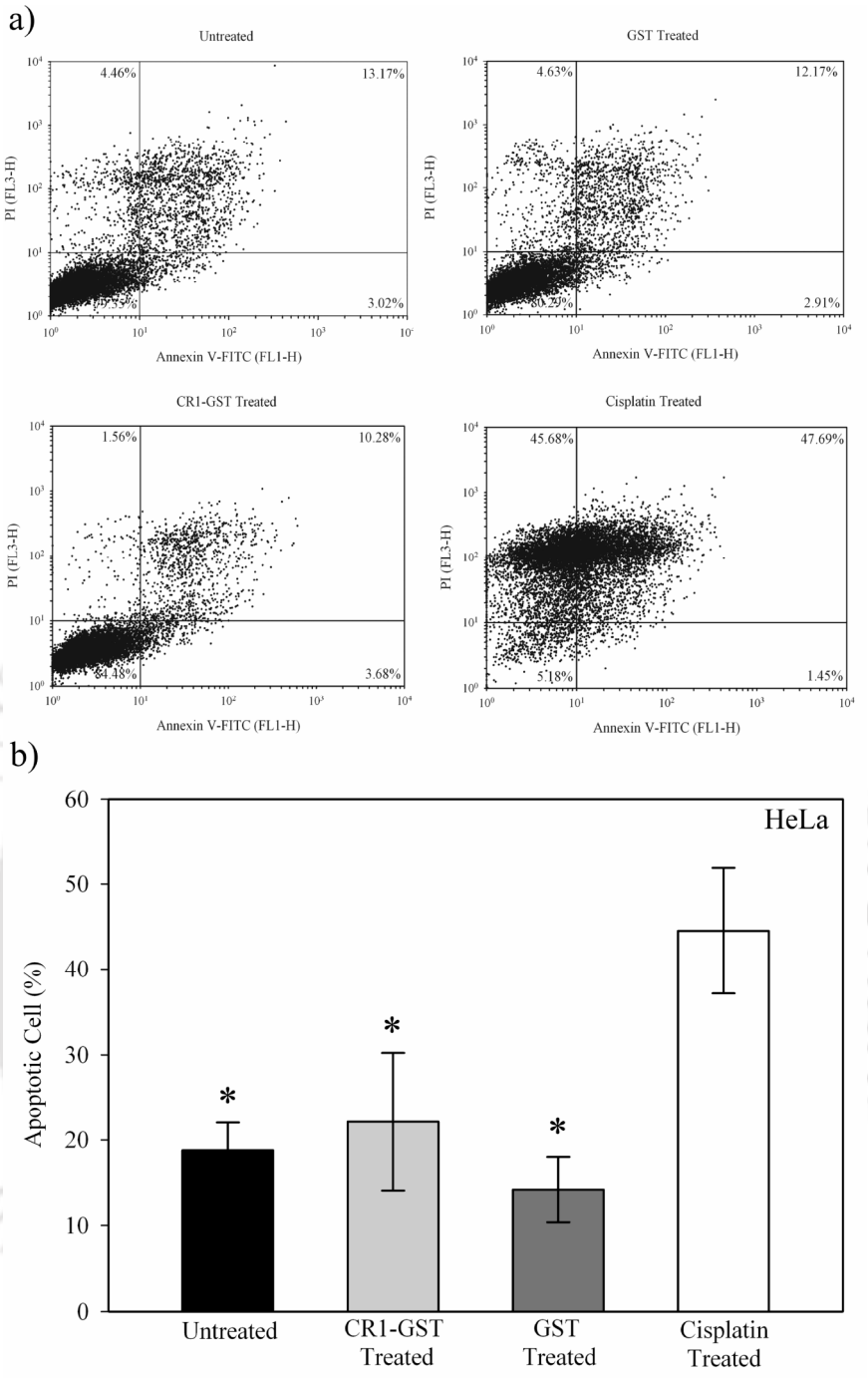

Figure 4.19 CR1-GST does not induce apoptosis in HeLa cells. HeLa cells were treated with either CR1-GST or GST (200 ng/ml) or left untreated for 72 hr in presence of serum and analyzed by flow cytometry after double staining with PI and Annexin-V-FITC. Cells treated with Cisplatin (3 mg/ml) were used as a positive control for apoptosis. (a) Dot plots showing the flow cytometric data of a representative experiment. Cells present in lower and upper right quadrants represent cells in early and late apoptosis respectively. (b) Bar plot showing percentage of apoptotic cells in each treatment group. Each bar represents mean of three independent experiments. *, no significant difference among these treatment groups, One-way ANOVA, $p > 0.05$.

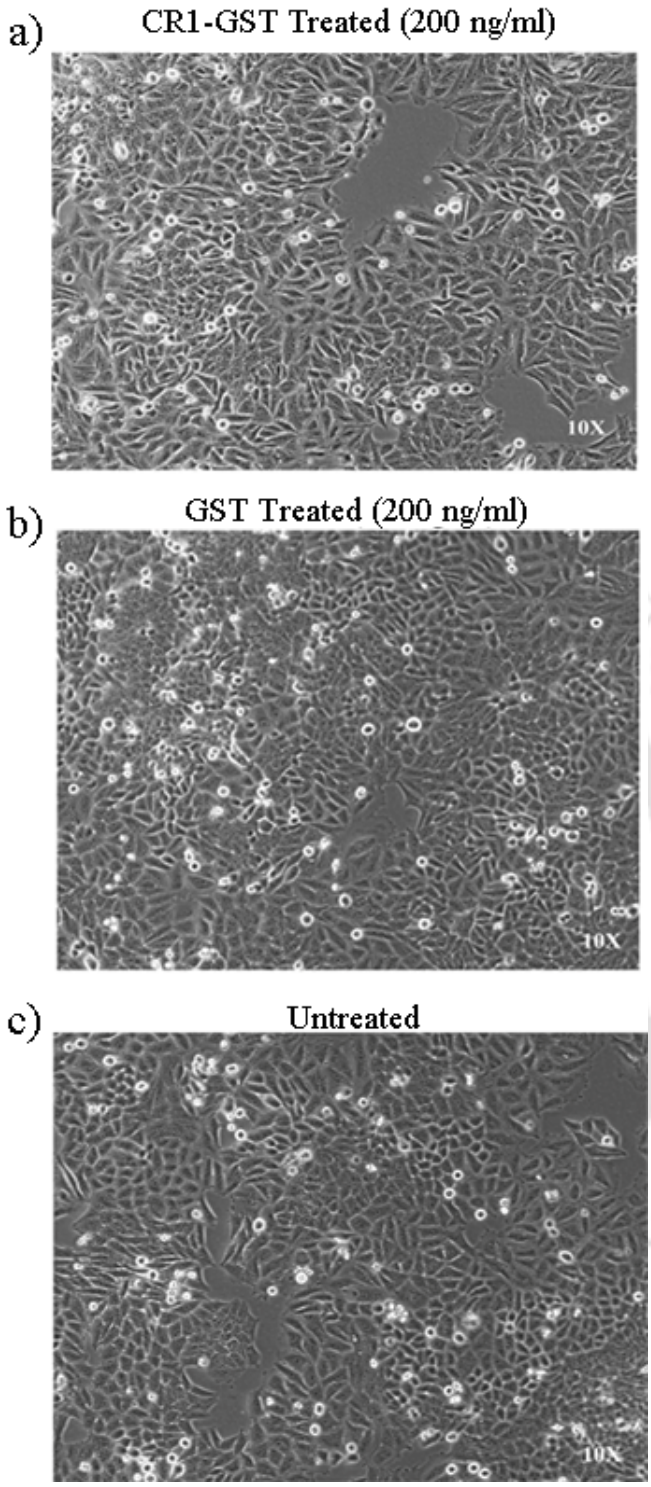

Figure 4.20 CR1-GST does not induce cell death or morphological changes in HeLa cells. Photomicrographs showing HeLa cells treated for 72 hr either with a) CR1-GST (200 ng/ml) or b) GST (200 ng/ml) or c) left untreated, in presence of serum. Cells treated with of CR1-GST were as healthy as untreated or GST treated cells. Phase contrast images were taken at 10X magnification with Eclipse Ti-U inverted microscope, Nikon.

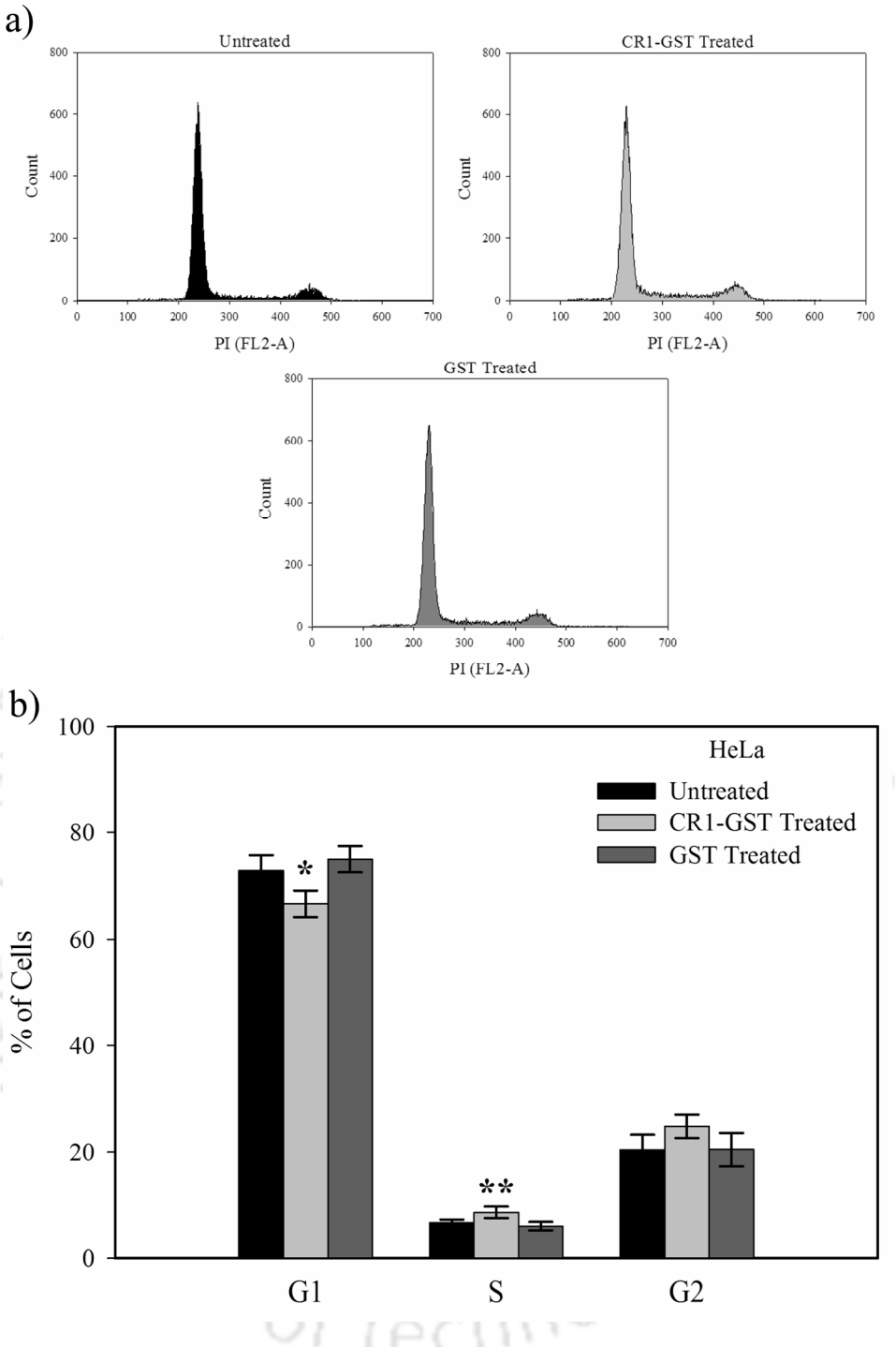

Figure 4.21 Effect of CR1-GST on distribution of cells in different stages of cell cycle. HeLa cells, treated with either CR1-GST or GST (200 ng/ml) or left untreated for 72 hr in presence of serum, were stained with PI and analyzed by flow cytometry. a) Histograms for PI intensity in different treatment groups in a representative experiment. b) Percentage of cells in different phases of cell cycle was calculated from flow cytometry data. Each bar represents mean of four independent experiments. * and ** represent significant differences with untreated and GST treated cells, One-way ANOVA, $p < 0.05$.

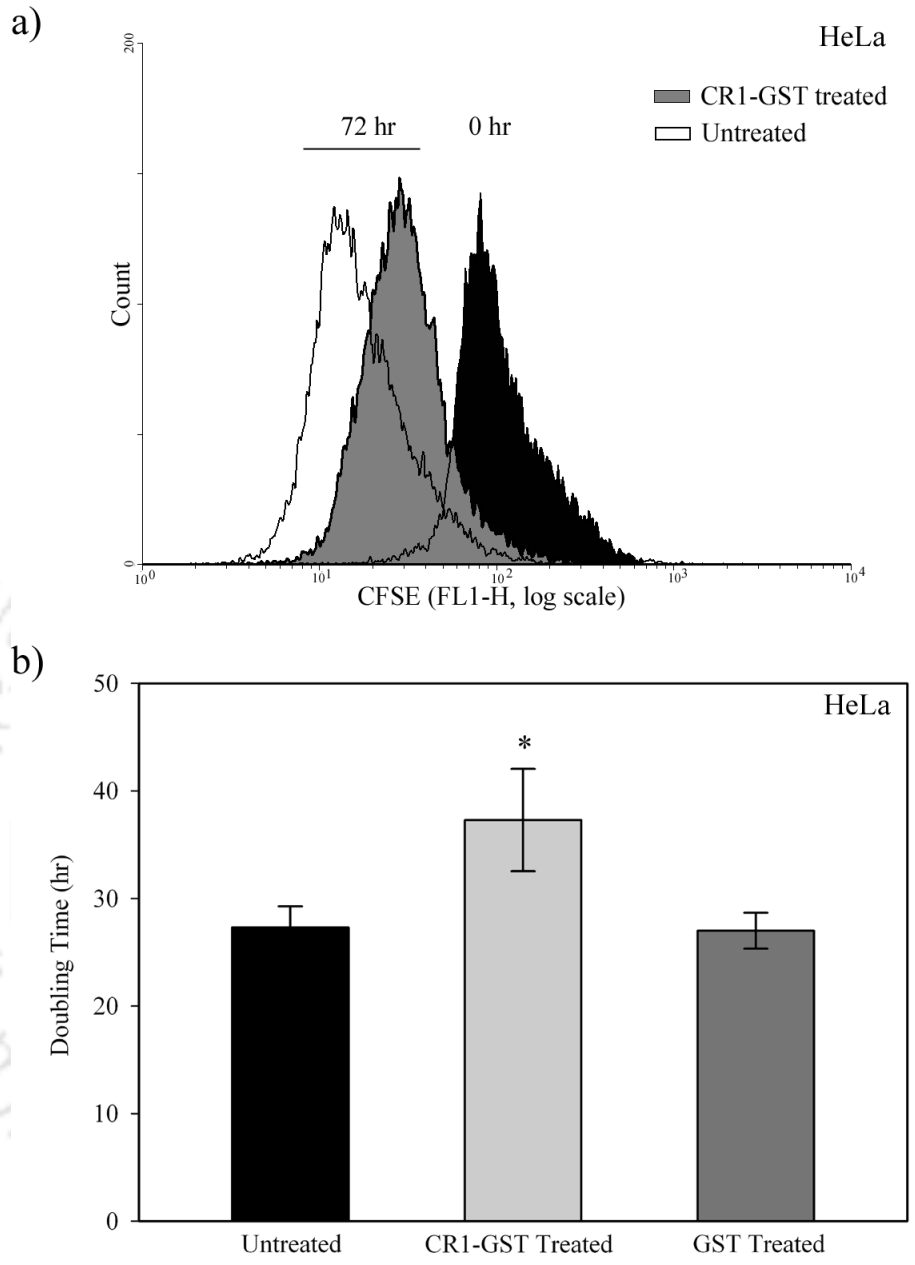

Figure 4.22 CR1-GST slows down cell division of HeLa cells. Cells loaded with CFDA-SE were treated with either CR1-GST or GST (200 ng/ml) or left untreated for 72 hr in presence of serum and analyzed by flow cytometry. (a) Flourescence intensity histograms for CFSE in cells of different treatment groups in a representative experiment. After 72 hr of incubation, CFSE histograms move leftward, indicating dye dilution due to cell division. Histogram corresponding to GST treated cells is not shown here as it overlaps with that of untreated cells. (b) Doubling time of cells of different treatment groups calculated from flow cytometry data. Each bar represents mean of three independent experiments. *, significantly different from other treatment groups, One-way ANOVA, $p < 0.05$.

Effect of CR1-GST on transcription profile of cell cycle regulatory molecules:

Cyclins are important cell cycle regulatory molecules which modulates the cell cycle progression. We have investigated the mRNA expression level of different cyclins in HeLa cells after 72 hr treatment with CR1-GST. Real-time PCR was used to estimate the level of expression of these molecules. Data of these experiments are shown in Figure 4.23. It was observed that expression of Cyclin A2 was marginally more in CR1-GST treated cells. Cyclin A2 is expressed both in S and G2 phases and expression peaks in G2. On the other hand, expression of Cyclin E1 peaks at G1/S boundary [119]. We observed that CR1-GST treated HeLa cells had slightly lesser amount of Cyclin E1. These marginal changes in expression of cyclin A2 and E1 can be explained in terms of our observations in cell cycle analysis. In CR1-GST treated cells, we had slightly lesser number of cells in G1 but more in S and G2 phases. It should be noted that changes in expression for both the cyclins, though statistically significant, were less than 2 fold. Therefore, such subtle changes may not be of biological significance but rather may have originated as cells were slightly out of phase.

Interestingly, we have not observed any change in the expression of Cyclin D1 in CR1-GST treated cells. Cyclin D1 is essential to make a cell committed at G1 phase to move through the cell cycle and its expression does not show significant oscillation across different phases of cell cycle [119]. Therefore, results of our real time PCR experiment, when read with other results, indicates that the recombinant CR1-GST does not halt cell cycle, and rather slows down the process.

We analyzed expression of three key cyclin-dependent kinase inhibitors, namely $p27^{Kip1}$, $p21^{Cip1}$ and $p57^{Kip2}$. These molecules inhibit activity of cyclin-Cdk complexes required for G1/S transition and progression through S phase [120]. Increase in their expression slows down cell cycle progression and even leads to cell cycle arrest [121-124]. The data of real-time PCR for these genes are shown in Figure 4.24. It was observed that CR1-GST treated cells have marginally higher expression of $p27^{Kip1}$, and the difference in expression was statistically significant. However, like cyclins the change in expression was less than two fold. It should be kept in mind that activity of Cdk inhibitors in a cell can be controlled by different mechanisms, including transcriptional control, and by control of degradation. Therefore, results of real-time

PCRs, alone, may not be a correct reflection of the activity of these proteins inside the cell. In essence, data obtained by real-time PCRs for cyclins and cyclin inhibitors did not give us conclusive evidence to understand the molecular mechanism behind reduced proliferation CR1-GST treated HeLa cells.

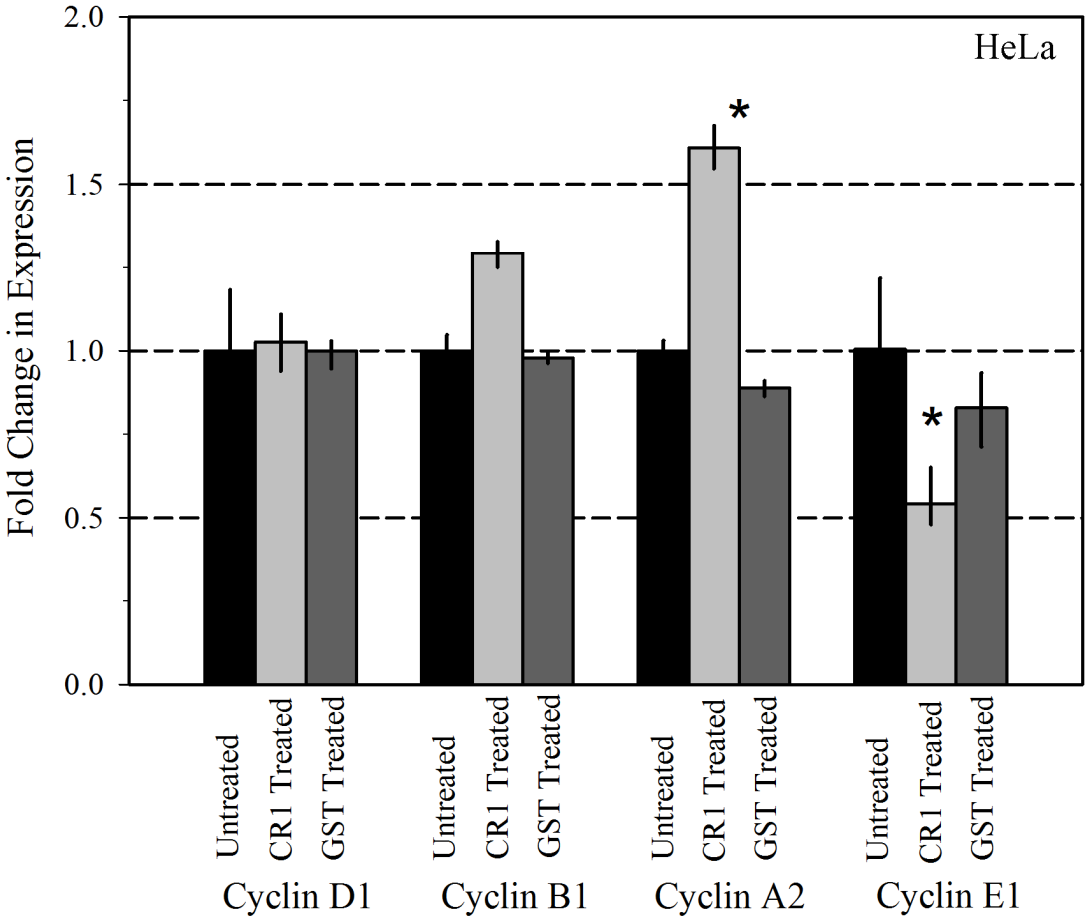

Figure 4.23 Effect of CR1-GST on expression of different cyclins in HeLa cells. Real-time PCR was used to calculate fold change in expression of four different cyclins. Cells were treated with either CR1-GST or GST (200 ng/ml) or kept untreated for 72 hr. Subsequently RNA was isolated and processed for the assay. Data of each treatment group was normalized with respect to untreated cells to calculate fold change. Each bar represents mean of three data points. Error bars represent maximum and minimum values. *: significantly different from untreated, $p < 0.05$. GAPDH, β-actin and PPIA were used as endogenous controls.

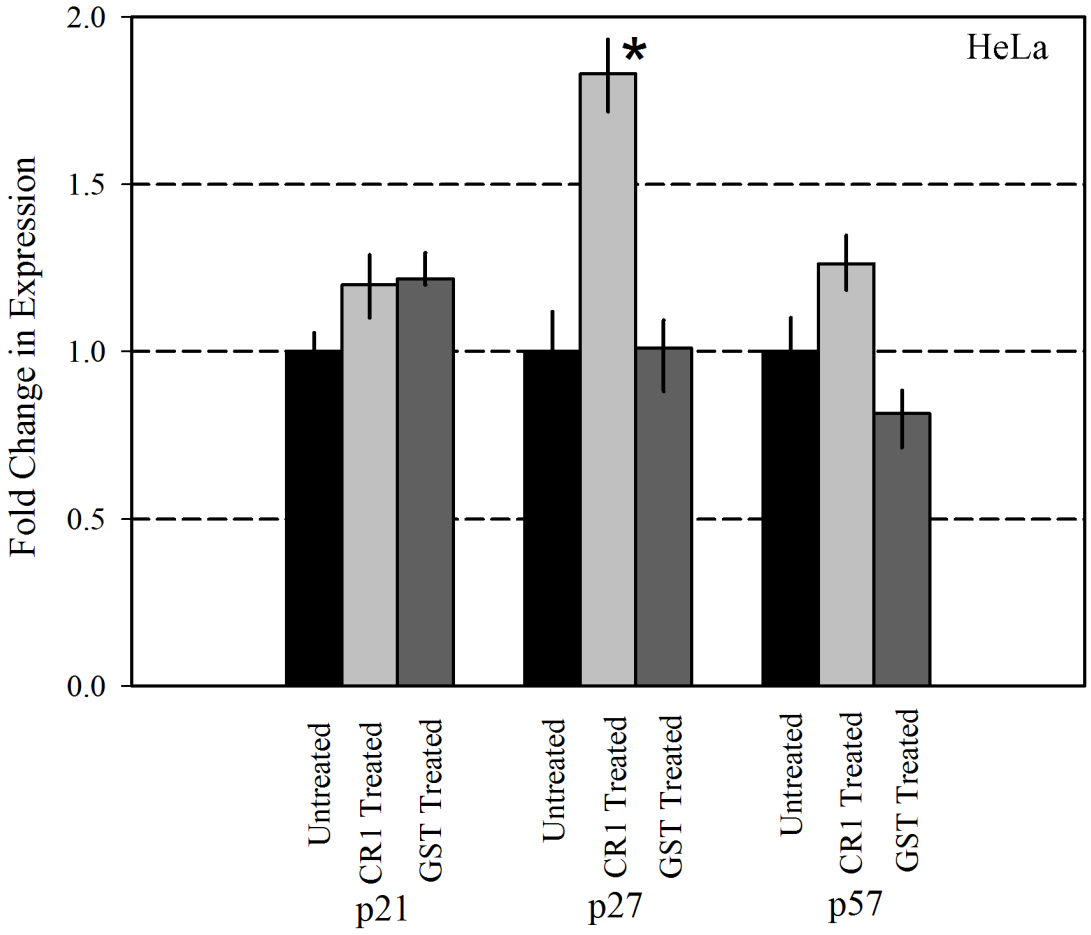

Figure 4.24 Effect of CR1-GST on expression of cyclin dependent kinase inhibitors in HeLa cells. Real-time PCR was used to calculate fold change in expression. Cells were treated with either CR1-GST or GST (200 ng/ml) or kept untreated for 72 hr. Subsequently RNA was isolated and processed for the assay. Data of each treatment group was normalized with respect to untreated cells to calculate fold change. Each bar represents mean of three data points. Error bars represent maximum and minimum values. *: significantly different from untreated/GST treated, $p < 0.05$. PPIA was used as endogenous control.

CR1-GST mediated anti-proliferative pathways:

We have observed that treatment with exogenous CR-1 reduces proliferation of HeLa cells by slowing down the overall cell cycle, without cell death or cell cycle arrest. To understand the molecular pathways that lead to such a phenomenon, we looked again to various molecules of MAPK and Akt pathways, two critical pathways that regulate cell proliferation. We have shown earlier that treatment with recombinant CR-1 does not activate these two pathways in HeLa cells. In those experiments, cells were treated only for a short duration. We have seen that the anti-proliferative effect depends upon treatment duration (Figure 4.11). Therefore, we looked into the status of various molecules of MAPK and PI3K/Akt pathways after long durations of treatment with CR1-GST.

Phosphatase and tensin homolog (PTEN) is a key phosphatase in PI3K/Akt pathway. PTEN dephosphorylates phosphatidylinositol-(3,4,5)-triphosphate (PIP3), a second messenger, lowering its level within the cell. PIP3 is necessary for activation of Akt (Figure 4.25a). Thus, PTEN negatively regulates PI3K/Akt pathway [125]. Several authors have shown that increased expression of PTEN reduces activation of Akt leading to suppression of cell proliferation, cell cycle arrest and cell death [126, 127]. Particularly, observations of Seminario *et al.* [128] on role of PTEN in cell cycle progression, are very relevant for our work. They observed reduced cell proliferation without cell cycle arrest or cell death when they overexpressed PTEN in Jurkat cells. We have done Western blot experiment to detect PTEN in HeLa cells treated with CR1-GST. As shown in Figure 4.25b, treatment with CR1-GST increased the amount of PTEN in HeLa cells and such increase was dependent on treatment duration. Increase in PTEN would reduce PIP3 and eventually would lead to decrease in phophorylated Akt. As expected, we have observed such synchronized decrease in phosphorylated Akt in CR1-GST treated HeLa cells (Figure 4.25b). This decrease in activation of Akt was also dependent on treatment duration.

Downregulation of PI3K/Akt pathways is a well known function of PTEN. However, there are some evidences indicating that PTEN can also downregulate Erk1/2 signaling pathway [129, 130]. Therefore, we have performed Western blot to detect the phosphorylation status of Erk1/2 in HeLa cells treated for long time with CR1-GST.

As shown in Figure 4.25b, prolonged treatment with CR1-GST reduced the amount of phosphorylated Erk1/2.

Apart from the Erk1/2 pathway, there are two other MAPK signaling pathways. These are Jun N-terminal kinase (JNK) and p38 MAPK pathways. These pathways are activated by wide varieties of environmental stimuli, including stress [131]. These two pathways work in context-specific and cell type-specific manner to integrate signals that affect proliferation, differentiation, survival and migration [132, 133]. Activation of JNK pathway often leads to reduced cell proliferation, cell cycle arrest and even apoptosis [133-135]. We have done Western blots to detect the phosphorylation status of JNK and p38. As shown in Figure 4.26, prolonged treatment with CR1-GST increased the phosphorylation of JNK in HeLa cells. But, phosphorylation status of p38 remained unchanged. It is clear from Figure 4.25 and 4.26 that activation of JNK is synchronized with increase in PTEN. Recent investigations have shown that PTEN can regulate activity of JNK [136, 137]. In studies involving ischemic brain injury, Zhang *et al.* [137] have shown that inhibition of PTEN expression decreases phosphorylation of JNK. They have shown that increased Akt activation inversely correlates with activation of JNK1/2. However, the exact molecular connectivity between PI3K/Akt and JNK pathways are not known. Therefore, the activation of JNK in CR1-GST treated HeLa cells may have originated through inhibition of PI3K/Akt pathway or by Akt independent mechanism of PTEN.

We have observed reduced proliferation of HeLa cells when treated with recombinant CR-1, both in presence and in absence of serum. However, Western blot experiments for signal transduction pathways involving protein phosphorylation are usually performed using cells maintained in serum starved condition. Serum starvation reduces background phosphorylation of signaling molecules. Western blots shown in Figure 4.25b and 4.26 have been performed using HeLa cells maintained in serum starved condition. One can argue that the results obtained in these experiments may have originated due to the stress created by serum starvation and are not a signature of CR-1 activity in these cells. Therefore, we have performed additional Western blot experiments with HeLa cells treated with CR1-GST in presence of serum. The results of these blots are shown in Figure 4.27. The increase in PTEN and phosphorylated JNK is quite evident in this experiment too. Though not visually very obvious,

densitometric analysis (Figure 4.27b) showed decrease in phosphorylation of Akt in CR1-GST treated cells. The dynamics of increase of PTEN, phospho-JNK and decrease in phospho-Akt is slower when the experiment was done in presence of serum. This is expected as growth factors present in the serum provides signals for proliferation and survival, thus opposing the anti-proliferative pathway of CR-1.

Our Western blot experiments have clearly elucidated that treatment with recombinant CR-1 increases PTEN, activates JNK and downregulates pro-proliferating Erk1/2 MAPK and PI3K/Akt pathways in HeLa cells. The signals through MAPK and PI3K/Akt pathways converge to modulate key molecules that control cell cycle. One such key molecule is $p27^{Kip1}$. To further elucidate the molecular mechanism that may be attributed to the increase in doubling time of CR-1 treated HeLa cells, we performed Western blot experiment for $p27^{Kip1}$. As a Cdk inhibitor, $p27^{Kip1}$ inhibits several cyclin-Cdk complexes involved in G1 and S phases, leading to reduced cell proliferation. Activity of $p27^{Kip1}$ is regulated by several mechanisms: change in expression, modulation of degradation and cellular localization [138, 139]. PTEN and PI3K/Akt pathway can regulate $p27^{Kip1}$ (Figure 4.28a). Members of Forkhead box transcription factor family induce expression of p27Kip1. Activated Akt phosphorylates these transcription factors, preventing their nuclear localization, leading to downregulation of $p27^{Kip1}$ expression [140]. Increase in expression of PTEN leads to upregulation of $p27^{Kip1}$ and such increase in $p27^{Kip1}$ is crucial for PTEN dependent growth arrest [141, 142]. PTEN dependent upregulation of $p27^{Kip1}$ is usually achieved through downregulation of Akt and subsequent nuclear localization of transcription factors. Like PI3K/Akt pathway, Erk1/2 MAPK pathway can also reduce expression of p27Kip1 [143]. The amount of $p27^{Kip1}$ in a cell is also regulated by ubiquitin-dependent proteolytic pathway. PTEN downregulates degradation of $p27^{Kip1}$. PTEN negatively regulates expression of S-phase kinase-associated protein 2 (SKP2) which is required for ubiquitin-dependent degradation of $p27^{Kip1}$ [144]. Treatment with recombinant CR-1 induces PTEN and downregulates PI3K/Akt and Erk1/2 pathways in HeLa cells. In accordance to this, we observed that CR1-GST upregulates the level of $p27^{Kip1}$ in HeLa cells (Figure 4.28b).

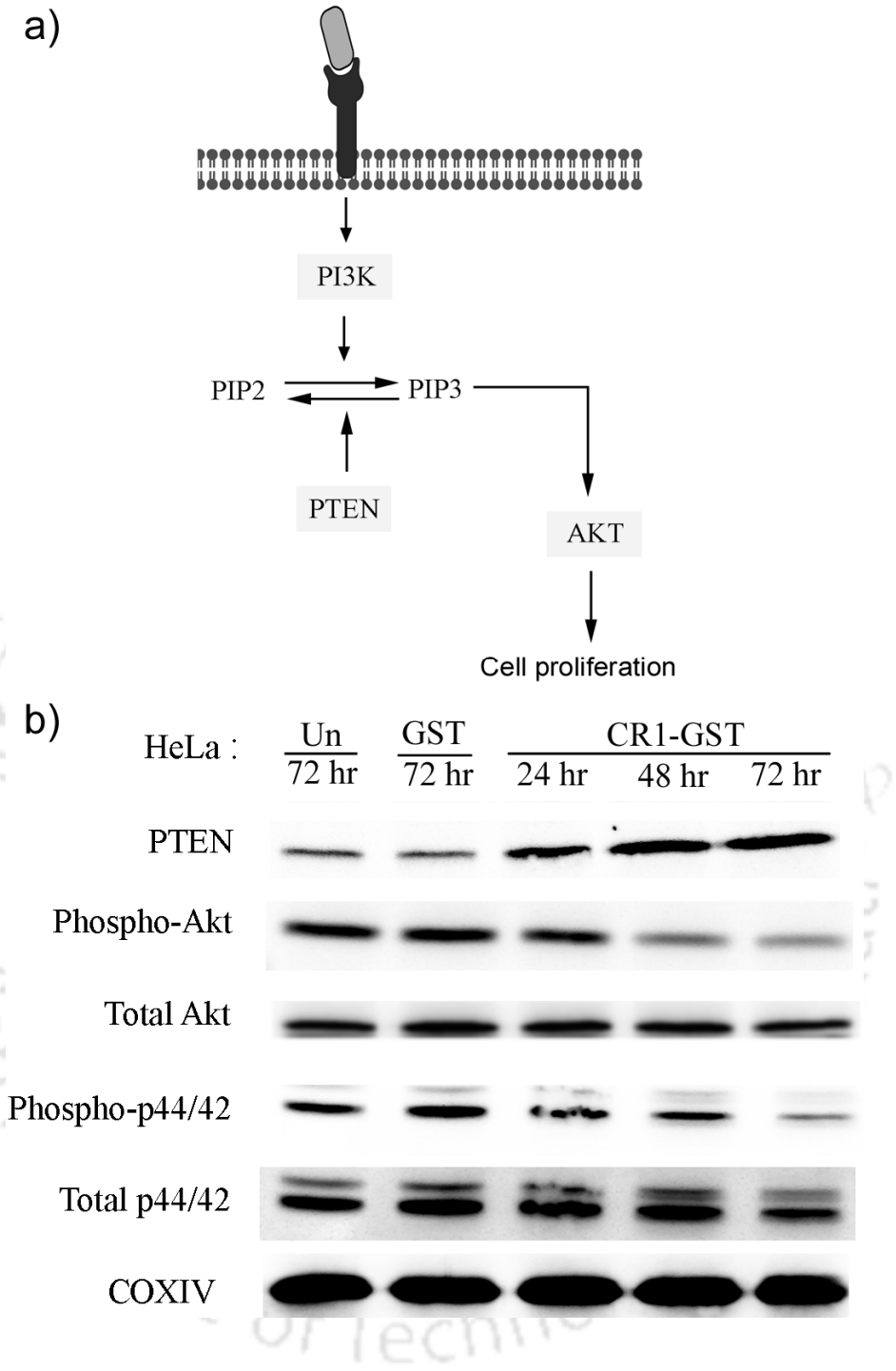

Figure 4.25 CR1-GST induces expression of PTEN. a) Simplified network diagram to show the role of PTEN in control of PI3K/Akt pathway. PTEN dephosphorylates PIP3 leading to reduced phosphorylation of Akt. b) Western blots to detect status of PTEN, Akt and p44/42. HeLa cells were treated with either CR1-GST (200 ng/ml for 24 hr, 48 hr and 72 hr) or GST (200 ng/ml for 72 hr) or left untreated for 72 hr in absence of serum. Expression of phosphorylated and total proteins was detected by Western Blot. Cox IV was used as loading control. Repeated experiments were performed and one representative blots are shown here. Un: Untreated cells.

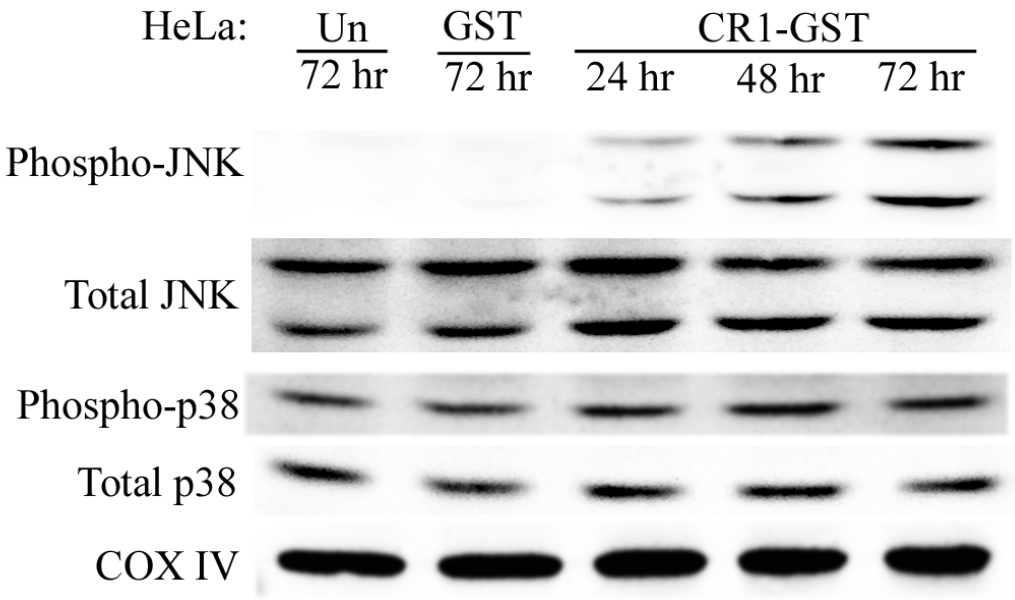

Figure 4.26 Effect of CR1-GST on JNK and p38 pathways. HeLa cells were treated with either CR1-GST (200 ng/ml for 24 hr, 48 hr and 72 hr) or GST (200 ng/ml for 72 hr) or left untreated for 72 hr in absence of serum. Expression of phosphorylated and total proteins was detected by Western Blot. Cox IV was used as loading control. Repeated experiments were performed and one representative blots are shown here. Un: Untreated cells.

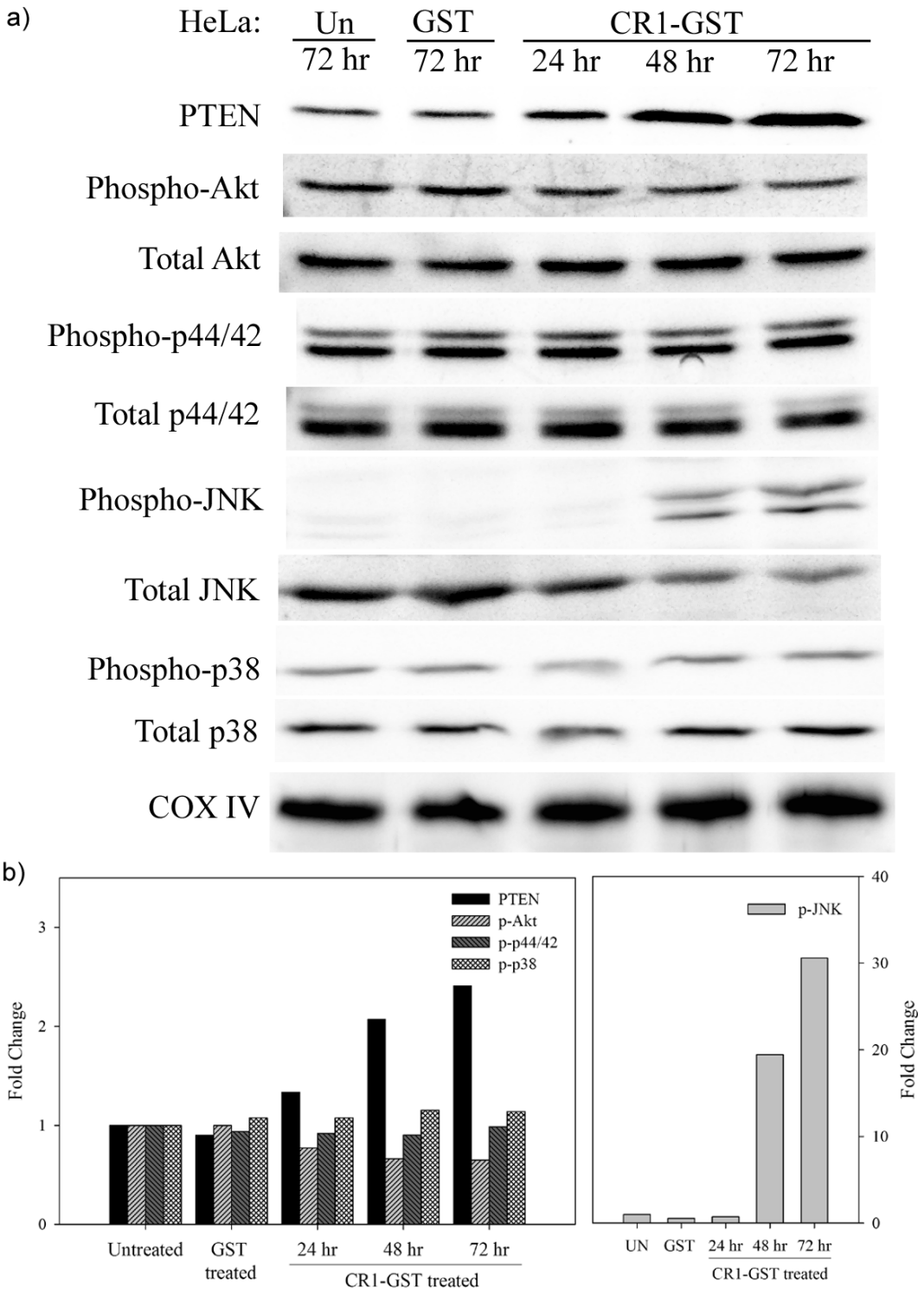

Figure 4.27 Western blots to detect effects of CR1-GST on different signaling molecules in HeLa cells maintained with serum. HeLa cells were treated with either CR1-GST (200 ng/ml for 24 hr, 48 hr and 72 hr) or GST (200 ng/ml for 72 hr) or left untreated for 72 hr in presence of serum. (a) Expression of phophorylated and total proteins was detected by Western Blot. Cox IV was used as loading control. (b) Densitometric analysis of Western blot data. Data of each treatment group was normalized with respect to untreated cells to calculate fold change. Un: Untreated cells.

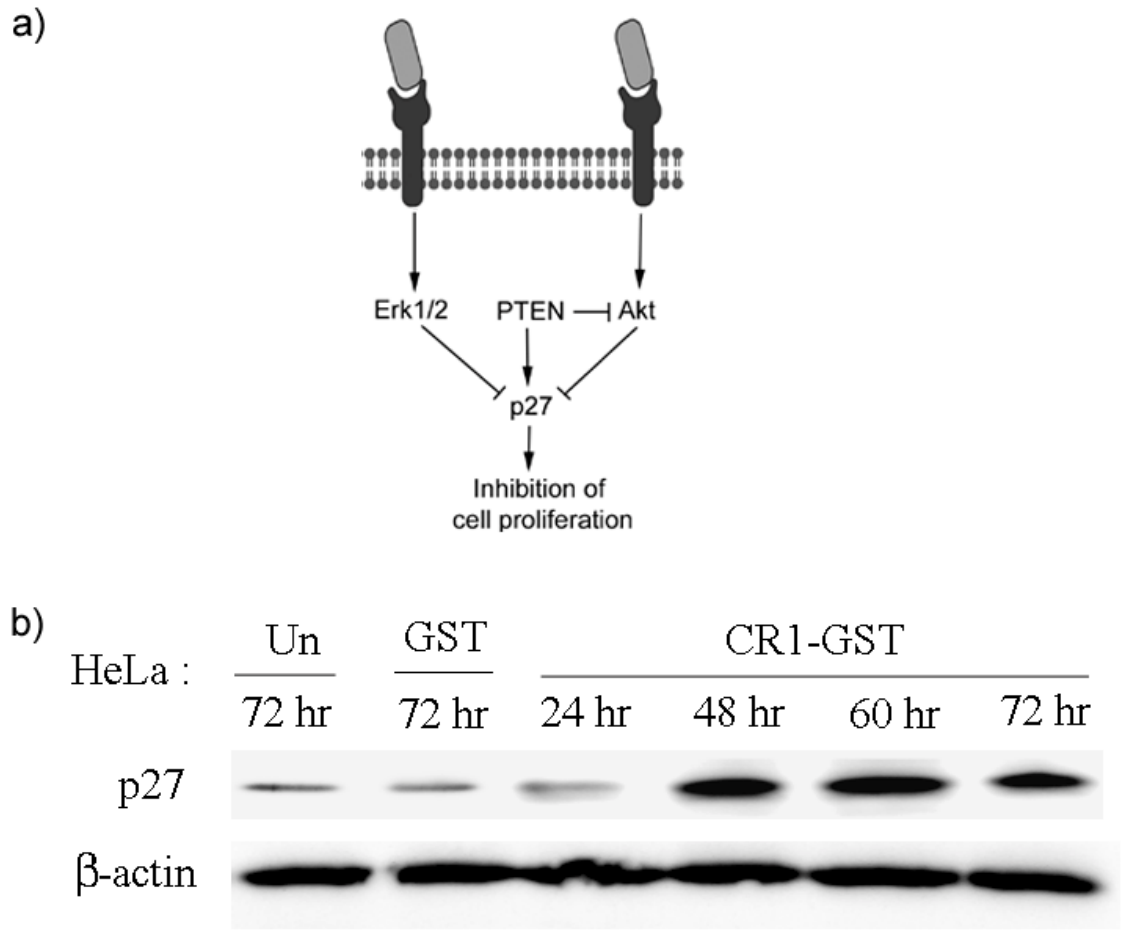

Figure 4.28 CR1-GST increases $p27^{Kip1}$ in HeLa cells. a) A simplified network diagram to show the control of p27Kip1 by PTEN, PI3K/Akt and Erk1/2 MAPK pathways. b) Western blot to detect $p27^{Kip1}$ in CR1-GST treated HeLa cells. HeLa cells were treated with either CR1-GST (200 ng/ml for 24 hr, 48 hr, 60hr and 72 hr) or GST (200 ng/ml for 72 hr) or left untreated for 72 hr in absence of serum. Expression of proteins was detected by Western Blot. β-actin was used as loading control. Un: Untreated cell

We have observed that the anti-proliferative pathway of CR-1 involves changes in levels of certain proteins, namely PTEN, and $p27^{Kip1}$. Phenomenon involving change in protein levels are usually delayed events and they can be modulated by interfering in processes of translation. In fact, changes in these key molecules happened only when HeLa cells were treated with CR1-GST for a long duration. We have also observed that the anti-proliferate effect is time-dependent. Therefore, we have investigated whether *de novo* protein synthesis is crucial for the anti-proliferative effect of CR-1. We have used Cycloheximide (CHX) in this investigation. Cycloheximide is a translation inhibitor, that blocks peptide chain elongation during protein synthesis [145]. HeLa cells were treated with different concentration of CHX alone for 48 hr in presence of serum. Viability of these treated cells was measured by MTT. The data is shown in the inset of Figure 4.29. As CHX causes global reduction in translation, treatment with CHX reduced proliferation of HeLa cells. Subsequently, we have treated HeLa cells with 200 ng/ml CR1-GST along with different concentrations of CHX. After 48 hr of treatment, viability was measured by MTT assay. The result is shown in Figure 4.29. Earlier we have shown that treatment with 200 ng/ml of CR1-GST reduces the viability of HeLa cells to ≤ 50% (Figure 4.9b). It is clear from Figure 4.29 that treatment with CHX blocks the anti-proliferative effect of CR1-GST in a dose-dependent fashion. This result confirmed that CR-1 mediated anti-proliferation pathway in HeLa cells is translation dependent.

As per our observations, PTEN is a key molecule in CR-1 mediated anti-proliferative pathway in HeLa cells. Treatment with CR1-GST fails to induce the mitogenic pathways in HeLa cells as expression of Glypican-1 is low, but increases PTEN that probably downregulates Akt and Erk1/2 pathways and upregulates $p27^{kip1}$. In contrast to HeLa cells, treatment with CR1-GST induces mitogenic pathways in U-87 MG cells. Treatment with growth factors usually triggers an early transient peak of activation of Erk1/2 and Akt [146, 147]. Similar observation has been made for Cripto-1 too [53, 54]. We have also observed such transient activation of these two molecules when U-87 MG cells were treated with CR1-GST. Subsequently, we looked into the status of Akt and Erk1/2 along with PTEN, JNK and p38 in U-87 MG cells after prolonged treatment with CR1-GST. In contrast to HeLa, U-87 MG is a PTEN null cell line due to homozygous mutation [148]. Therefore PTEN was not detected in these samples (Figure 4.30). Consequently, treatment with CR1-GST did

not lead to any change in the phosphorylation status of Akt, Erk1/2 and JNK (Figure 4.30).

We have used a systematic approach to understand the molecular mechanism behind the anti-proliferative effect of CR-1. All of our observations are shown in brief as a flowchart in Figure 4.31. We have shown that treatment with recombinant Cripto-1 reduces cell proliferation by increasing the doubling time of HeLa cells but induces proliferation in U-87 MG cells. Such differential effect indicates that this protein can activate both pro-proliferating and anti-proliferating pathways in a contextual fashion and the fate of the cell depends upon the relative strength of these two opposing pathways. In HeLa cells, the pro-proliferative pathways of CR-1 are very weak due to low expression of Glypican-1, whereas the same pathways are active in U-87 MG cells. On the other hand, the anti-proliferative pathway of CR-1 involving PTEN is active in HeLa cells but absent in PTEN null U-87 MG cells. The interactions between these two opposing pathways are shown in Figure 4.32. Though we have shown that the anti-proliferative pathway involves increase in PTEN and downregulation of PI3K/Akt and Erk1/2 pathways, the exact mechanism by which CR-1 increases PTEN is not known. Additionally, the biphasic effect of CR-1 on proliferation of U-87 MG cells can not be explained in terms of increase in PTEN, as it is a PTEN null cell line. Further investigations using U-87 MG may help to identify other pathways through which CR-1 may exert anti-proliferative effect.

The molecular signaling pathways, shown in Figure 4.32, expose an intriguing feature of CR-1 signaling. CR-1 can activate the PI3K/Akt pathway as well as can trigger the molecular mechanism that downregulates the same pathway. It can activate PI3K that catalyzes formation of PIP3, whereas it can also activate PTEN that catalyzes just the opposite reaction. This point of convergence of two opposing pathways constitutes a network motif which is known as Incoherent Feed-forward (Figure 4.33) [149]. Such network motifs can generate pulsed output and therefore can work as a self-limiting network motif. Pulsed output is quite common in mitogenic pathways. Treatment with growth factors usually triggers an early transient peak of activation of both Erk1/2 and Akt that decays fast to normal basal level [146, 147]. Such observation has also been made for Cripto-1 too [53, 54]. Such transient pulse of activation is crucial for determining the cell fate. It has been reported that transient activation of a mitogenic

pathway triggers cell proliferation, while sustained activation leads to cellular differentiation [97]. A negative feedback can also generate a transient pulse and such feedbacks are known to exist in mitogenic pathways [147, 150]. However, existence of incoherent feed-forward motifs in mitogenic pathways is not well documented. An important feature of an incoherent feed-forward motif is that it can provide robustness in cellular response. Robustness allows a cell to adapt in a noisy environment where the strength of input signals as well as concentrations of molecules of the signaling pathways varies. Robustness can be achieved through a feedback loop or by an incoherent feed-forward loop [151]. In case of an abrupt increase in input signal, such network motifs allow the output to transiently increase and then fall back to the basal level, thereby buffering the noise. Ma *et. al.* have shown that in comparison to feedback loops, incoherent feed-forward loops can provide robustness in a broader parameter space [151]. Although investigated extensively using mathematical tools, little work has been done to identify and understand incoherent feed-forward loops in real biological signaling pathways. Very recently, Takeda *et. al.* [152] have identified and analyzed an incoherent feed-forward loop in the chemotaxis pathway of *Dictyostelium*. They have shown that the input signal simultaneously activates the RasGEF and RasGAP. RasGEF activates Ras-GTP, whereas RasGAP deactivates Ras-GTP. They have further shown that this incoherent feed-forward loop provides robust activation of Ras in these cells. This incoherent feed-forward loop in Ras-GTP pathway is almost similar to what we have observed in CR-1 pathway. However, in our experimental system (*i.e.* HeLa cells) the positive path is very weak and did not allow us to check the capability of this network motif to provide robustness. Further experiments, with cells expressing both PTEN and Glypican-1 at an adequate level may help to further investigate this motif.

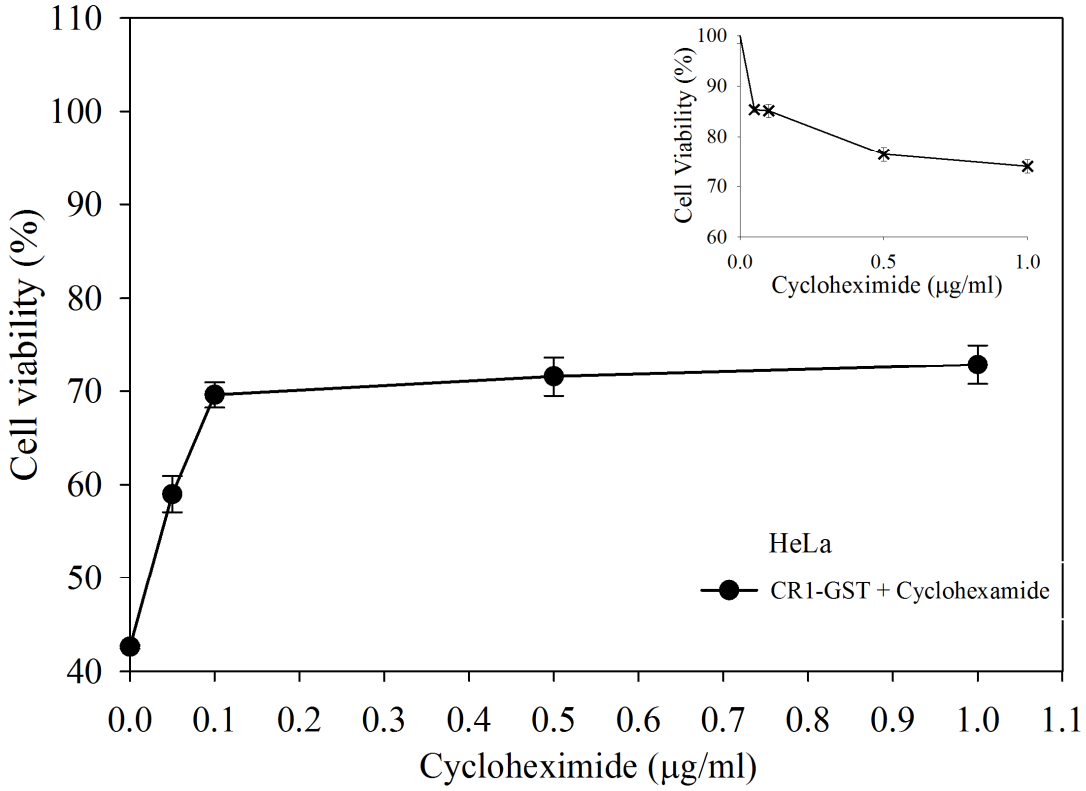

Figure 4.29 Anti-proliferative effect of CR1-GST is translation dependent. Combined effect of CR1-GST (200 ng/ml) and different concentrations of Cycloheximide (CHX), on HeLa cells after 48 hr of treatment in presence of serum was measured by MTT assay. Cell viability was estimated by dividing the measurement for treated cells by that of untreated cells. CHX is an inhibitor of translation. Effect of CHX alone on viability of HeLa cells is shown in inset.

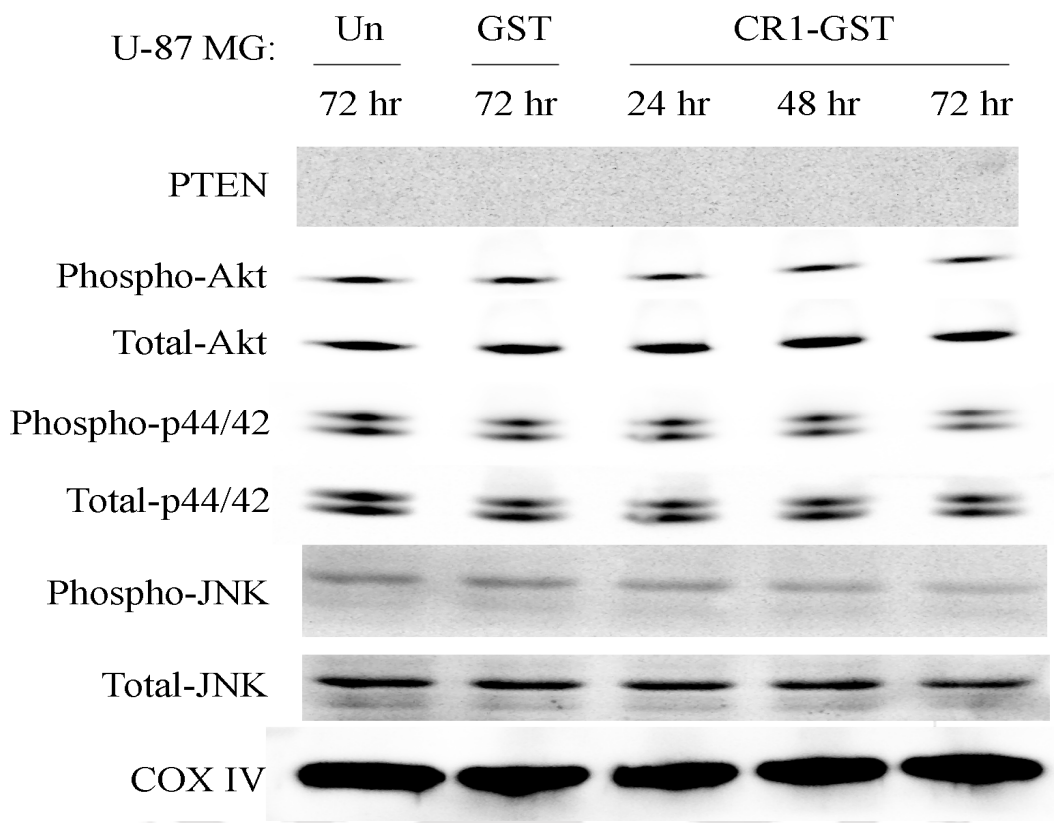

Figure 4.30 Treatment CR1-GST does not induce the anti-proliferative pathway involving PTEN in U-87 MG cells. U-87 MG is a PTEN-null cell line. U-87 MG cells were treated with either CR1-GST (200 ng/ml for 24 hr, 48 hr and 72 hr) or GST (200 ng/ml for 72 hr) or left untreated for 72 hr in absence of serum. Expression of phosphorylated and total proteins was detected by Western Blot. Cox IV was used as loading control. Un: Untreated cells.

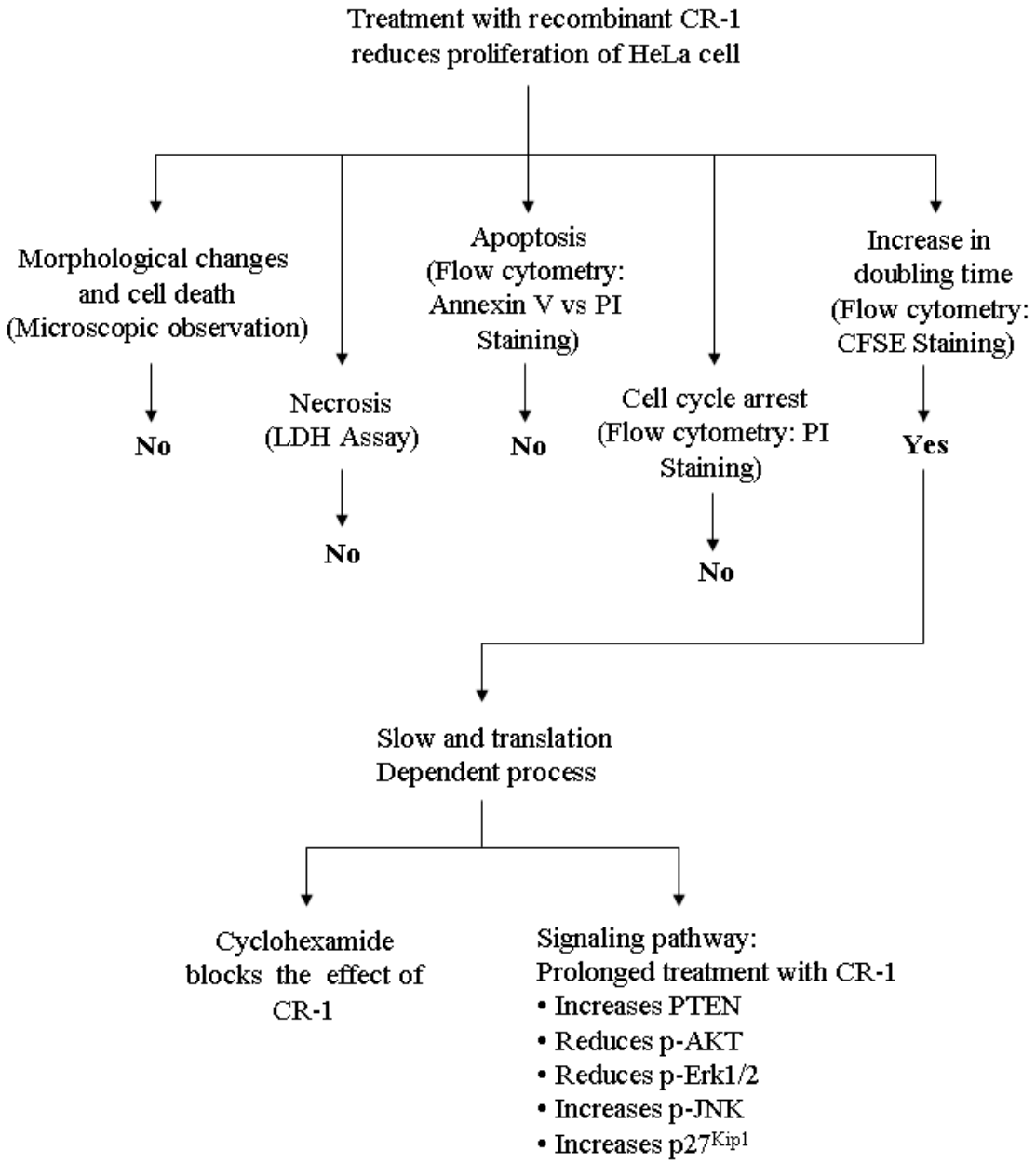

Figure 4.31 Flowchart to briefly explain our observations on the anti-proliferative effect of CR-1.

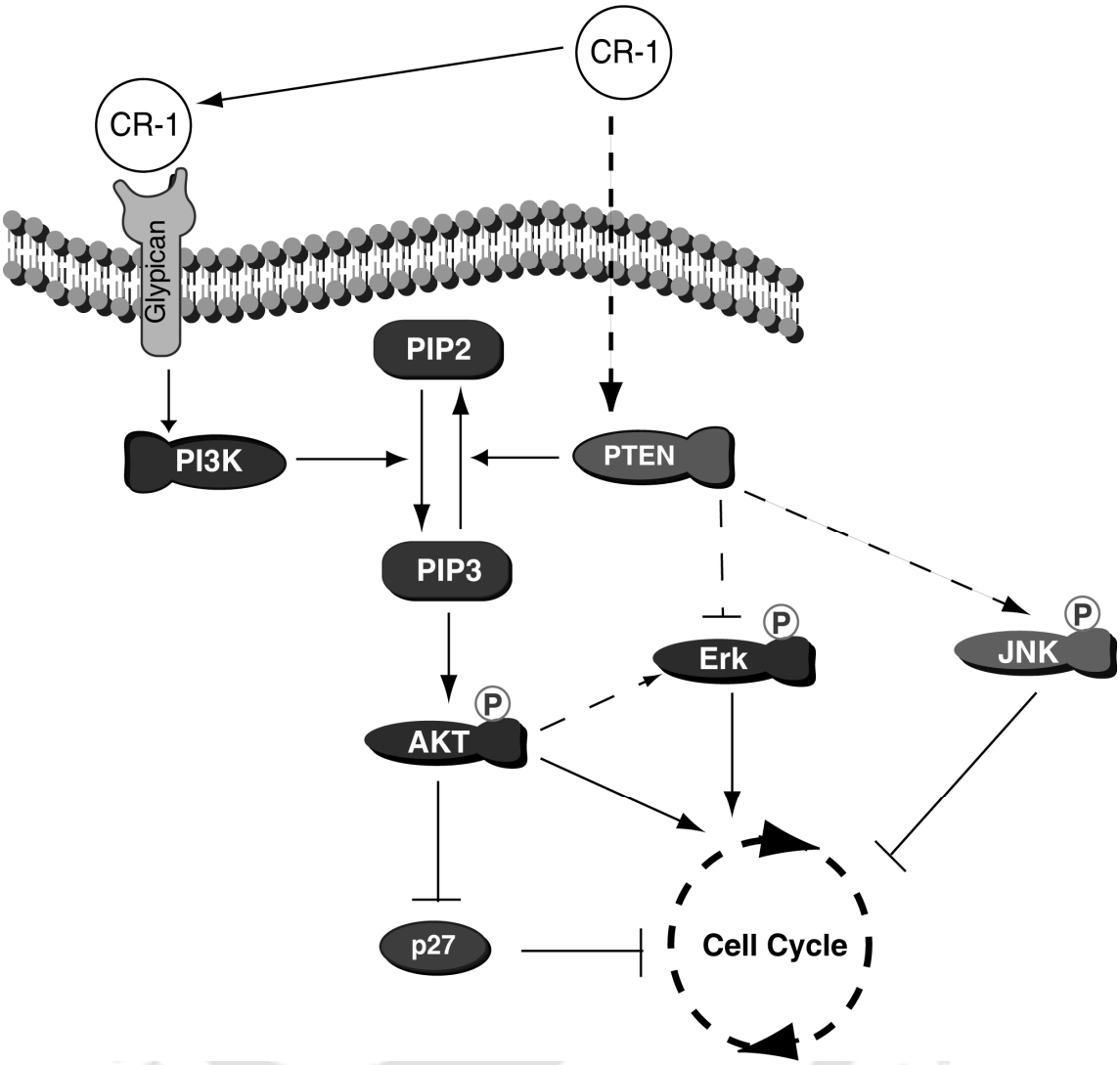

Figure 4.32 Schematic diagram to show the interactions between the anti-proliferative and pro-proliferative signaling pathways of Cripto-1. CR-1 induces proliferation through the well known mitogenic pathway involving Glypican-1/PI3K/Akt. This pathway is weak in HeLa cells due to low expression of Glypican-1. We have shown that CR-1 increases PTEN in HeLa cells, thereby inhibiting mitogenic PI3K/Akt and Erk1/2 MAPK pathway. Consequently it increases $p27^{Kip1}$ that acts as an inhibitor to cell cycle progression. Treatment with CR-1 also activates JNK that can reduce cell proliferation. The molecular mechanisms which are not clearly elucidated or not known are shown by dotted arrows. CR-1 can activate cell proliferation through several other pathways, including Glypican-1/Erk1/2 MAPK pathway. These pathways are not shown here to maintain clarity.

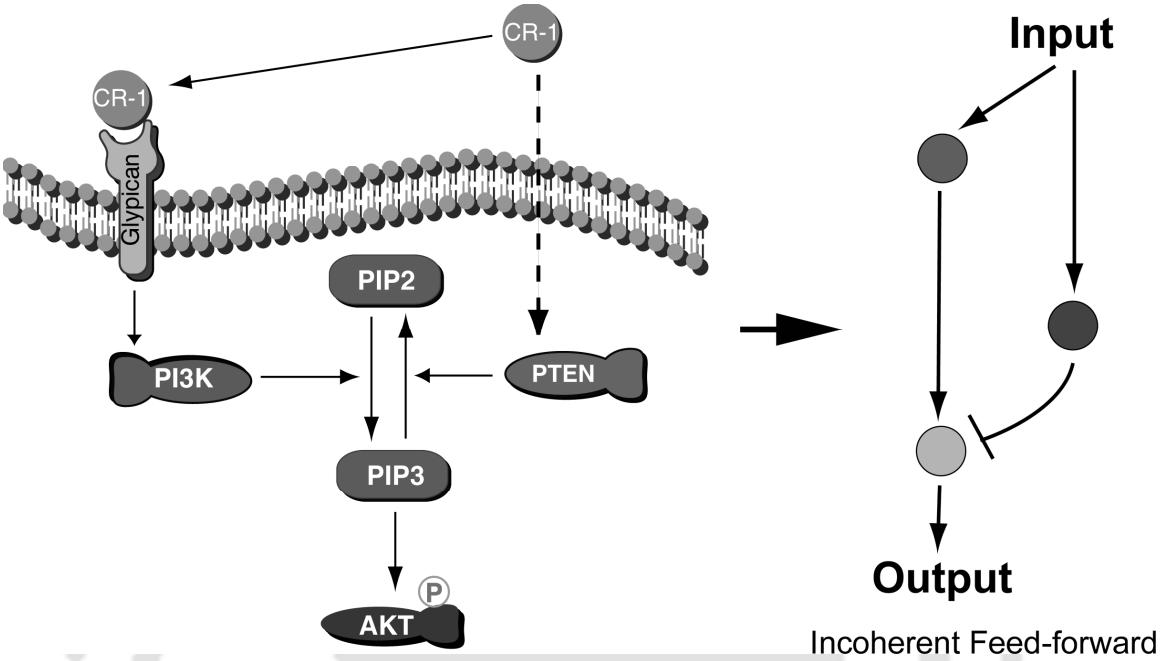

Figure 4.32 An Incoherent feed-forward motif in CR-1 signaling network. CR-1 (the input signal) generates PIP3 through Glypican-1/PI3K pathway. The same input signal (*i.e* CR-1) activates PTEN that reduces PIP3. Information transferred through these two opposing pathways converges on PIP3. Level of PIP3 determines the state of activation of Akt (the output). This type of incoherent feed-forward network motifs usually work as pulse generators, controlled signal attenuators, and are known to provide robustness.

5 Conclusions & Scope for future work

We have cloned, expressed and purified recombinant human Cripto-1 using an *E. coli* expression system. We have used this protein to understand the molecular signaling pathways of Cripto-1. Two different cell lines, U-87 MG and HeLa, were used in our work to elucidate and explore the contextual effect of CR-1 on cell proliferation. U-87 MG expresses Glypican-1, a cell surface molecule, through which CR-1 triggers mitogenic pathways. However, the expression of Glypican-1 is comparatively very low in HeLa cells. Treatment with recombinant CR-1 activates mitogenic pathways and triggers cell proliferation in U-87 MG cells. In contrast, we have shown that treatment with recombinant CR-1 monotonically reduces proliferation of HeLa cells in a dose- and time-dependent fashion. This anti-proliferative effect was re-confirmed using two other recombinant CR-1, one expressed in mammalian system and the other in insect expression system. Further, we have shown that inhibition of Erk1/2 MAPK and PI3K/Akt pathways potentiate the anti-proliferative effect of CR-1. These observations indicate that CR-1 can activate both pro- and anti-proliferative pathways in a cell and the fate of the cell depends upon the relative strength of these two opposing pathways.

Further, we have looked into the molecular mechanism of CR-1 induced reduction in proliferation of HeLa cells. We have shown that treatment with recombinant CR-1 does not induce necrosis or apoptosis of these cells. Such treatment does not even block cells in any phase of cell cycle. Rather, it was found that CR-1 reduces cell proliferation by increasing the doubling time of HeLa cells. Subsequently, we have investigated the signaling pathways that usually control progression of cell cycle. We have observed that treatment with recombinant CR-1 increases PTEN in HeLa cells. PTEN negatively regulates the PI3K/Akt pathway. Consequently, treatment with CR-1 reduces activation of Akt pathway in HeLa cells leading to increase in $p27^{Kip1}$ which is an inhibitor of cell cycle. It is now known that PI3K/Akt pathway has cross-talks with Erk1/2 pathway. We have also observed that treatment with recombinant CR-1 suppresses both Akt and Erk1/2 MAPK pathways in HeLa cells. Additionally, treatment with recombinant CR-1

activates JNK pathway in HeLa cells. This pathway is also known to inhibit cell proliferation. Therefore, treatment with CR-1 can activate two opposing processes: one that activates mitogenic PI3K/Akt and Erk1/2 MAPK pathways and the other that suppresses these pathways through increase in PTEN. In HeLa cells, the pro-proliferative pathways of CR-1 are very weak due to low expression of Glypican-1, whereas the same pathways are active in U-87 MG cells. On the other hand, anti-proliferative pathway of CR-1 involving PTEN is active in HeLa cells but absent in PTEN null U-87 MG cells.

This integration of two opposing pathways clearly explains the cell-specific effect of CR-1 that we have observed in our experiments. However, the exact mechanism by which CR-1 increases PTEN is still unknown to us and requires further explorations. PTEN is not expressed in U-87 MG cells. Therefore, the anti-proliferative pathway of CR-1 involving PTEN is not functional in U-87 MG cells. Still, we have observed that recombinant CR-1 induces proliferation of U-87 MG cells in a biphasic fashion with lesser proliferation at higher doses. This indicates that there must be additional mechanism, independent of PTEN, by which CR-1 can inhibit cell proliferation. Therefore, we require further investigations to identify all the components of CR-1 signaling circuit.

It should be noted that this is the first study to show that Cripto-1 can increase the doubling time of a cell and can modulate PTEN and JNK. This is also the first work to successfully express recombinant CR-1 in *E. coli* in soluble form without any additional step like *in vitro* refolding. Additionally, the results shown in this work lead us to a very interesting feature of CR-1 signaling. Treatment with recombinant CR-1 activates the PI3K/Akt pathway as well as triggers the molecular mechanism that downregulates the same pathway. It seems that the CR-1 signaling has an integral self-limiting control which can be contextually modulated to decide the fate of a cell. Such self-limiting control is crucial for any molecule that modulates proliferation and differentiation of a cell and is involved in embryonic development. As discussed earlier, convergence of two opposing pathways activated by CR-1 constitutes an Incoherent Feed-forward loop. Such loops are crucial for signal attenuation and can work as an ultra-sensitive switch. Mathematical modeling has proved that such a network motif is very efficient in dampening the effect of sudden change in input signals, thus helping in adaptation.

Signal transduction pathways are not static. The dynamics of information transfer in signaling network determines the eventual cellular behavior. The dynamics is controlled by multiple switches, integrators, feedbacks and feed-forwards. Understanding of these elements is crucial to understand the functioning of the signaling molecule. Observations made in the present work add newer elements in the known circuit of CR-1 signaling. Further investigations in this direction would help us to understand the complete design of this network.

Extensive work has been done to investigate expression of CR-1 in different types of cancer and its role in oncogenesis. These studies have confirmed the mitogenic role of CR-1. However, extrapolation and generalization of these observations may not be appropriate in all cellular systems. We have shown that CR-1 affects cell proliferation in cell-specific fashion. This contexuality depends upon molecules involved in CR-1 signaling. Loss of expression or mutation of PTEN is frequent in cancer cells. However, varying level of expression of PTEN has also been detected in different types of cancer. Similarly, expression of glypican-1 also varies with cell type. Therefore, expression of CR-1 will have different effects in different types of cancer cells. The emphasis of most of the works on the role of CR-1 in oncogensis lies on its effects on cancer cells. In contrast, little attention has been paid on the role of CR-1 in tumor microenvironment remodeling. Normal cells present in tumor microenvironment express functional PTEN and JNK. CR-1 expressed by tumor cells may induce the anti-proliferative pathways in the surrounding normal cells, affecting their proliferation and survival. Therefore, investigations on role of CR-1 on the survival and growth of normal cells present in a tumor microenvironment will be very interesting.

Bibliography

1. Shen, M.M., H. Wang, and P. Leder, *A differential display strategy identifies Cryptic, a novel EGF-related gene expressed in the axial and lateral mesoderm during mouse gastrulation.* Development, 1997. **124**(2): p. 429-42.
2. Kinoshita, N., J. Minshull, and M.W. Kirschner, *The identification of two novel ligands of the FGF receptor by a yeast screening method and their activity in Xenopus development.* Cell, 1995. **83**(4): p. 621-30.
3. Zhang, J., W.S. Talbot, and A.F. Schier, *Positional cloning identifies zebrafish one-eyed pinhead as a permissive EGF-related ligand required during gastrulation.* Cell, 1998. **92**(2): p. 241-51.
4. Shen, M.M. and A.F. Schier, *The EGF-CFC gene family in vertebrate development.* Trends Genet, 2000. **16**(7): p. 303-9.
5. Ciardiello, F., et al., *Differential expression of epidermal growth factor-related proteins in human colorectal tumors.* Proc Natl Acad Sci U S A, 1991. **88**(17): p. 7792-6.
6. Kuniyasu, H., et al., *Expression of cripto, a novel gene of the epidermal growth factor family, in human gastrointestinal carcinomas.* Jpn J Cancer Res, 1991. **82**(9): p. 969-73.
7. Friess, H., et al., *Cripto, a member of the epidermal growth factor family, is over-expressed in human pancreatic cancer and chronic pancreatitis.* Int J Cancer, 1994. **56**(5): p. 668-74.
8. Qi, C.F., et al., *Expression of transforming growth factor alpha, amphiregulin and cripto-1 in human breast carcinomas.* Br J Cancer, 1994. **69**(5): p. 903-10.
9. Brandt, R., et al., *Identification and biological characterization of an epidermal growth factor-related protein: cripto-1.* J Biol Chem, 1994. **269**(25): p. 17320-8.
10. Saloman, D.S., et al., *The EGF-CFC family: novel epidermal growth factor-related proteins in development and cancer.* Endocr Relat Cancer, 2000. **7**(4): p. 199-226.
11. Bianco, C., et al., *Cripto-1 indirectly stimulates the tyrosine phosphorylation of erb B-4 through a novel receptor.* J Biol Chem, 1999. **274**(13): p. 8624-9.
12. Bianco, C., et al., *Role of human cripto-1 in tumor angiogenesis.* J Natl Cancer Inst, 2005. **97**(2): p. 132-41.
13. Shi, S., et al., *The threonine that carries fucose, but not fucose, is required for Cripto to facilitate Nodal signaling.* J Biol Chem, 2007. **282**(28): p. 20133-41.

14. Seno, M., et al., *Purification and characterization of a recombinant human cripto-1 protein.* Growth Factors, 1998. **15**(3): p. 215-29.
15. Xu, C., et al., *Abrogation of the Cripto gene in mouse leads to failure of postgastrulation morphogenesis and lack of differentiation of cardiomyocytes.* Development, 1999. **126**(3): p. 483-94.
16. Minchiotti, G., et al., *Structure-function analysis of the EGF-CFC family member Cripto identifies residues essential for nodal signalling.* Development, 2001. **128**(22): p. 4501-10.
17. Bianco, C., et al., *Detection and localization of Cripto-1 binding in mouse mammary epithelial cells and in the mouse mammary gland using an immunoglobulin-cripto-1 fusion protein.* J Cell Physiol, 2002. **190**(1): p. 74-82.
18. Bianco, C., et al., *A Nodal- and ALK4-independent signaling pathway activated by Cripto-1 through Glypican-1 and c-Src.* Cancer Res, 2003. **63**(6): p. 1192-7.
19. Yan, Y.T., et al., *Dual roles of Cripto as a ligand and coreceptor in the nodal signaling pathway.* Mol Cell Biol, 2002. **22**(13): p. 4439-49.
20. Bianco, C., et al., *Identification of Cripto-1 in human milk.* Breast Cancer Res Treat, 2001. **66**(1): p. 1-7.
21. Bianco, C., et al., *Identification of cripto-1 as a novel serologic marker for breast and colon cancer.* Clin Cancer Res, 2006. **12**(17): p. 5158-64.
22. Baldassarre, G., et al., *Expression of teratocarcinoma-derived growth factor-1 (TDGF-1) in testis germ cell tumors and its effects on growth and differentiation of embryonal carcinoma cell line NTERA2/D1.* Oncogene, 1997. **15**(8): p. 927-36.
23. De Santis, M.L., et al., *Cripto-1 inhibits beta-casein expression in mammary epithelial cells through a p21ras-and phosphatidylinositol 3'-kinase-dependent pathway.* Cell Growth Differ, 1997. **8**(12): p. 1257-66.
24. Ciccodicola, A., et al., *Molecular characterization of a gene of the 'EGF family' expressed in undifferentiated human NTERA2 teratocarcinoma cells.* Embo J, 1989. **8**(7): p. 1987-91.
25. Scognamiglio, B., et al., *Assignment of human teratocarcinoma derived growth factor (TDGF) sequences to chromosomes 2q37, 3q22, 6p25 and 19q13.1.* Cytogenet Cell Genet, 1999. **84**(3-4): p. 220-4.
26. Minchiotti, G., et al., *Role of the EGF-CFC gene cripto in cell differentiation and embryo development.* Gene, 2002. **287**(1-2): p. 33-7.
27. Niemeyer, C.C., M.G. Persico, and E.D. Adamson, *Cripto: roles in mammary cell growth, survival, differentiation and transformation.* Cell Death Differ, 1998. **5**(5): p. 440-9.

28. Kenney, N.J., et al., *Detection and location of amphiregulin and Cripto-1 expression in the developing postnatal mouse mammary gland.* Mol Reprod Dev, 1995. **41**(3): p. 277-86.
29. Bhattacharya, B., et al., *Gene expression in human embryonic stem cell lines: unique molecular signature.* Blood, 2004. **103**(8): p. 2956-64.
30. Hu, X.F. and P.X. Xing, *Cripto as a target for cancer immunotherapy.* Expert Opin Ther Targets, 2005. **9**(2): p. 383-94.
31. Herrington, E.E., et al., *Expression of epidermal growth factor-related proteins in the aged adult mouse mammary gland and their relationship to tumorigenesis.* J Cell Physiol, 1997. **170**(1): p. 47-56.
32. Fontanini, G., et al., *Evaluation of epidermal growth factor-related growth factors and receptors and of neoangiogenesis in completely resected stage I-IIIA non-small-cell lung cancer: amphiregulin and microvessel count are independent prognostic indicators of survival.* Clin Cancer Res, 1998. **4**(1): p. 241-9.
33. D'Antonio, A., et al., *Transforming growth factor alpha, amphiregulin and cripto-1 are frequently expressed in advanced human ovarian carcinomas.* Int J Oncol, 2002. **21**(5): p. 941-8.
34. Ding, J., et al., *Cripto is required for correct orientation of the anterior-posterior axis in the mouse embryo.* Nature, 1998. **395**(6703): p. 702-7.
35. Warga, R.M. and D.A. Kane, *One-eyed pinhead regulates cell motility independent of Squint/Cyclops signaling.* Dev Biol, 2003. **261**(2): p. 391-411.
36. Bamford, R.N., et al., *Loss-of-function mutations in the EGF-CFC gene CFC1 are associated with human left-right laterality defects.* Nat Genet, 2000. **26**(3): p. 365-9.
37. Salomon, D.S., C. Bianco, and M. De Santis, *Cripto: a novel epidermal growth factor (EGF)-related peptide in mammary gland development and neoplasia.* Bioessays, 1999. **21**(1): p. 61-70.
38. Bianco, C., et al., *Cripto-1: an oncofetal gene with many faces.* Curr Top Dev Biol, 2005. **67**: p. 85-133.
39. Normanno, N., et al., *Cripto-1 overexpression leads to enhanced invasiveness and resistance to anoikis in human MCF-7 breast cancer cells.* J Cell Physiol, 2004. **198**(1): p. 31-9.
40. Wechselberger, C., et al., *Human Cripto-1 overexpression in the mouse mammary gland results in the development of hyperplasia and adenocarcinoma.* Oncogene, 2005. **24**(25): p. 4094-105.
41. Normanno, N., et al., *CRIPTO-1: a novel target for therapeutic intervention in human carcinoma.* Int J Oncol, 2004. **25**(4): p. 1013-20.

42. Strizzi, L., et al., *Cripto-1: a multifunctional modulator during embryogenesis and oncogenesis.* Oncogene, 2005. **24**(37): p. 5731-41.
43. Ciardiello, F., et al., *Expression of cripto, a novel gene of the epidermal growth factor gene family, leads to in vitro transformation of a normal mouse mammary epithelial cell line.* Cancer Res, 1991. **51**(3): p. 1051-4.
44. Strizzi, L., et al., *Epithelial mesenchymal transition is a characteristic of hyperplasias and tumors in mammary gland from MMTV-Cripto-1 transgenic mice.* J Cell Physiol, 2004. **201**(2): p. 266-76.
45. Savagner, P., *Leaving the neighborhood: molecular mechanisms involved during epithelial-mesenchymal transition.* Bioessays, 2001. **23**(10): p. 912-23.
46. Steinert, P.M. and D.R. Roop, *Molecular and cellular biology of intermediate filaments.* Annu Rev Biochem, 1988. **57**: p. 593-625.
47. Gilles, C., et al., *Vimentin contributes to human mammary epithelial cell migration.* J Cell Sci, 1999. **112 (Pt 24)**: p. 4615-25.
48. Ebert, A.D., et al., *Cripto-1-induced increase in vimentin expression is associated with enhanced migration of human Caski cervical carcinoma cells.* Exp Cell Res, 2000. **257**(1): p. 223-9.
49. Bianco, C., et al., *Role of the cripto (EGF-CFC) family in embryogenesis and cancer.* Growth Factors, 2004. **22**(3): p. 133-9.
50. Zhang, W. and H.T. Liu, *MAPK signal pathways in the regulation of cell proliferation in mammalian cells.* Cell Res, 2002. **12**(1): p. 9-18.
51. Bianco, C., et al., *Cripto-1 activates nodal- and ALK4-dependent and -independent signaling pathways in mammary epithelial Cells.* Mol Cell Biol, 2002. **22**(8): p. 2586-97.
52. Bianco, C., et al., *Activation of a Nodal-independent signaling pathway by Cripto-1 mutants with impaired activation of a Nodal-dependent signaling pathway.* FEBS Lett, 2008. **582**(29): p. 3997-4002.
53. Kannan, S., et al., *Cripto enhances the tyrosine phosphorylation of Shc and activates mitogen-activated protein kinase (MAPK) in mammary epithelial cells.* J Biol Chem, 1997. **272**(6): p. 3330-5.
54. Ebert, A.D., et al., *Cripto-1 induces phosphatidylinositol 3'-kinase-dependent phosphorylation of AKT and glycogen synthase kinase 3beta in human cervical carcinoma cells.* Cancer Res, 1999. **59**(18): p. 4502-5.
55. Kuan, C.T., C.J. Wikstrand, and D.D. Bigner, *EGF mutant receptor vIII as a molecular target in cancer therapy.* Endocr Relat Cancer, 2001. **8**(2): p. 83-96.
56. Turner, N. and R. Grose, *Fibroblast growth factor signalling: from development to cancer.* Nat Rev Cancer. **10**(2): p. 116-29.
57. Shi, Y. and J. Massague, *Mechanisms of TGF-beta signaling from cell membrane to the nucleus.* Cell, 2003. **113**(6): p. 685-700.

58. Gray, P.C., et al., *Cripto binds transforming growth factor beta (TGF-beta) and inhibits TGF-beta signaling.* Mol Cell Biol, 2006. **26**(24): p. 9268-78.
59. Shani, G., et al., *GRP78 and Cripto form a complex at the cell surface and collaborate to inhibit transforming growth factor beta signaling and enhance cell growth.* Mol Cell Biol, 2008. **28**(2): p. 666-77.
60. Massague, J., *TGF-beta signal transduction.* Annu Rev Biochem, 1998. **67**: p. 753-91.
61. Schier, A.F. and M.M. Shen, *Nodal signalling in vertebrate development.* Nature, 2000. **403**(6768): p. 385-9.
62. Foley, S.F., et al., *The CRIPTO/FRL-1/CRYPTIC (CFC) domain of human Cripto. Functional and structural insights through disulfide structure analysis.* Eur J Biochem, 2003. **270**(17): p. 3610-8.
63. Yeo, C. and M. Whitman, *Nodal signals to Smads through Cripto-dependent and Cripto-independent mechanisms.* Mol Cell, 2001. **7**(5): p. 949-57.
64. Reissmann, E., et al., *The orphan receptor ALK7 and the Activin receptor ALK4 mediate signaling by Nodal proteins during vertebrate development.* Genes Dev, 2001. **15**(15): p. 2010-22.
65. Morkel, M., et al., *Beta-catenin regulates Cripto- and Wnt3-dependent gene expression programs in mouse axis and mesoderm formation.* Development, 2003. **130**(25): p. 6283-94.
66. Adkins, H.B., et al., *Antibody blockade of the Cripto CFC domain suppresses tumor cell growth in vivo.* J Clin Invest, 2003. **112**(4): p. 575-87.
67. Xing, P.X., et al., *Cripto: a novel target for antibody-based cancer immunotherapy*. Cancer Res, 2004. **64**(11): p. 4018-23.
68. *The TGF-β Family*. Cold Spring Harbor Monograph Series 50, ed. K.M. Rik Derynck. 2008: Cold Spring Harbor Laboratory Press.
69. Bruce Alberts, A.J., Julian Lewis, Martin Raff, Keith Roberts, and Peter Walter., *Molecular Biology of the Cell*. 4th edition ed. 2002.
70. Streuli, C.H. and N. Akhtar, *Signal co-operation between integrins and other receptor systems.* Biochem J, 2009. **418**(3): p. 491-506.
71. Aksamitiene, E., A. Kiyatkin, and B.N. Kholodenko, *Cross-talk between mitogenic Ras/MAPK and survival PI3K/Akt pathways: a fine balance.* Biochem Soc Trans. **40**(1): p. 139-46.
72. Hasson, P. and Z. Paroush, *Crosstalk between the EGFR and other signalling pathways at the level of the global transcriptional corepressor Groucho/TLE.* Br J Cancer, 2006. **94**(6): p. 771-5.
73. Albert, R., H. Jeong, and A.L. Barabasi, *Error and attack tolerance of complex networks.* Nature, 2000. **406**(6794): p. 378-82.

74. Lee, M.K., et al., *TGF-beta activates Erk MAP kinase signalling through direct phosphorylation of ShcA.* Embo J, 2007. **26**(17): p. 3957-67.
75. Moustakas, A., et al., *Mechanisms of TGF-beta signaling in regulation of cell growth and differentiation.* Immunol Lett, 2002. **82**(1-2): p. 85-91.
76. Li, C.Y., L. Suardet, and J.B. Little, *Potential role of WAF1/Cip1/p21 as a mediator of TGF-beta cytoinhibitory effect.* J Biol Chem, 1995. **270**(10): p. 4971-4.
77. Maliekal, T.T., R.J. Anto, and D. Karunagaran, *Differential activation of Smads in HeLa and SiHa cells that differ in their response to transforming growth factor-beta.* J Biol Chem, 2004. **279**(35): p. 36287-92.
78. Roberts, A.B., et al., *Type beta transforming growth factor: a bifunctional regulator of cellular growth.* Proc Natl Acad Sci U S A, 1985. **82**(1): p. 119-23.
79. Kawamoto, T., et al., *Relation of epidermal growth factor receptor concentration to growth of human epidermoid carcinoma A431 cells.* J Biol Chem, 1984. **259**(12): p. 7761-6.
80. Luciano, A.M., et al., *Epidermal growth factor inhibits large granulosa cell apoptosis by stimulating progesterone synthesis and regulating the distribution of intracellular free calcium.* Biol Reprod, 1994. **51**(4): p. 646-54.
81. Coles, H.S., J.F. Burne, and M.C. Raff, *Large-scale normal cell death in the developing rat kidney and its reduction by epidermal growth factor.* Development, 1993. **118**(3): p. 777-84.
82. Gulli, L.F., et al., *Epidermal growth factor-induced apoptosis in A431 cells can be reversed by reducing the tyrosine kinase activity.* Cell Growth Differ, 1996. **7**(2): p. 173-8.
83. Armstrong, D.K., et al., *Epidermal growth factor-mediated apoptosis of MDA-MB-468 human breast cancer cells.* Cancer Res, 1994. **54**(20): p. 5280-3.
84. Filmus, J., et al., *MDA-468, a human breast cancer cell line with a high number of epidermal growth factor (EGF) receptors, has an amplified EGF receptor gene and is growth inhibited by EGF.* Biochem Biophys Res Commun, 1985. **128**(2): p. 898-905.
85. Reddy, K.B., *Epidermal growth factor induced apoptosis.* Apoptosis, 1996. **1**(1): p. 33-39.
86. Song, J.Y., et al., *Epidermal growth factor competes with EGF receptor inhibitors to induce cell death in EGFR-overexpressing tumor cells.* Cancer Lett, 2009. **283**(2): p. 135-42.
87. Casaccia-Bonnefil, P., H. Kong, and M.V. Chao, *Neurotrophins: the biological paradox of survival factors eliciting apoptosis.* Cell Death Differ, 1998. **5**(5): p. 357-64.

88. Casaccia-Bonnefil, P., et al., *Death of oligodendrocytes mediated by the interaction of nerve growth factor with its receptor p75.* Nature, 1996. **383**(6602): p. 716-9.
89. Sedel, F., C. Bechade, and A. Triller, *Nerve growth factor (NGF) induces motoneuron apoptosis in rat embryonic spinal cord in vitro.* Eur J Neurosci, 1999. **11**(11): p. 3904-12.
90. Soilu-Hanninen, M., et al., *Nerve growth factor signaling through p75 induces apoptosis in Schwann cells via a Bcl-2-independent pathway.* J Neurosci, 1999. **19**(12): p. 4828-38.
91. Descamps, S., et al., *Nerve growth factor stimulates proliferation and survival of human breast cancer cells through two distinct signaling pathways.* J Biol Chem, 2001. **276**(21): p. 17864-70.
92. Molloy, N., H. , D.E. Read, and A.M. Gorman, *Nerve Growth Factor in Cancer Cell Death and Survival.* Cancers, 2011. **3**: p. 510-530.
93. Cordeiro, M.F., et al., *TGF-beta1, -beta2, and -beta3 in vitro: biphasic effects on Tenon's fibroblast contraction, proliferation, and migration.* Invest Ophthalmol Vis Sci, 2000. **41**(3): p. 756-63.
94. Krall, J.A., E.M. Beyer, and G. MacBeath, *High- and low-affinity epidermal growth factor receptor-ligand interactions activate distinct signaling pathways.* PLoS One, 2011. **6**(1): p. e15945.
95. De Santis, M.L., et al., *Cripto-1 induces apoptosis in HC-11 mouse mammary epithelial cells.* Cell Death Differ, 2000. **7**(2): p. 189-96.
96. Merlo, G.R., et al., *p53-dependent and p53-independent activation of apoptosis in mammary epithelial cells reveals a survival function of EGF and insulin.* J Cell Biol, 1995. **128**(6): p. 1185-96.
97. Marshall, C.J., *Specificity of receptor tyrosine kinase signaling: transient versus sustained extracellular signal-regulated kinase activation.* Cell, 1995. **80**(2): p. 179-85.
98. Tyson, J.J., K.C. Chen, and B. Novak, *Sniffers, buzzers, toggles and blinkers: dynamics of regulatory and signaling pathways in the cell.* Curr Opin Cell Biol, 2003. **15**(2): p. 221-31.
99. Alon, U., *Network motifs: theory and experimental approaches.* Nat Rev Genet, 2007. **8**(6): p. 450-61.
100. Cloutier, M. and E. Wang, *Dynamic modeling and analysis of cancer cellular network motifs.* Integr Biol (Camb), 2011. **3**(7): p. 724-32.
101. Chandarlapaty, S., et al., *AKT inhibition relieves feedback suppression of receptor tyrosine kinase expression and activity.* Cancer Cell, 2011. **19**(1): p. 58-71.

102. Carracedo, A. and P.P. Pandolfi, *The PTEN-PI3K pathway: of feedbacks and cross-talks.* Oncogene, 2008. **27**(41): p. 5527-41.
103. Fritsche-Guenther, R., et al., *Strong negative feedback from Erk to Raf confers robustness to MAPK signalling.* Mol Syst Biol, 2011. **7**: p. 489.
104. Bradford, M.M., *A rapid and sensitive method for the quantitation of microgram quantities of protein utilizing the principle of protein-dye binding.* Anal Biochem, 1976. **72**: p. 248-54.
105. Lowry, O.H., et al., *Protein measurement with the Folin phenol reagent.* J Biol Chem, 1951. **193**(1): p. 265-75.
106. Joseph Sambrook, D.R., *Molecular Cloning: A Laboratory Manual*. 3rd ed, Cold Spring Harbor, New York: Cold Spring Harbor Laboratory Press.
107. Laemmli, U.K., *Cleavage of structural proteins during the assembly of the head of bacteriophage T4.* Nature, 1970. **227**(5259): p. 680-5.
108. Ramakers, C., et al., *Assumption-free analysis of quantitative real-time polymerase chain reaction (PCR) data.* Neurosci Lett, 2003. **339**(1): p. 62-6.
109. Pfaffl, M.W., G.W. Horgan, and L. Dempfle, *Relative expression software tool (REST) for group-wise comparison and statistical analysis of relative expression results in real-time PCR.* Nucleic Acids Res, 2002. **30**(9): p. e36.
110. Mosmann, T., *Rapid colorimetric assay for cellular growth and survival: application to proliferation and cytotoxicity assays.* J Immunol Methods, 1983. **65**(1-2): p. 55-63.
111. Butler, M., *Cell Counting and Viability Measurements*, in *Animal Cell Biotechnology: Methods and Protocols*, J. N, Editor. 1999, Humana Press: New Jersey. p. 131-144.
112. Huong, P.L., et al., *Measurement of antigen specific lymphocyte proliferation using 5-bromo-deoxyuridine incorporation. An easy and low cost alternative to radioactive thymidine incorporation.* J Immunol Methods, 1991. **140**(2): p. 243-8.
113. Riccardi, C. and I. Nicoletti, *Analysis of apoptosis by propidium iodide staining and flow cytometry.* Nat Protoc, 2006. **1**(3): p. 1458-61.
114. Watanabe, K., et al., *Growth factor induction of Cripto-1 shedding by glycosylphosphatidylinositol-phospholipase D and enhancement of endothelial cell migration.* J Biol Chem, 2007. **282**(43): p. 31643-55.
115. Terpe, K., *Overview of bacterial expression systems for heterologous protein production: from molecular and biochemical fundamentals to commercial systems.* Appl Microbiol Biotechnol, 2006. **72**(2): p. 211-22.
116. Majno, G. and I. Joris, *Apoptosis, oncosis, and necrosis. An overview of cell death.* Am J Pathol, 1995. **146**(1): p. 3-15.

117. Koh, J.Y. and D.W. Choi, *Quantitative determination of glutamate mediated cortical neuronal injury in cell culture by lactate dehydrogenase efflux assay.* J Neurosci Methods, 1987. **20**(1): p. 83-90.
118. Quah, B.J., H.S. Warren, and C.R. Parish, *Monitoring lymphocyte proliferation in vitro and in vivo with the intracellular fluorescent dye carboxyfluorescein diacetate succinimidyl ester.* Nat Protoc, 2007. **2**(9): p. 2049-56.
119. Whitfield, M.L., et al., *Identification of genes periodically expressed in the human cell cycle and their expression in tumors.* Mol Biol Cell, 2002. **13**(6): p. 1977-2000.
120. Morgan, D.O., *The Cell Cycle: Principles of Control (Primers in Biology)*. 1 ed. 2006, London: New Science Press, Ltd.
121. Mitsuhashi, T., et al., *Overexpression of p27Kip1 lengthens the G1 phase in a mouse model that targets inducible gene expression to central nervous system progenitor cells.* Proc Natl Acad Sci U S A, 2001. **98**(11): p. 6435-40.
122. Zou, L., Z. Ding, and P. Roy, *Profilin-1 overexpression inhibits proliferation of MDA-MB-231 breast cancer cells partly through p27kip1 upregulation.* J Cell Physiol. **223**(3): p. 623-9.
123. Scandura, J.M., et al., *Transforming growth factor beta-induced cell cycle arrest of human hematopoietic cells requires p57KIP2 up-regulation.* Proc Natl Acad Sci U S A, 2004. **101**(42): p. 15231-6.
124. Volakaki, A.A., et al., *Essential role of p21/waf1 in the mediation of the anti-proliferative effects of GHRH antagonist JMR-132.* J Mol Endocrinol, 2008. **41**(5): p. 389-92.
125. Vazquez, F. and W.R. Sellers, *The PTEN tumor suppressor protein: an antagonist of phosphoinositide 3-kinase signaling.* Biochim Biophys Acta, 2000. **1470**(1): p. M21-35.
126. Radu, A., et al., *PTEN induces cell cycle arrest by decreasing the level and nuclear localization of cyclin D1.* Mol Cell Biol, 2003. **23**(17): p. 6139-49.
127. Davies, M.A., et al., *Adenoviral-mediated expression of MMAC/PTEN inhibits proliferation and metastasis of human prostate cancer cells.* Clin Cancer Res, 2002. **8**(6): p. 1904-14.
128. Seminario, M.C., et al., *PTEN expression in PTEN-null leukaemic T cell lines leads to reduced proliferation via slowed cell cycle progression.* Oncogene, 2003. **22**(50): p. 8195-204.
129. Chetram, M.A., V. Odero-Marah, and C.V. Hinton, *Loss of PTEN permits CXCR4-mediated tumorigenesis through ERK1/2 in prostate cancer cells.* Mol Cancer Res, 2011. **9**(1): p. 90-102.

130. Chung, J.H., et al., *The ERK1/2 pathway modulates nuclear PTEN-mediated cell cycle arrest by cyclin D1 transcriptional regulation.* Hum Mol Genet, 2006. **15**(17): p. 2553-9.
131. Davis, R.J., *Signal transduction by the JNK group of MAP kinases.* Cell, 2000. **103**(2): p. 239-52.
132. Wada, T. and J.M. Penninger, *Mitogen-activated protein kinases in apoptosis regulation.* Oncogene, 2004. **23**(16): p. 2838-49.
133. Wagner, E.F. and A.R. Nebreda, *Signal integration by JNK and p38 MAPK pathways in cancer development.* Nat Rev Cancer, 2009. **9**(8): p. 537-49.
134. Lin, A. and B. Dibling, *The true face of JNK activation in apoptosis.* Aging Cell, 2002. **1**(2): p. 112-6.
135. Ordan, O., et al., *Stress-responsive JNK mitogen-activated protein kinase mediates aspirin-induced suppression of B16 melanoma cellular proliferation.* Br J Pharmacol, 2003. **138**(6): p. 1156-62.
136. Vivanco, I., et al., *Identification of the JNK signaling pathway as a functional target of the tumor suppressor PTEN.* Cancer Cell, 2007. **11**(6): p. 555-69.
137. Zhang, Q.G., et al., *Critical role of PTEN in the coupling between PI3K/Akt and JNK1/2 signaling in ischemic brain injury.* FEBS Lett, 2007. **581**(3): p. 495-505.
138. le Sage, C., R. Nagel, and R. Agami, *Diverse ways to control p27Kip1 function: miRNAs come into play.* Cell Cycle, 2007. **6**(22): p. 2742-9.
139. Vervoorts, J. and B. Luscher, *Post-translational regulation of the tumor suppressor p27(KIP1).* Cell Mol Life Sci, 2008. **65**(20): p. 3255-64.
140. Stahl, M., et al., *The forkhead transcription factor FoxO regulates transcription of p27Kip1 and Bim in response to IL-2.* J Immunol, 2002. **168**(10): p. 5024-31.
141. Bruni, P., et al., *PTEN expression is reduced in a subset of sporadic thyroid carcinomas: evidence that PTEN-growth suppressing activity in thyroid cancer cells mediated by p27kip1.* Oncogene, 2000. **19**(28): p. 3146-55.
142. Li, D.M. and H. Sun, *PTEN/MMAC1/TEP1 suppresses the tumorigenicity and induces G1 cell cycle arrest in human glioblastoma cells.* Proc Natl Acad Sci U S A, 1998. **95**(26): p. 15406-11.
143. Rivard, N., et al., *MAP kinase cascade is required for p27 downregulation and S phase entry in fibroblasts and epithelial cells.* Am J Physiol, 1999. **277**(4 Pt 1): p. C652-64.
144. Mamillapalli, R., et al., *PTEN regulates the ubiquitin-dependent degradation of the CDK inhibitor p27(KIP1) through the ubiquitin E3 ligase SCF(SKP2).* Curr Biol, 2001. **11**(4): p. 263-7.
145. Baliga, B.S., A.W. Pronczuk, and H.N. Munro, *Mechanism of cycloheximide inhibition of protein synthesis in a cell-free system prepared from rat liver.* J Biol Chem, 1969. **244**(16): p. 4480-9.

146. Kumar, N., et al., *Quantitative analysis of Akt phosphorylation and activity in response to EGF and insulin treatment.* Biochem Biophys Res Commun, 2007. **354**(1): p. 14-20.
147. Borisov, N., et al., *Systems-level interactions between insulin-EGF networks amplify mitogenic signaling.* Mol Syst Biol, 2009. **5**: p. 256.
148. Pore, N., et al., *PTEN mutation and epidermal growth factor receptor activation regulate vascular endothelial growth factor (VEGF) mRNA expression in human glioblastoma cells by transactivating the proximal VEGF promoter.* Cancer Res, 2003. **63**(1): p. 236-41.
149. Mangan, S. and U. Alon, *Structure and function of the feed-forward loop network motif.* Proc Natl Acad Sci U S A, 2003. **100**(21): p. 11980-5.
150. Amit, I., et al., *A module of negative feedback regulators defines growth factor signaling.* Nat Genet, 2007. **39**(4): p. 503-12.
151. Ma, W., et al., *Defining network topologies that can achieve biochemical adaptation.* Cell, 2009. **138**(4): p. 760-73.
152. Takeda, K., et al., *Incoherent feedforward control governs adaptation of activated ras in a eukaryotic chemotaxis pathway.* Sci Signal. **5**(205): p. ra2.

Appendix

General reagents: Acetic acid, chloroform, di-sodium hydrogen phosphate, glycerol, hydrochloric acid, isopropyl alcohol, isoamyl alcohol, methanol, potassium acetate, sulphuric acid, ethanol, sodium chloride (all of AR grade) – from SRL, India and Merck, India.

Molecular biology grade reagents/ chemicals: Acrylamide, APS, bis-acryl amide, EDTA, IPTG, lysozyme, TEMED, G418, phenol, DAB, tween 20, triton X 100 - from Sigma-Aldrich, USA or SRL, India. PCR Master mix, dNTPs agarose from Bioline, UK. Cyber green master mix –from Applied Biosystem, U.S.A. Magnesium chloride, disodium citrate, boric acid, SDS, Tris–base - from Merck, India. Ampicillin, chloramphenicol, tetracycline from Himedia, India. PI3 kinase inhibitor, MEK1/2 inhibitor from Cell Signaling Technology, U.S.A.

Components for bacterial culture medium: Bacto-agar, yeast extract, tryptone- from Himedia, India.

Components for mammalian cell culture medium: DMEM and antibiotic from Invitogen, fetal calf serum- from PAA, sodium bicarbonate- from Sigma-Aldrich, U.S.A.

Enzymes: Taq DNA polymerase– from Bangalore Genei, India. *BamHI*, *Xho I*, *EcoRI*, – from NEB, UK. RNaseA – from Sigma-Aldrich. T4 DNA ligase from- Promega,U.S.A. Reverse transcriptase- from MBI Fermentas, Lithuania.

Blotting Membranes and Filters: PVDF membrane (0.2 µm) - from Milipore, U.S.A. 3mm filter paper - from Whatman, USA.

DNA and protein markers: 100 bp and 1 kb DNA ladder and protein molecular weight marker (14-100KD) - from Bangalore Genei, India.

Plastic and Glasswares: PCR tubes - from Axygen, USA; micro pipette tips, micro centrifuge tubes, petri dishes and other plastic wares- from Tarson Products Pvt. Ltd., India. Glassware- from Borosil International, India.

Cell lines: All the cell lines were procured from National Centre for Cell Science, Pune, India.

Table A1. List of Plasmid Vector

Name	Use	Promoter	Selection marker(s)	Cloning Site
pGEM-T Easy (Promega)	T/A cloning. Vector		Amp^R	T/A cloning *EcoRI* for screening of clone)
pGEX-4T-2 (G.E Healthcare)	Bacterial Expression Vector	ptac	Amp^R	ΔC-CR1 cloned at BamHI/xhoI site
pCI-neo (Promega)	Mammalian expression Vector	pCMV	Amp^R, Neo^R	Full length CR1 cloned at EcoRI site (gifted by Dr. D. S . salomon, NIH, USA)

Table. A2. List of Bacterial Strain

Strain	Description
Escherichia coli DH5α	$F^{'}$ ϕ80d*lac*ZΔM15 Δ (*lac*ZYA- *arg*F) U169 *end*A1 *rec*A1 *hsd*R17 ($r_k^- m_k^+$) *deo*R *thi*-1 *pho*A *sup*E44 λ^- *gyr*A96 *rel*A1
Escherichia coli Rosetta Gami (DE3) (Novagen)	F^- *ompT hsdS*$_B$ (r_B^- m_B^-) *gal dcm lacY1 ahpC* (DE3) *gor522*::Tn*10 trxB* pRARE (Cam^R, Kan^R, Tet^R)

Table. A3. Culture Medium for Bacteria

Media	Constituents	Concentration	pH
Luria broth (LB)	Bactotryptone	1.0%	7.2
	Yeast extract	0.5%	
	NaCl	0.5%	
2xTY	Bactotryptone	1.6%	7.2
	Yeast extract	1.0%	
	NaCl	0.5%	
TYA	Bactotryptone	1.0%	7.2
	Yeast extract	0.5%	
	NaCl	0.8%	
	Agar	1.5%	
TYA/AMP	TYA media		7.2
	Ampicillin	100 µg/ ml	
TYA/AMP/Glu	TYA/AMP media		7.2
	Glucose	1%	

Table. A4. Culture Medium for Animal Cell

Media	Constituents	pH
DMEM	DMEM poweder with high glucose for 1 liter, 3.7g $NaHCO_3$.	7.4, adjusted with 1N HCL
DMEM with serum	DMEM, 10% serum, 1x Antibiotic.	7.4

Table. A5. List of Buffers and Solutions

Buffers / Solutions	Composition
Tris-EDTA (TE) buffer	0.01 M Tris-HCl (pH 7.4), 0.001 M Na_2-EDTA (pH 8.0)
TAE - Tris Acetate EDTA buffer, 50x (100ml)	24.2 g Tris base, 5.71 ml CH_3COOH, 10 ml of 0.5 M EDTA.
Phosphate buffer saline (PBS)	0.137 M NaCl, 2.68 mM KCl, 7.98 mM Na_2HPO_4, 1.4 mM KH_2PO_4, pH 7.2.
PBST	PBS containing 0.1% Tween -20
TBS	50mM tris base, 150mM NaCl
TBST	TBS containing 0.1% Tween -20
STE	150 mM NaCl, 10 mM Tris-cl (pH 8.0), 1mM EDTA (pH 8.0).
Trypsin- EDTA	0.05% Trypsin, 0.53mM EDTA in PBS
RIPA buffer	50 mM Tris-HCl, pH 7.5, 150 mM NaCl, 1% Nonidet P40, 0.5% sodium deoxycholat, 0.1% SDS.
<u>Buffers/solutions for SDS-PAGE</u>	
30 % acrylamide-bisacrylamide solution (100ml)	29.2 g Acrylamide, 0.8 g Bisacrylamide
Tris.HCl, pH 6.8, 0.5 M (100 ml)	6.06 g of Tris base, pH adjusted to 6.8 with 2 N HCl.
Tris.HCl, pH 8.8, 1.5 M (100 ml)	18.18 g of Tris base, pH adjusted to 8.8 with 2 N HCl.
Gel Running Buffer	25 mM Tris base, 250 mM, 0.1% SDS
Sample Loading Buffer (1X)	50 mM Tris-HCl pH 6.8, 2% SDS, 10% glycerol, 1% β-mercaptoethanol, 0.02 % bromophenol blue
Staining solution	50% Methanol, 10% Acetic acid, 40% Water, 0.25% CBB R250
Destaining solution	30% Methanol, 10% Acetic acid, 60% Water.

Buffers/solutions for Western Blot

Transfer buffer	25 mM Tris base, 39 mM Glycine, 20 % Methanol
Ponceau solution (Sigma)	0.1% PonceauS in 5% acetic acid
Blocking Solution	5% non fat milk in PBST or 5% BSA in TBST.
Washing buffer	PBST or TBST

Solutions for Plasmid Isolation

Solution I	50 mM Glucose , 25 mM Tris.HCl, 10 mM EDTA (pH 8.0)
Solution II	0.2 N NaOH, 1% SDS
Solution III	5 M potassium acetate, pH adjusted to 4.8 with acetic acid

Buffers/Solutions for Cell cycle analysis

Fixation Solution	70% ice cold ethanol in PBS , 1mM EDTA
DNA Extraction Buffer	192 ml of 0.2 M Na_2HPO4 with 8 ml of 0.1% Triton X-100 (v/v
DNA staining Solution	20 µg/ml propidium iodide and 200 µg/ml RNase A in PBS

Solutions for BrdU ELISA

Substrate solution	O-phenylenediamine (0.4 mg/ml) diluted in 0.05 M citric acid and 0.1 M Na_2HPO_4, pH 5.0 and 0.03% H_2O_2.

Table. A6. List of Antibody

Name	Sourse/ Type	Working condition	Working dilution	Use
Anti-human Cripto-1 (R&D System, U.S.A, #AF145)	Goat/ monoclonal	4 °C/ ON	1:500	WB
Anti-GST (B.Genei, India, # 105644)	Mose /	RT/ 2 h	1:500	WB
Anti-human phospho- p44/42 MAPK (Erk1/2) (Thr202/Tyr204) (Cell signaling, U.S.A, # 4370)	Rabbit/ monoclonal	4 °C/ ON	1:1000	WB
Anti-human p44/42 MAPK (Erk1/2) (Cell Signaling,U.S.A, # 4695)	Rabbit/ monoclonal	4 °C/ ON	1:1000	WB
Anti-human Phospho-Akt (Ser473) (Cell Signaling, U.S.A, # 4060)	Rabbit/ monoclonal	4 °C/ ON	1:1000	WB
Anti-human Akt (pan) (Cell Signaling, U.S.A, # 4691)	Rabbit/ monoclonal	4 °C/ ON	1:1000	WB
Anti-human Phospho- JNK (Thr183/Tyr185) (Cell Signaling, U.S.A, # 4668)	Rabbit/ monoclonal	4 °C/ ON	1:1000	WB
Anti-human JNK (Cell signaling, U.S.A, # 9258)	Rabbit/ monoclonal	4 °C/ ON	1:1000	WB
Anti-human Phospho-p38 MAPK (Thr180/Tyr182) (Cell Signaling, U.S.A, # 4511)	Rabbit/ monoclonal	4 °C/ ON	1:1000	WB
Anti-human p38 MAPK (Cell Signaling, U.S.A, # 9212)	Rabbit/ monoclonal	4 °C/ ON	1:1000	WB

Anti-human PTEN (Cell Signaling, U.S.A, # 9188)	Rabbit/ monoclonal	4 °C/ ON	1:1000	WB
Anti-human p27 (Cell Signaling, U.S.A, # 3686)	Rabbit/ monoclonal	4 °C/ ON	1:1000	WB
Anti-human COXIV (Cell Signaling, U.S.A, # 4850)	Rabbit/ monoclonal	4 °C/ ON	1:2000	WB
Anti-human beta actin (Cell Signaling, U.S.A, # 4970)	Rabbit/ monoclonal	4 °C/ ON	1:2000	WB
Anti-human GAPDH (Cell Signaling, U.S.A, # 2118)	Rabbit/ monoclonal	4 °C/ ON	1:2000	WB
Anti-BrdU (BD Pharmigen, U.S.A, # 555627)	Mouse/ monoclonal	RT/1 hr	1:500	ELISA
Anti Mouse-HRP (Sigma, U.S.A, # A0412)	Goat	RT/ 2 hr	1:2000	ELISA, WB
Anti Rabbit-HRP (Cell Signaling, U.S.A, # 7074)	Goat	RT/ 2 hr	1:5000	WB
Anti Goat-HRP (Bangalore Genei, India, # 105500)	Rabbit	RT/ 2 hr	1:2000	WB

RT: Room Temperature, ON: Over Night, W.B: Western Blot.

Table A7. List of Primers

Name	Sequence	Annealing Temp.(°C)	Final Conc (nM)
	Primers set for cloning		
Cripto-1	CRF : 5'- CGCGGATCCATGGACTGCAGGAAGATGG -3' CRR: 5'- CCGCTCGAGCAGACGGTGGTAGTTCTGG-3'	60	500
	Primers set for real time PCR		
Cyclin D1	CD1F : 5'-CGCCCCACCCCTCCAG -3' CD1R : 5'-CGCCCAGACCCTCAGACT -3'	60	100
Cyclin B1	CB1F 5'- TCTGGATAATGGTGAATGGACA-3' CB1R : 5'-CGATGTGGCATACTTGTTCTTG-3'	60	100
Cyclin A2	CA2F : 5'- ACGGCGCTCCAAGAGGACCA-3' CA2R : 5'- AGCCAGGGCATCTTCACGCT-3'	60	100
Cyclin E1	CE1F: 5'- CCACACCTGACAAAGAAGATGATGAC-3' CE1R: 5'- GAGCCTCTGGATGGTGCAATAAT-3'	60	100
Glypican-1	GLPF : 5'-CCGGAAGGTCAGCAGGAAGAGCTCC-3' GLPR : 5'- GGCCTGGCTACTGTAAGGGCCA-3'	60	200
p21	FP21: 5'- GGACAGCAGAGGAAGACCATGT -3' RP21: 5'- TGGAGTGGTAGAAATCTGTCATGC -3'	60	100

p27	FP27: 5'- CTGCAACCGACGATTCTTCTACT -3' RP27: 5'- GGGCGTCTGCTCCACAGA -3'	60	100
p57	FP57: 5'- CAGAACCGCTGGGATTACGA -3' RP57: 5'- CACCGAGTCGCTGTCCACTT -3'	60	100
Beta actin	actinF : 5'-CTGTCTGGCGGCACCACCAT-3' actinR : 5'- GCAACTAAGTCATAGTCCGC-3'	60	100
PPIA	CycloF: 5'-ACACGCCATAATGGCACTGG-3' CycloR: 5'-ATTTGCCATGGACAAGATGCC-3'	60	200
GAPDH	GAPF: 5'-GAAGGTGAAGGTCGGAGTC-3' GAPR: 5'-GAAGATGGTGATGGGATTTC-3'	60	500

Figure A1: Melting curve profile of amplicon of each primer set using SYBR Green as a reporter dye.

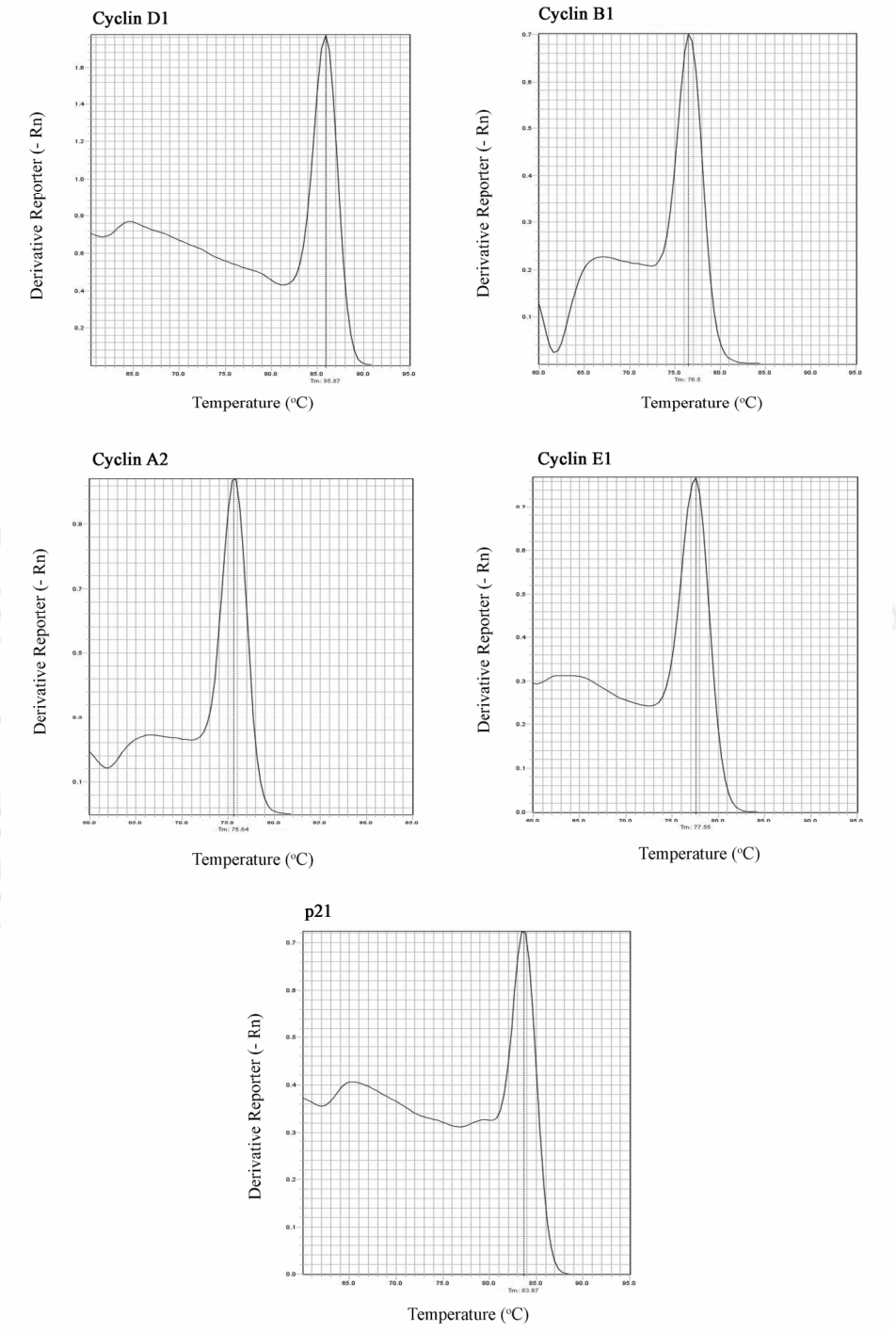

Figure A2: Melting curve profile of amplicon of each primer set using SYBR Green as a reporter dye

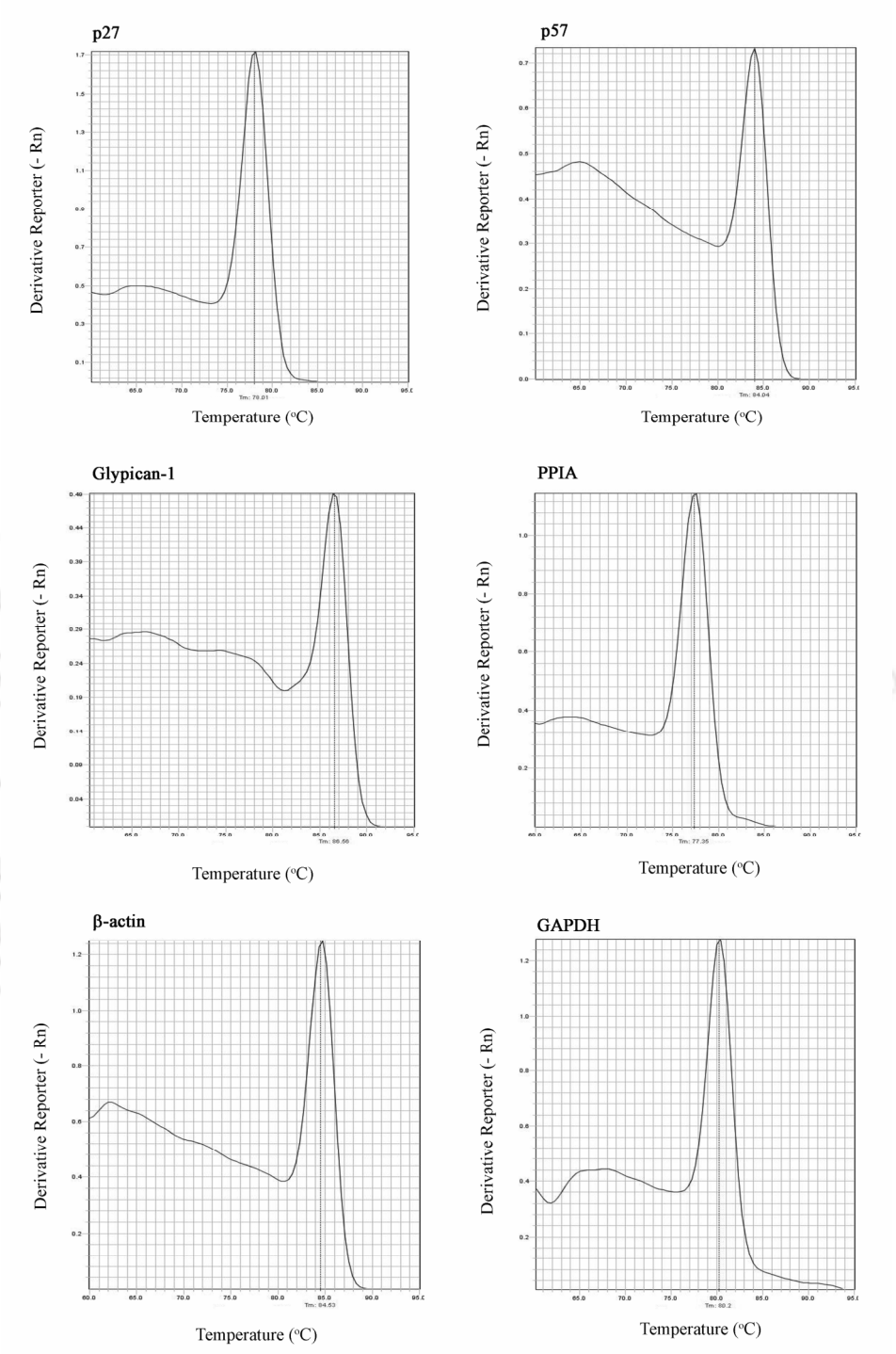

Table. A8. List of Antibiotic

Name	Stock Conc.(mg/ml)	Solvent	Working Conc.(µg/ml)
Ampicillin	100	Water	50-100
Chloramphenicol	50	50% ethanol	50
Tetracycline	25	70% ethanol	12
G418	20	HEPES buffer	400-800

Table. A9. List of Inhibitors

Name	Stock Conc.(mM)	Solvent
PI3 Kinase Inhibitor (LY294002)	10	DMSO
MEK1/2 Inhibitor **(**U0126)	10	DMSO

Publications

1. **Das AB**, Loying P, Bose B. Human recombinant Cripto-1 increases doubling time and reduces proliferation of HeLa cells independent of pro-proliferation pathways. *Cancer Lett.* 2011, *in press*.
   (DOI: http://dx.doi.org/10.1016/j.canlet.2011.12.013) [PMID: 22182448]

Abstract:

1. **Das AB**, Bose B. Heterologous Expression of Human Oncofetal Protein Cripto-1. *77th Annual meeting of Society Of Biological Chemists (India)*, IIT Madras, Chennai, India, December, 2008.